


2019

Mechanistic Study of Diatrizoic Acid Induced Proximal Tubule Cytotoxicity

Dakota Blake Ward

Follow this and additional works at: <https://mds.marshall.edu/etd>

 Part of the [Medical Cell Biology Commons](#), [Medical Toxicology Commons](#), and the [Reproductive and Urinary Physiology Commons](#)

**MECHANISTIC STUDY OF DIATRIZOIC ACID INDUCED PROXIMAL TUBULE
CYTOTOXICITY**

A dissertation submitted to
the Graduate College of
Marshall University
In partial fulfillment of
the requirements for the degree of
Doctor of Physiology
In
Biomedical Sciences

by
Dakota Blake Ward

Approved by

Dr. Monica Valentovic, Committee Chairperson

Dr. Gary Rankin

Dr. Richard Egleton

Dr. Travis Salisbury

Dr. Todd Green

Marshall University
July 2019

APPROVAL OF THESIS

We, the faculty supervising the work of Dakota Blake Ward, affirm that the dissertation, *Mechanistic Study of Diatrizoic Acid Induced Proximal Tubule Cytotoxicity*, meets the high academic standards for original scholarship and creative work established by the Biomedical Sciences Program and the Graduate College of Marshall University. This work also conforms to the editorial standards of our discipline and the Graduate College of Marshall University. With our signatures, we approve the manuscript for publication.



June 6, 2019

Dr. Monica Valentovic,

Department of Biomedical Sciences

Committee Chairperson

Date



Dr. Gary Rankin,

6/6/19

Department of Biomedical Sciences

Committee Member

Date



Dr. Richard Egleton,

6/6/19

Department of Biomedical Sciences

Committee Member

Date



Dr. Travis Salisbury,

6/6/19

Department of Biomedical Sciences

Committee Member

Date



Dr. Todd Green,

6/6/19

Department of Biomedical Sciences

Committee Member

Date

© 2019
Dakota Blake Ward
ALL RIGHTS RESERVED

DEDICATION

I dedicate this work to my incredible wife Paige. It is impossible to say where I would be without your support, understanding, and love, but it is safe to say it would not be writing a dedication page. Although it is no secret how difficult and time consuming getting a doctorate is, no one explains the burdens it puts on the people you love. I am beyond thankful for you being there for me throughout this chapter in our lives. I cannot wait to build the life we have always dreamed of together. I love you, Das.

ACKNOWLEDGMENTS

First and foremost, I want to acknowledge my advisor and mentor, Dr. Monica Valentovic. Our relationship has had its fair share of ups and downs, however, my respect and admiration for her has never wavered. I always joke and say, “if I knew half of what she has forgotten, I’d be set for life.” Dr. Valentovic sees things in people that they cannot see in themselves and I am no exception. Her recognition has driven me to be the scientist and person I am today. Dr. Valentovic is the type of person that you can always count on and I could not be happier with an advisor. Thank you, Dr. V. Also, thanks for all the snacks.

I would like to extend a special thanks to Dr. Gary Rankin. My first experiences in research began in Dr. Rankin’s laboratory. Through working in his lab, I realized that research is the career path that I wanted to follow. I was a lost kid with an interest in science prior to meeting Dr. Rankin and I will be forever grateful for the opportunity.

To the rest of my committee, Dr. Egleton, Dr. Salisbury, and Dr. Green, I want to thank you all individually. Dr. Egleton, thank you for being a source of great conversation and the occasional beer. Your stream of consciousness is unrivalled. Every time I eat a piece of ginger candy, I will think of you. Dr. Salisbury, thank you for being an absolute machine of a human being. Your drive and determination inspire me daily. I cannot think of a day where I was at the lab that I did not see you, late nights and weekends included. Dr. Green, a more helpful person does not exist, and I definitely cannot think of a person happier to help. You always seem to have a smile on and you never fail to put a smile on my face. Thank you all.

Quickly, I want to thank Jamie Friedman. You started as a peer and colleague. Then you became a friend. Now, you’re a lifer.

Finally, I want to thank Katie Brown, better known as BJ. I owe the vast majority of the work in this dissertation to you. All the problems that I was having in the lab seemed to vanish when you became a part of our lab. I truly wish I could bring you with me on all of my future endeavors.

To the countless people that impacted my life positively or negatively to lead me to where I am today, I cannot thank you enough.

TABLE OF CONTENTS

Approval of Thesis.....	ii
Dedication.....	iv
Acknowledgments.....	v
List of Tables	x
List of Figures	xi
Abstract.....	xiii
Chapter 1: Contrast Induced Acute Kidney Injury and Direct Cytotoxicity of Iodinated Radiocontrast Media on Renal Proximal Tubule Cells.....	
1	1
Abstract.....	2
Introduction.....	2
Radiocontrast Media	3
Renal Pathogenesis	7
Risk Factors	10
Cytotoxicity.....	15
Interventions for Cytotoxicity by Hydration, Drugs, and Natural Products	24
Conclusions.....	29
Chapter 2: General Methods, Materials, and Statement of Hypothesis	
30	30
The HK-2 Cell Model.....	30
Experimental Protocol	30
General Protocol for Western Blotting and OxyBlot®.....	32
Seahorse XFe Assays.....	33
Cell and Protein Normalization	36

Statistical Analysis.....	36
Statement of Hypothesis	37
Chapter 3: Radiocontrast Agent Diatrizoic Acid Induces Mitophagy and Oxidative Stress Via Calcium Dysregulation	
Abstract.....	40
Introduction.....	40
Methods.....	42
Chemicals and Reagents	42
Cell Line and Diatrizoic Acid (DA) Treatment	43
Mitochondrial and Cell Viability.....	43
Mitochondrial Isolation.....	44
Oxyblot and Western Blot	45
Seahorse XF Assays.....	46
TNF α in Cell Media and Cell Lysate.....	47
SOD Activity Assay.....	48
Calcium Assays.....	48
Statistical Analysis.....	49
Results.....	49
DA Effects on Mitochondrial and Cell Viability.....	49
DA Effects on Mitochondrial Function and Energy Utilization.....	51
DA Effects on Mitophagy.....	56
DA Effects on Endoplasmic Reticulum Stress	59
DA Effects on Oxidative Stress	61

DA Effects on Mitochondrial Membrane Leakage and Apoptosis Initiation	69
DA Effects on Calcium Homeostasis	70
Discussion	76
Conclusion	97
Acknowledgments.....	99
Chapter 4: Summary, Conclusions, and Future Directions.....	100
Clinically Relevant Concentrations of DA is Cytotoxic to HK-2 Cells	100
DA Alters Mitochondrial Function and Induces Mitophagy in HK-2 Cells.....	101
DA Causes Oxidative Stress in HK-2 Cells.....	103
DA Induces Apoptosis in HK-2 Cells.....	105
DA Causes Dysregulation of Calcium Homeostasis in HK-2 Cells	106
Conclusions.....	107
Future Directions	107
References.....	110
Appendix A: Office of Research Integrity Approval Letter	133
Appendix B: List of Abbreviations.....	134
Appendix C: Vita	139

LIST OF TABLES

Table 1. Summary of various parameters of RCM.	8
Table 2. Common predisposing risk factors for CI-AKI	10
Table 3. Primary and secondary antibodies used in current work.	33

LIST OF FIGURES

Figure 1. Relationship between osmolality and viscosity for RCM agents.....	6
Figure 2. Molecular structures of different RCM.	7
Figure 3. ROS scavenging pathways in renal epithelial cells.....	19
Figure 4. Pathways involved in the UPR.....	22
Figure 5. Agilent Seahorse XF cell mito stress test profile and electron transport chain.	35
Figure 6. Hypothesized sequence of events following exposure of HK-2 cells to DA.	38
Figure 7. Diatrizoic acid cytotoxic effects on mitochondrial viability in HK-2 cells using MTT.50	
Figure 8. Diatrizoic acid cytotoxic effects on cell viability in HK-2 cells using Trypan Blue Exclusion.....	50
Figure 9. Diatrizoic acid effects on various parameters of mitochondrial respiration in HK-2 cells.	52
Figure 10. Diatrizoic acid effects on various parameters of glycolysis in HK-2 cells.....	53
Figure 11. Diatrizoic acid effects on mitochondrial, glycolytic, and total ATP production.....	55
Figure 12. Diatrizoic acid effects on mitochondrial fuel oxidation in HK-2 cells.....	56
Figure 13. Diatrizoic acid effects on LC3B expression in HK-2 cells following 8 hr exposure ..	57
Figure 14. Diatrizoic acid effects on LC3B expression in HK-2 cells following 24 hr exposure	58
Figure 15. Diatrizoic acid effects on GRP78 expression in HK-2 cells.....	60
Figure 16. Diatrizoic acid effects on CHOP expression in HK-2 cells.....	61
Figure 17. Diatrizoic acid effects on protein carbonylation in HK-2 cells	62
Figure 18. Diatrizoic acid effects on 4-HNE adduct formation in HK-2 cells	63
Figure 19. Diatrizoic acid effects on superoxide dismutase expression and activity in cellular fractions of HK-2 cells.....	65

Figure 20. Diatrizoic acid effects on oxidative stress within cellular fractions of HK-2 cells.	66
Figure 21. Diatrizoic acid effects on TNF α and NOX4 expression in HK-2 cells.	68
Figure 22. Diatrizoic acid effects on mitochondrial membrane integrity in HK-2 cells.....	69
Figure 23. Diatrizoic acid effects on the expression of caspase 4, caspase 12, and caspase 3 in HK-2 cells.	70
Figure 24. Effects of EGTA, BAPTA-AM, or 2-APB pretreatment on mitochondrial viability in HK-2 cells.	72
Figure 25. Diatrizoic acid effects on calpain activity in HK-2 cells.....	73
Figure 26. Effects of BAPTA-AM or calpeptin pretreatment on LC3B expression in HK-2 cells.	74
Figure 27. Effects of BAPTA-AM or calpeptin pretreatment on oxidative stress in HK-2 cells..	75
Figure 28. Effects of BAPTA-AM or calpeptin pretreatment on caspase 12 activity in HK-2 cells.	76
Figure 29. Summary of DA-induced cytotoxicity.....	109

ABSTRACT

Radiocontrast media (RCM) are necessary for many diagnostic procedures such as arteriography, percutaneous coronary intervention (PCI), and computed tomography. Contrast-induced acute kidney injury (CI-AKI) is the third most common cause of hospital-associated kidney damage accounting for 10-25% of cases worldwide. The mechanisms of contrast-induced renal impairment are not entirely known, but diminished renal hemodynamics, inflammatory responses, and direct cytotoxicity have been hypothesized. The purpose of this study was to investigate the mechanisms of direct cytotoxicity observed in HK-2 cells following treatment with diatrizoic acid (DA) and to determine the source of this damage. Mitochondrial function, endoplasmic reticulum (ER) stress, oxidative stress, and the role of calcium were examined in response to exposure to DA. HK-2 cells were grown to confluency for 48 hr and exposed to 0-30 mg I/mL of DA for 2, 8, or 24 hr. The vehicle used for all studies was phosphate buffered saline (PBS). Mitochondrial and cell viability were decreased within 2 and 24 hr, respectively, as shown by MTT assays and trypan blue exclusion cell counts. Mitochondrial function was monitored using an Agilent Seahorse analyzer and cell mito stress tests, cell glycolysis stress tests, mito fuel flex tests, and real-time ATP rate assays. Oxidative stress, ER stress, and mitophagy were assessed in whole cell lysate and cell fractions using OxyBlot and Western blot analysis for 4-hydroxynonenol (4-HNE), tumor necrosis factor alpha (TNF α), NADPH oxidase 4 (NOX4), manganese superoxide dismutase (MnSOD), glucose-regulated protein 78 (GRP78), C/EBP homologous protein (CHOP), microtubule-associated proteins 1A/1B light chain 3B (LC3B), cytochrome c, and caspases 3, 4, and 12. The role of calcium in mitophagy and apoptosis was determined by pretreating HK-2 cells with various calcium modulators such as BAPTA-AM, EGTA, 2-APB, or calpeptin prior to the addition of DA. Studies conducted using

Seahorse XF technology and analysis of LC3BI and II expression determined that DA alters mitochondrial function within 8 hr. MTT and calpain activity assays indicated that disruption of calcium homeostasis plays a role in DA induced cytotoxicity within 8 hr. An increase in oxidative stress and loss of mitochondrial membrane integrity was evident within 24 hr exposure to 18 mg I/mL DA. DA induces apoptosis at 24 hr exposure as shown by Western blot analysis of cytochrome c leakage and activation of caspase 3 and 12. These studies indicate that mitochondrial damage and oxidative stress occur in HK-2 cells treated with DA, and maintaining calcium homeostasis may help prevent DA-induced cytotoxicity.

**CHAPTER 1: CONTRAST INDUCED ACUTE KIDNEY INJURY AND DIRECT
CYTOTOXICITY OF IODINATED RADIOCONTRAST MEDIA ON RENAL
PROXIMAL TUBULE CELLS**

A manuscript published in the *Journal of Pharmacology and Experimental Therapeutics*.

Dakota B. Ward; Monica A. Valentovic

Reprinting for dissertation is part of the author's rights and permission is not required from the American Society for Pharmacology and Experimental Therapeutics (ASPET), the copyright holder.

Dakota B. Ward*, Monica A. Valentovic*¹

* Department of Biomedical Sciences, Joan C. Edwards School of Medicine, Marshall University, Huntington, WV 25755

¹Correspondence should be addressed to: Department of Biomedical Sciences; 1 John Marshall Drive, Joan C. Edwards School of Medicine, Marshall University, Huntington, WV, 25755.

Phone (307-696-7332) Fax (304-696-7391) Email: valentov@marshall.edu

ABSTRACT

The administration of intravenous iodinated radiocontrast media (RCM) to visualize internal structures during diagnostic procedures has increased exponentially since their first use in 1928. A serious side effect of RCM exposure is contrast-induced acute kidney injury (CI-AKI), which is defined as an abrupt and prolonged decline in renal function occurring 48–72 hours after injection. Multiple attempts have been made to decrease the toxicity of RCM by altering ionic strength and osmolarity, yet there is little evidence to substantiate that a specific RCM is superior in avoiding CI-AKI. RCM-associated kidney dysfunction is largely attributed to alterations in renal hemodynamics, specifically renal vasoconstriction; however, numerous studies indicate direct cytotoxicity as a source of epithelial damage. Exposure of in vitro renal proximal tubule cells to RCM has been shown to affect proximal tubule epithelium in the following manner: 1) changes to cellular morphology in the form of vacuolization; 2) increased production of reactive oxygen species, resulting in oxidative stress; 3) mitochondrial dysfunction, resulting in decreased efficiency of the electron transport chain and ATP production; 4) perturbation of the protein folding capacity of the endoplasmic reticulum (ER) (activating the unfolded protein response and inducing ER stress); and 5) decreased activity of cell survival kinases. The present review focuses on the direct cytotoxicity of RCM on proximal tubule cells in the absence of in vivo complications, such as alterations in renal hemodynamics or cytokine influence.

INTRODUCTION

Administration of radiocontrast media (RCM) necessary for X-ray based imaging procedures such as percutaneous coronary intervention and cardiac angiography may lead to contrast-induced acute kidney injury (CI-AKI). The severity of this dysfunction can range from

non-symptomatic increases in serum creatinine (SCr) to severe and permanent renal damage resulting in the need for dialysis (Brown et al., 2016). CI-AKI is defined as an absolute increase in SCr greater than 0.5 mg/dl or a relative increase of greater than 25% of baseline SCr peaking 3-5 days after administration and returning to baseline within 10-14 days in the absence of other contributing factors (Mehran & Nikolsky, 2006; Thomsen & Morcos, 2003). Currently, the exact mechanisms of RCM nephrotoxicity have not been fully elucidated; however, hypothesized sources include alterations in renal hemodynamics and direct toxicity to renal epithelium mutually resulting in an increase in reactive oxygen species (ROS) and oxidative damage. Renal ischemia is a complex result of severe renal vasoconstriction, decreased oxygen supply, and increased oxygen demand within the renal outer medulla (J. S. Yang et al., 2018). Although a vast number of clinical reports and observational studies have explored the incidence of CI-AKI following administration of RCM, most finding significant risk, little is known about the direct cellular toxicity induced by RCM. To determine the source of RCM induced cytotoxicity, *in vitro* models must be implemented to eliminate renal hemodynamic and inflammatory responses to RCM administration. This minireview briefly discusses the characterization of RCM, renal pathogenesis, and risk factors involved in CI-AKI, as well as the direct toxic effects of RCM on cellular antioxidant systems, mitochondria, the endoplasmic reticulum (ER) and the unfolded protein response (UPR), and activity of stress kinases in *in vitro* systems. This short review also briefly addresses current and experimental preventative measures for CI-AKI.

RADIOCONTRAST MEDIA

The first RCM developed for intravenous administration, uroselectan, diodrast and hippuran, were synthesized in the late 1920s for use in urography procedures (Swick, 1930). During this time, advances to understand the relationships between chemical structure, toxicity,

and pharmacokinetics were being made, resulting in the discovery of the parent compound to all modern RCM, acetrizoic acid (Wallingford, 1953). Continuation of these developments led to the detection of RCM that are much more tolerable and increasingly radiopaque compared to early radiopaque compounds.

The first generation of modern RCM are derivatives of acetrizoic acid, ionic monomers, and have osmolalities 5-8 fold greater than plasma, thus were denoted high-osmolar contrast media (HOCM). The ionization of early RCM have been associated with many toxic reactions including: severe nephrotoxicity (Schreiner, 1966; Stokes & Bernard, 1961), induction of convulsions and seizures (Melartin, Tuohimaa, & Dabb, 1970), pancreatitis in patients undergoing endoscopic retrograde cholangio-pancreatography (Banerjee, Grainger, & Thompson, 1990), severe and potentially fatal thrombi in patients with sickle-cell anemia (McNair, 1972), inhibition of platelet aggregation *in vivo* and *in vitro* (Gaffer et al., 1979), and blood volume expansion leading to right heart volume overload in patients with poor cardiac function (Widmark, 2007). The theory that first generation RCM ionicity and osmolality were critical contributors to toxicity led to the dimerization or replacement of carboxyl groups with non-dissociating hydrophilic groups (Stratta, Quaglia, Airoidi, & Aime, 2012). The resulting generation of RCM consisted of ionic dimers and non-ionic monomers that had osmolalities 2-3 fold greater than plasma and were labeled low-osmolar contrast media (LOCM). The practice of decreasing RCM osmolality continued resulting in the third generation of RCM of non-ionic-dimers that exhibit osmolality that is equivalent to plasma and are designated iso-osmolar contrast media (IOCM).

Following intravenous administration, RCM are rapidly diluted and distributed by circulating plasma reaching concentrations adequate for visualization in approximately 5-10

minutes. First generation RCM have a low serum-albumin binding of 0-10% while second and third generation RCM show no notable serum protein binding. RCM of all generations show no significant metabolism and are excreted unchanged predominately through the kidneys by glomerular filtration with a very small percentage, less than 2%, recovered in the feces (Amersham-Health, 2007; GE-Healthcare, 2006). The pharmacokinetics of RCM can be described by a two-compartment model consisting of a rapid distribution alpha phase and a slow excretion beta phase. In patients with normal kidney function, the alpha phase and beta phase half-lives for diatrizoic acid are 30 minutes and 120 minutes, respectively. However, in patients with significant renal impairment, the beta phase half-life can be prolonged for several days (Amersham-Health, 2007).

The indications for RCM change in accordance to procedure and risk of the patient involved. All generations of RCM are used for angiocardiology, although the use of HOCM is not recommended in patients with renal or cardiac insufficiencies. HOCM are used specifically for nonvascular procedures such as pyelography, cystography, and routine computed tomography procedures. LOCM and IOCM are used for vascular procedures and multi-detector computed tomography (Radiology, 2018). It is commonly accepted that a major portion of the toxicity of RCM is due to elevated osmolalities, however, reducing the osmolality of RCM results in a substantial increase in RCM viscosity (Figure 1). High injection rates of RCM with higher viscosities could be a contributing factor in stasis of renal tubular function (Ueda, Nygren, Hansell, & Ulfendahl, 1993). Although there is considerable dissension as to which generation of RCM is the safest, IOCM are thought to be optimal as they deliver the most iodine per molecule with the least impact on osmolality. Figure 2 describes the physical structures of various RCM. Table 1 summarizes several parameters of the various generations of RCM.

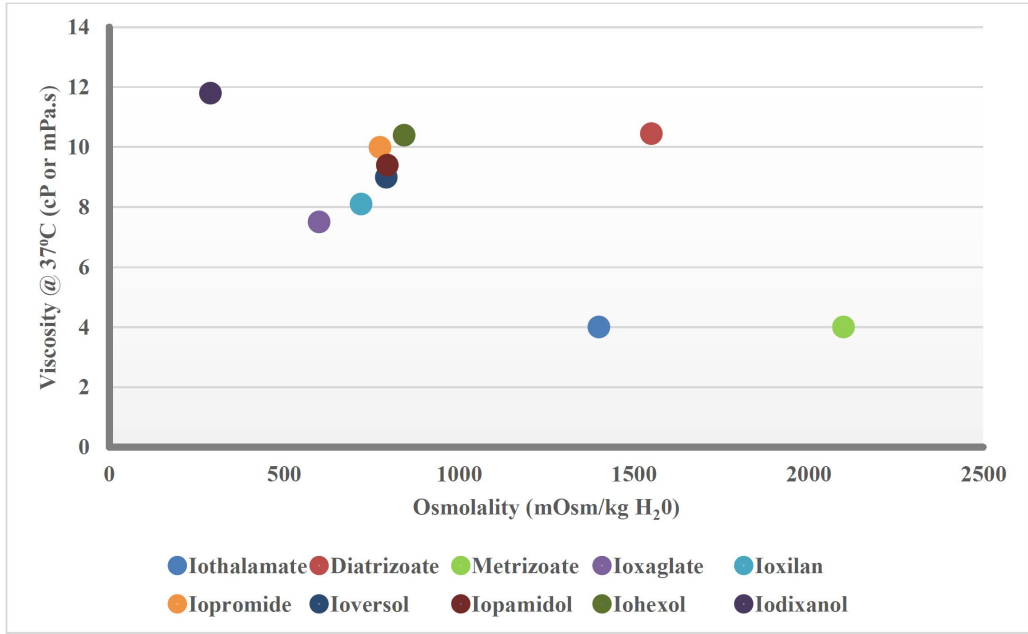


Figure 1. Relationship between osmolality and viscosity for RCM agents. Maximum concentrations of iodine provided by the manufactures and corresponding viscosities at 37°C. Refer to Table 1 for values.

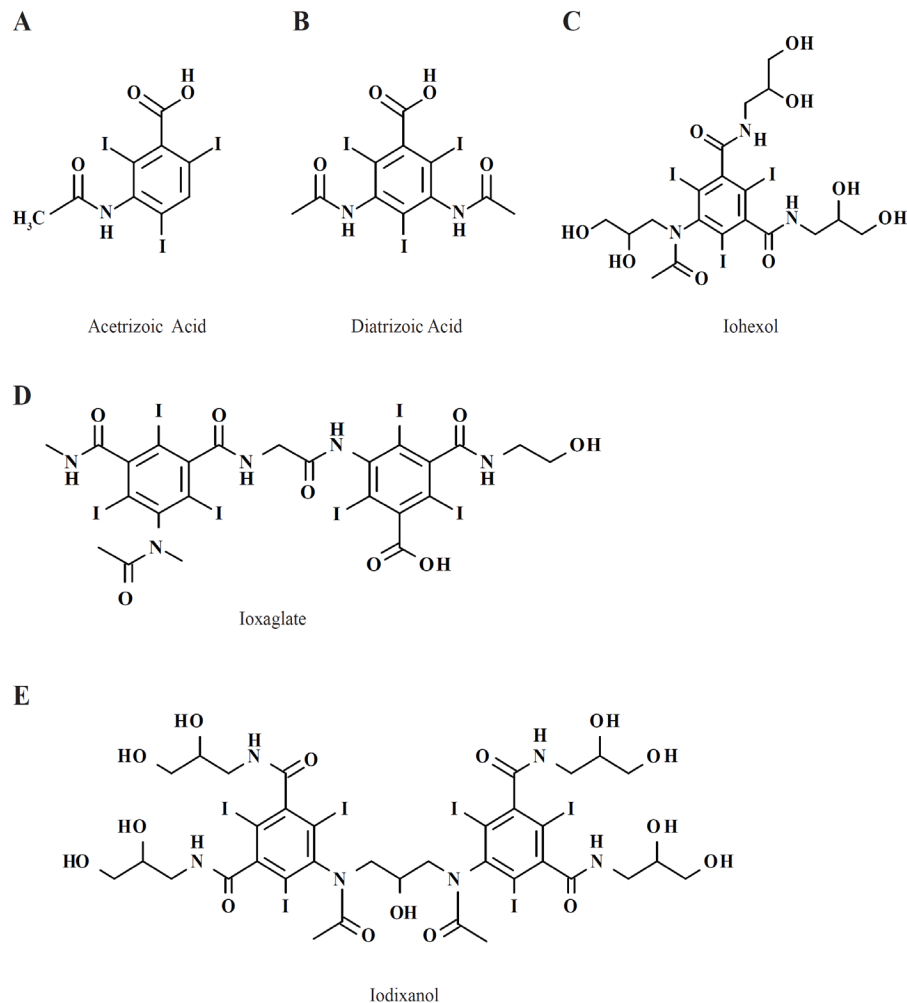


Figure 2. Molecular structures of different RCM. Parent compound to modern RCM, acetrizic acid (A), first generation ionic monomer, diatrizoic acid (B), second generation non-ionic monomer, Iohexol (C) and ionic dimer, ioxaglate (D), and third generation non-ionic dimer, iodixanol (E).

RENAL PATHOGENESIS

The administration of intravenous iodinated RCM for diagnostic procedures and medical interventions have increased exponentially since their introduction in the late 1920s.

Unfortunately, CI-AKI is the third most common cause of hospital-acquired kidney damage, accounting for 12% of cases (Gleeson & Bulugahapitiya, 2004; Nash, Hafeez, & Hou, 2002).

The level of this dysfunction can vary from a mild increase in SCr to permanent renal failure resulting in dialysis (Brown et al., 2016). Although the definition of CI-AKI varies in the

literature, it is generally defined as an absolute increase in SCr greater than 0.5 mg/dl or a relative increase of greater than 25% of baseline SCr peaking 3-5 days after administration and returning to baseline within 10-14 days (Mehran & Nikolsky, 2006; Thomsen & Morcos, 2003). The incidence of CI-AKI is low, less than 2%, in patients with normal to slightly diminished renal function (GFR > 60 ml/min per 1.73 m²) (Berns, 1989; Weisbord & Palevsky, 2008); however, in high-risk patients with moderate to severe renal impairment the incidence is as high as 55% (Mehran & Nikolsky, 2006).

Generations of Radiocontrast Media

Generation	RCM Name	Osmolality (mOsmol/Kg)	Iodine Content (mg I/mL)	Viscosity 25°C/37°C (cP or mPa.s)	Ionicity	Iodine-to-molecule Ratio
First Generation	Iothalamate	600-1400	141-282	2.0/1.5 - 6.0/4.0	Ionic Monomer	1.5 : 1
	Diatrizoate	1551	370	16.4/10.45		
	Metrizoate	2100	370	-/4		
Second Generation	Ioxaglate	600	320	15.7/7.5	Ionic Dimer	3 : 1
	Ioxilan	721	350	16.3/8.1	Nonionic Monomer	
	Iopromide	328-774	150-370	2.3/1.5 - 22.0/10.0		
	Ioversol	502-792	240-350	4.6/3.0 - 14.3/9.0		
	Iopamidol	524-796	250-370	5.1/3.0 - 20.9/9.4		
	Iohexol	322-844	140-350	2.3/1.5 - 20.4/10.4		
Third Generation	Iodixanol	290	270-320	12.7/6.3 - 26.6/11.8	Nonionic Dimer	6 : 1

Table 1. Summary of various parameters of RCM. (Radiology, 2018)

Although the exact mechanisms of toxicity of RCM have not been fully elucidated, it is hypothesized that the acute deterioration of kidney function is caused by a combination of renal medullary hypoxia and direct toxicity to renal epithelial cells. Intravenous administration of RCM induces transient vasodilation of renal vasculature followed by severe, sustained vasoconstriction, specifically of the afferent arterioles, resulting in decreased oxygen supply and oxidative damage to the outer medulla (Z. Z. Liu et al., 2012; Persson, Hansell, & Liss, 2005). This response is likely due to modifications of endogenous renal vasomodulators, specifically nitric oxide (NO), endothelin, and adenosine (Hall et al., 1992). The production of the

vasodilator NO decreases in response to RCM resulting in exacerbation of renal vasoconstriction (Touati et al., 1993). Levels of endothelin, a vasoconstrictive peptide released by endothelial cells to maintain blood pressure, have been shown to increase after RCM exposure (Clark, Kim, & Epstein, 1997). It is also apparent that adenosine plays a role in inducing CI-AKI. Intrarenally administered adenosine produces biphasic hemodynamic alterations that are similar to those induced by RCM (Arend et al., 1987).

The oxidative damage induced by vasoconstriction is compounded in the relatively hypoxic renal medullae. Under normal physiological function, the medulla functions at very low O₂ tension as the result of limited blood flow and the ‘oxygen shunt’ caused by the anatomy of the outer medullary vasculature (Heyman, Rosen, & Brezis, 1997; Leong, Anderson, O'Connor, & Evans, 2007). Along with poor O₂ delivery, O₂ consumption within the outer medullae is high due to ion reabsorption by the thick ascending limb (TAL) of the nephron (Heyman et al., 1997). The combined effects of low O₂ delivery and high O₂ consumption renders the renal medullae particularly susceptible to hypoxic injury. RCM exposure has been shown to further decrease O₂ tension within the renal medulla and simultaneously induce osmotic diuresis and increase ion transport and O₂ consumption at the TAL (Cronin, 2010; Heyman et al., 1991). Additionally, an increase in tubular pressure secondary to RCM induced diuresis, increased urinary viscosity, and tubular obstruction result in increased oxygen consumption, worsening ischemic damage (Gleeson & Bulugahapitiya, 2004). The combination of alterations in vasomodulators and increased oxidative damage may exert direct tubular and vascular endothelial damage leading to a vicious cycle of hypoxic damage in the renal parenchyma (Heyman et al., 2010). Although renal papillary necrosis is not a hallmark of CI-AKI, administration of RCM is contraindicated in patients that are undergoing selective or nonselective nonsteroidal anti-inflammatory drug

(NSAID) therapy. Concomitant use may aggravate NSAID induced renal vasoconstriction, therefore, NSAID therapy should be suspended 48 hours prior to RCM administration (Horl, 2010).

RISK FACTORS

Prevention and treatment of CI-AKI depends solely on the ability of the provider to assess the relative risk of patients undergoing radiopaque imaging procedures. Those at the highest risk for CI-AKI are patients with chronic kidney disease with associated diabetes mellitus. Other factors that increase the risk for CI-AKI include congestive heart failure (CHF), salt depletion/dehydration, prolonged hypotension, low hematocrit, age > 70 years, multiple myeloma, sepsis, and concomitant use of a variety of specific drugs. Table 2 contains a list of common risk factors.

Predisposing Risk Factors

Preexisting Renal Impairment
Diabetes Mellitus
Congestive Heart Failure
Decreased Effective Intravascular Volume
Salt Depletion
Dehydration
Prolonged Hypotension
Low Hematocrit
Age > 70 Years
Multiple Myeloma
Sepsis
Concomitant Use of Various Drugs

Table 2. Common predisposing risk factors for CI-AKI

Preexisting renal dysfunction is the most decisive risk factor in the development of CI-AKI. Due to the inverse relationship of estimated glomerular filtration rate (eGFR) and the risk for CI-AKI, the defined eGFR cut-off point for classifying patients as high risk is ≤ 60

mL/min/1.73 m² (Tsai et al., 2014). The incidence of CI-AKI in patients with underlying chronic renal failure ranges from 14.8 to 55%, and risk can double in patients with concomitant diabetes mellitus when compared to nondiabetic patients (Mehran & Nikolsky, 2006).

Any extrarenal condition that effectively lowers intravascular volume profoundly increases the risk of CI-AKI. Conditions that reduce effective intravascular volume include: CHF, prolonged dehydration, and salt depletion. CHF activates numerous humoral and neurohumoral mechanisms resulting in sodium and water reabsorption by the kidneys. These mechanisms result in expansion of extracellular fluid by increasing venous capillary pressure, decreasing plasma oncotic pressure, and promoting fluid extravasation and edema formation (Navas & Martinez-Maldonado, 1993). Compromised left ventricle systolic performance often apparent in CHF patients has also been linked to increased risk of CI-AKI (Gruberg et al., 2000; Martin-Paredero et al., 1983). Severe dehydration and salt depletion secondary to abnormal fluid losses associated with insufficient salt intake have been shown to play a role in CI-AKI (Detrenis, Meschi, Musini, & Savazzi, 2005). Prolonged hypotension as a result of decreased effective intravascular volume or induced by antihypertensive treatment using angiotensin-converting enzyme inhibitors (ACEI), angiotensin-II receptor blockers (ARB), or diuretics heighten risk for CI-AKI (Barrett & Parfrey, 1994). Decreased effective intravascular volume contributes to CI-AKI risk by reducing renal perfusion and GFR resulting in decreased O₂ delivery and increasing the concentration of RCM within the renal tubules furthering ischemic insult and direct cytotoxicity.

Anemia, or low hematocrit, is an independent risk factor for CI-AKI (J. Y. Cho et al., 2010; Murakami et al., 2013; Nikolsky et al., 2005). A study of 510 patients indicated that individuals with lower hematocrit were more likely to develop CI-AKI (J. Y. Cho et al., 2010).

In an earlier study with patients who displayed both reduced eGFR and hematocrit, rates of CI-AKI were as high as 28.8%, whereas patients with only a diminished eGFR and normal hematocrit had significantly lower rates of CI-AKI (Nikolsky et al., 2005). The mechanism for increased CI-AKI risk in patients with low hematocrit may be partially attributed to diminished oxygen delivery to renal tissue which could increase susceptibility to renal damage. A study of 200 patients revealed less CI-AKI in patients provided oxygen 10 minutes prior to angiography compared to room air (Sekiguchi et al., 2018). These findings suggest sufficient oxygenation may be beneficial to reduce renal damage by RCM, but further studies are warranted to explore the beneficial effect of oxygen.

Advanced age is considered an independent predictor of CI-AKI, although the increased risk to develop CI-AKI is almost certainly multifactorial (Gussenhoven et al., 1991). Age-related alterations in renal function including decreases in GFR, tubular secretion, and urine concentrating ability (Denic, Glassock, & Rule, 2016; Sands, 2012) play a role, as well as the requirement for larger doses of RCM in elderly patients with calcified vasculature (Mehran & Nikolsky, 2006).

Many radiologists and physicians consider RCM use a contraindication in patients with multiple myeloma (Bartels, Brun, Gammeltoft, & Gjorup, 1954; Killmann, Gjorup, & Thaysen, 1957; Scheitlin, Martz, & Brunner, 1960). CI-AKI in myeloma patients has been attributed to precipitation of RCM with Tamm-Horsfall glycoprotein, resulting in increased ischemic injury and desquamation of renal proximal tubule (PT) cells (Dawnay et al., 1985). A more recent retrospective study reviewed 46 patients with myeloma who underwent RCM-enhanced CT scans of the chest, abdomen, and pelvis (Pahade et al., 2011). Of the 46 patients, 12 (26.1%) developed CI-AKI; however, there was no significant difference in peak SCr levels in patients

that obtained CI-AKI when compared to the patients that did not. Of the parameters obtained, only serum levels of β 2-microglobulin increase in both patients with high tumor burden and decreased renal function indicating a statistically significant correlation with the development of CI-AKI. According to the authors, a threshold value of $<2.8\text{mg/L}$ of β 2-microglobulin could essentially eliminate the risk of CI-AKI in patients with multiple myeloma. The European Society of Urogenital Radiology concluded multiple myeloma was not a risk factor following evaluation of a retrospective study of 13 studies (Stacul et al., 2018). However, ESUR concluded that myeloma patients with diminished renal function, dehydration, or hypercalcemia were at a much higher risk for CI-AKI (Stacul et al., 2018).

Sepsis is a life-threatening medical condition most often caused by an overwhelming immune response to a body-wide bacterial infection. Sepsis affects both adult and pediatric patients and is associated with numerous changes to renal function that may be mediated by release of these inflammatory agents as well as direct tubular insult (Alobaidi, Basu, Goldstein, & Bagshaw, 2015). Pro-inflammatory cytokines are released into the bloodstream to combat the infection triggering widespread inflammation, thrombus formation, and endothelial damage (Cavaillon et al., 2003). In cases of septic shock, side-effects include: reduced blood pressure, abnormalities in microcirculatory blood flow, coagulopathy, and endothelial dysfunction resulting in severely reduced oxygen delivery and organ dysfunction or failure (Angus & van der Poll, 2013). However, further studies are needed to evaluate the contribution of renal perfusion as animal studies and human studies have reported both increased and decreased renal blood flow (Langenberg et al., 2005; Langenberg et al., 2006). Autopsy series fail to detect extensive cellular necrosis in victims of septic shock (Takasu et al., 2013); this may be due to sepsis promoting mitochondrial damage in renal tubular epithelial cells resulting in decrease oxygen

consumption (Tran et al., 2011). In addition to decreased oxygenation, renal epithelium experience activation of an innate immune response, giving rise to pathogenic oxidative stress and further tissue injury (Wiersinga, Leopold, Cranendonk, & van der Poll, 2014). The use of nephrotoxic antibiotics to combat the infection can complicate the diagnosis and treatment of sepsis-associated acute kidney injury. Perhaps one, or all, of these factors play a role in why patients undergoing radiopaque imaging procedures are at increased risk of sepsis (Matejovic et al., 2011). Due to the bidirectional nature of sepsis, additional studies are needed to evaluate the connections between CI-AKI and sepsis.

Concomitant use of drugs that are nephrotoxic or impair kidney function increase the risk of CI-AKI. Directly nephrotoxic drugs such as aminoglycosides, cyclosporine A, amphotericin B, and cisplatin have been reported to increase kidney susceptibility to RCM-induced toxicity (Kolonko, Kokot, & Wiecek, 1998; Morcos, 1998). Aminoglycosides and amphotericin B exert a direct nephrotoxic effect via disruption of normal phospholipid trafficking and the induction of severe renal vasoconstriction (Fanos & Cataldi, 2000; Swan, 1997). Cyclosporin A impairs lysosomal function and damages both proximal and distal convoluted tubules resulting in changes to tubulointerstitial transport (Kolonko et al., 1998). Cisplatin, and other platinum derivatives, impair proper enzyme function by binding to sulfhydryl groups resulting in direct toxicity to PT cells (Hanigan & Devarajan, 2003). Long-term ingestion of high doses of NSAIDs, certain penicillins, and sulfonamides can lead to acute tubulointerstitial nephritis which increases the risk of CI-AKI (Kolonko et al., 1998; Morcos, 1998). Although the role of ACEIs and ARBs in CI-AKI is controversial, many providers still believe that concomitant use should be avoided (Toprak, 2007). According to the Council on the Kidney in Cardiovascular Disease and the Council for High Blood Pressure Research of the American Heart Association, the use of

ACEIs or ARBs in radiopaque imaging procedures depends on multiple factors. If the patient's renal perfusion pressure is adequate and volume depletion is not severe, the use of ACEIs or ARBs is acceptable and can even improve renal hemodynamics and salt excretion. However, angiotensin II is essential in the autoregulation of GFR and renal perfusion, and the use of these agents in hypovolemic patients can induce a dramatic decrease in GFR and subsequent oliguric or anuric renal failure (Schoolwerth et al., 2001). Conversely, the Kidney Disease Improving Global Outcomes Clinical Practice Guideline for Acute Kidney Injury states that there is not enough evidence to recommend the discontinuation of ACEIs or ARBs prior to RCM administration (Kellum, 2012). Loop diuretics, specifically furosemide, have been shown to increase the risk of CI-AKI (Majumdar et al., 2009). Other studies have stated that although loop diuretic exposure is associated with acute kidney injury in hospitalized patients, the change in renal function is small and loop diuretic use does not explain the variability in overall renal function (El-Refai et al., 2011).

CYTOTOXICITY

The cytotoxic effects of RCM on PT cells have been extensively studied. The most commonly reported responses to the interaction between RCM and PT cells are vacuolization of the PT cells, increased production of ROS and induction of oxidative stress, mitochondrial dysfunction and an ensuing decline in ATP production, activation of the UPR and ER stress, and alterations in activity of stress kinases (Andersen, Christensen, & Vik, 1994; Andersen, Vik, Eikesdal, & Christensen, 1995; Tervahartiala et al., 1997; Tervahartiala et al., 1991).

Epithelial PT cell vacuolization is generally interpreted as an indicator of drug toxicity and is a histopathological feature of CI-AKI. One route in which RCM are influxed into PT cells is via pinocytosis. During the process of urine production, RCM is concentrated in the renal

tubules. As a result, PT cells are exposed to increasing concentrations of RCM, inducing a rise in pinocytic vessels containing RCM, formation of large vacuoles, alterations in renal histology, and epithelial damage (Andreucci, Solomon, & Tasanarong, 2014; Dickenmann, Oettl, & Mihatsch, 2008). An early study on vacuolization of PT in response to RCM demonstrated that male Sabra rats experienced vacuolar changes in the early segments of the PT within 120 minutes of administration to 2.9 g I/kg of iohalamate. The changes were described as being similar in nature and closely resembled what has been described in human contrast nephropathy (Heyman et al., 1988). A study performed by Tervahartiala et al. demonstrated that 3 g I/kg of diatrizoic acid or iopromide induced statistically significant PT cell vacuolization within 2 hours of administration in diabetic Wistar rats of both sexes (Tervahartiala et al., 1991). Iohexol and iotrolan caused longer lasting and more pronounced vacuolization (Tervahartiala et al., 1991). A separate study on male Sprague-Dawley rats showed a low-level increase in cytoplasmic vacuoles in PT cells occurred in as little as 5 minutes and continued to increase in size and number for 24 hours after single-dose administration of 3 g I/kg iotrolan (Rees, Old, & Rowlands, 1997). A more modern study performed on male Wistar rats demonstrated that a concentration as low as 10ml/kg of iodixanol can induce vacuolization in PT cells in 24 hours (Nasri et al., 2015). Although RCM from each generation induce vacuolization, the lack of *in vitro* studies makes it impossible to determine if this is a direct toxic side effect of RCM.

CI-AKI is the result of a combination of alterations in renal hemodynamics and toxic renal parenchymal damage. Aside from hypoxia induced by low oxygen supply, it is believed that the latter of the two is due to oxidative stress induced by an increase in ROS. Additionally, exposure to RCM results in diminished availability and activity of cellular antioxidant systems. Under physiological conditions, the production of ROS within renal parenchyma is connected to

tubular transport, specifically in areas of the nephron that have dense mitochondrial populations such as the PT, the convoluted tubules, or the TAL of the nephron. A major source of production of superoxide anions ($O_2^{\cdot-}$) and hydroxyl radicals (OH^{\cdot}) takes place within the mitochondria via NAD(P)H-oxidases (Heyman et al., 2010). Additionally, as the consumption of oxygen begins to overwhelm available oxygen during periods of hypoxia, there is an increase in the complete conversion of ATP to hypoxanthine by 5'-nucleotidase. From this, hypoxanthine is converted to uric acid and hydrogen peroxide (H_2O_2) via xanthine oxidase. Consequently, H_2O_2 and $O_2^{\cdot-}$ can react with NO to form peroxynitrite leading to renal vasoconstriction and epithelial damage by decreasing the vasodilatory effects of NO and interacting with protein and DNA, respectively. Although there is evidence that peroxynitrite can induce a degree of vasodilation initially, long-term exposure to peroxynitrite in an environment devoid of NO can lead to irreversible endothelial and epithelial damage (Pacher, Beckman, & Liaudet, 2007).

Several experimental studies have shown that exposure of renal cells to RCM enhances ROS production resulting in oxidative stress. Huang and colleagues noted that exposure of a non-cancerous, immortalized human renal proximal tubule epithelial cell line (HK-2) to the HOCM ioxitalamate induced an increase in cytoplasmic ROS production and formation of 8-hydroxy-2'-deoxyguanosine (8-OHdG), indicating oxidative damage following a 48 hour treatment (Huang et al., 2016). A significant increase of cytosolic superoxide formation took place only 2 hours after exposure of HK-2 cells to 150 mg I/mL of the LOCM iohexol (Jeong et al., 2018). A similar study using a canine distal convoluted tubule cell line (MDCK) showed that exposure to 50, 100, or 200 mg I/mL of iobitridol, iopamidol, or iodixanol induced a dose-dependent increase in ROS production within 3 hours (Quintavalle et al., 2011). A study performed by Netti et al. demonstrated that a statistically significant increase NADPH oxidase-

dependent ROS can be seen in HK-2 cells within 30 minutes of exposure to 200 mg I/mL of LOCM iohexol or iopamidol (Netti et al., 2014). An increase in intracellular ROS can be seen regardless of generation of RCM.

Although there are several *in vitro* studies pertaining to the effect of RCM on the production of ROS, very little has been done to examine the source of ROS production. A rise in ROS concentrations could be, in part, due to a reduction in the efficacy of intracellular antioxidant systems. Figure 3 shows the intracellular antioxidant systems. At the time of this review, a study performed by Jeong et al. is a lone study examining RCM effects on intracellular antioxidant systems *in vitro*. The Jeong group determined that HK-2 cells exposed to 150 mg I/mL of iohexol induced a significant decrease in manganese superoxide dismutase (MnSOD) and glutathione peroxidase (GPx) after 2 hours (Jeong et al., 2018). It is apparent that there is a significant gap in knowledge pertaining to the effects of RCM on antioxidant systems *in vitro*; however, the effects of RCM on reduced glutathione (GSH), GPx, MnSOD, and Catalase (CAT), have been studied extensively *in vivo*. A study performed by Gong et al. determined that male Sprague-Dawley rats exposed to 1.5-2 g I/kg of iohexol resulted in a decrease MnSOD and GSH after 24 hours (Gong et al., 2016). Tasanarong et al. showed in a similar study that exposing male Sprague-Dawley rats to 1.6 g I/kg of iopromide induced a significant decrease in MnSOD and CAT after 24 hours (Tasanarong, Kongkham, & Itharat, 2014). GSH, GPx, MnSOD, and CAT were all significantly reduced in male Sprague-Dawley rats exposed to 3 g I/kg of iodixanol (N. Liu et al., 2018). It should be stated that these changes in cellular oxidant defenses may not be a direct result of RCM toxicity and could be induced, in part, by alterations in renal hemodynamics. Taken together, increased ROS production and a decrease in the efficacy of

renal antioxidant systems plays an important role in CI-AKI; however, the effects of RCM on antioxidant systems on in vitro systems needs to be studied more in depth.

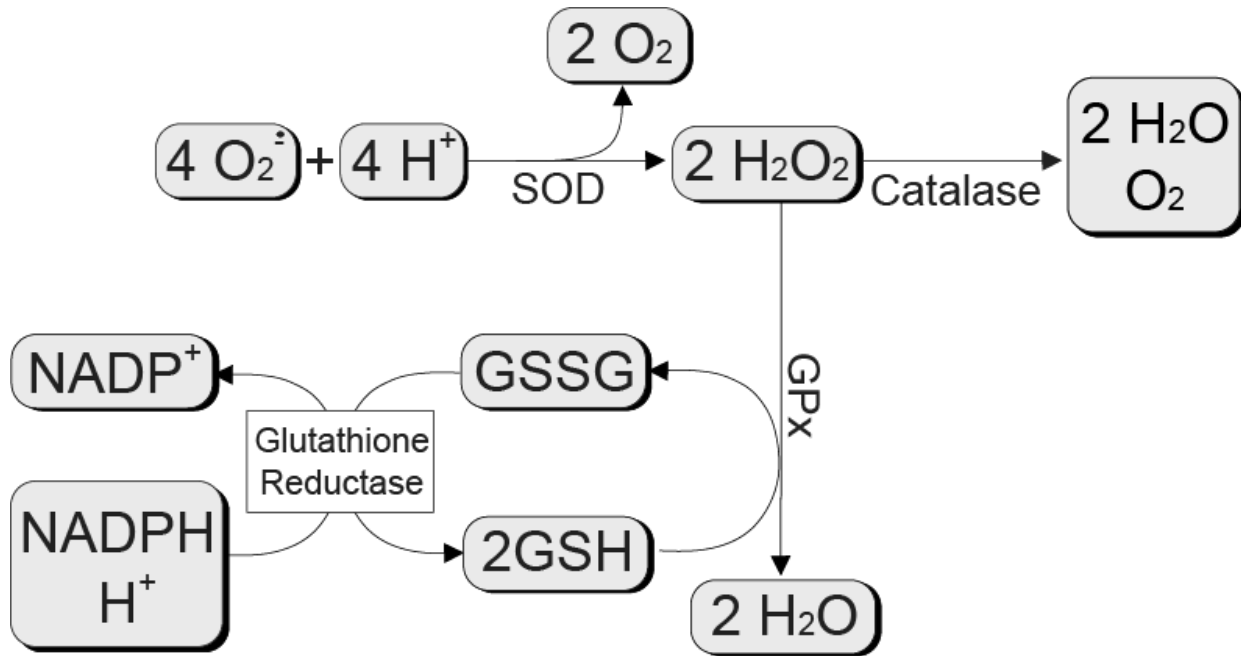


Figure 3. ROS scavenging pathways in renal epithelial cells.

Under normal physiological conditions, the mitochondria are one of the main sources of intracellular ROS and the main organelle target for ROS (Cho, Nakamura, & Lipton, 2010). Previous studies indicate that mitochondrial injury plays an important role in various types of acute kidney injury (Tang et al., 2018; Xiao et al., 2014). Humes et al. noted that PT segments isolated from New Zealand white rabbits incubated with diatrizoate demonstrated significant reductions in basal and uncoupled respiration and intracellular ATP levels indicating an interaction between diatrizoic acid and PT cell mitochondria (Humes, Hunt, & White, 1987). A follow up study using the same model compared the mitochondrial toxicity of diatrizoic acid and iopamidol (Messana, Cieslinski, Nguyen, & Humes, 1988). The authors determined that

diatrizoic acid induced greater reductions in intracellular ATP, basal respiration, and uncoupled respiration when compared to iopamidol and both RCM were toxic when compared to control. Messana et al. continued their studies of the effects of RCM on isolated proximal tubules by comparing the mitochondrial toxicity of the non-ionic monomer iopamidol and ionic dimer ioxaglate. The authors determined that both RCM induced mitochondrial damage but the differences in direct nephrotoxic potential become insignificant when normalized for iodine content (Messana, Cieslinski, & Humes, 1990). Exposure of a porcine kidney cell line that express characteristics similar to PT cells (LLC-PK1) to ioversol caused depolarization of mitochondrial membranes and stimulated the release of cytochrome c activating caspase-9 through the action of the adaptor molecule apoptotic protease-activating factor-1 (Itoh et al., 2006). Lei et al. determined that exposure to iohexol or iodixanol induced a significant increase in mitochondrial ROS and mitochondrial membrane potential in HK-2 cells (Lei et al., 2018). An *in vivo* investigation on the effects of RCM on the electron transport chain determined that exposure of male Wistar albino rats to 1.95 g I/mL of diatrizoate induced decreased activity in complex I and complex III within the kidneys, although not to a significant degree (Roza et al., 2011). As one would expect, significant mitochondrial dysfunction results insufficient ATP for a cell to maintain its cellular functions resulting in activation of the intrinsic apoptotic pathways; however, the source of mitochondrial dysfunction in response to RCM exposure has yet to be identified (Haller & Hizoh, 2004).

The primary role of the ER is the synthesis and folding of secreted, membrane-bound, and some organelle-targeted proteins. The environment within the ER is optimal for protein folding and management, as well as ATP storage and calcium transport (Gaut & Hendershot, 1993). Perturbations of cellular ATP levels, calcium concentration, and/or the redox status within

a cell can lead to a decline in the protein folding ability of the ER (Bravo et al., 2013). An accumulation of unfolded or misfolded proteins activates a pro-survival response responsible for restoring protein folding function within the ER called the unfolded protein response (UPR) (Schroder & Kaufman, 2005). Prolonged activation of the UPR will promote a shift from pro-survival to pro-apoptotic signaling, designated ER stress (Szegezdi, Logue, Gorman, & Samali, 2006). ER stress can lead to the activation of multiple signaling pathways that induce cellular apoptosis (Figure 4) and its role in CI-AKI has recently become a topic of interest. An initial study performed by Wu et al. determined the effects of diatrizoic acid on rat renal proximal tubule cells (NRK52E). Exposure of NRK52E cells to 40 mg I/mL of diatrizoic acid induced an increase in multiple ER stress markers including glucose-regulated protein 78 (GRP78), RNA-dependent protein kinase-like ER kinase (PERK), and inositol-requiring ER-to-nucleus signal kinase 1 (IRE1) within 24 hours (Wu et al., 2010). An additional study by Wu et al. on NRK52E cells determined that 40 mg I/mL of diatrizoic acid induced significant increases in the ER stress markers activating transcription factor 6 (ATF6), C/EBP homologous protein (CHOP), and the ER stress dependent caspase, caspase-12 within 24 hours (Wu et al., 2013). Peng et al. showed that HK-2 cells exposed to 40 mg I/mL of diatrizoic acid induced statistically different increases in GRP78, activating transcription factor 4 (ATF4), CHOP, and caspase-12 within 4 hours (P. A. Peng et al., 2015).

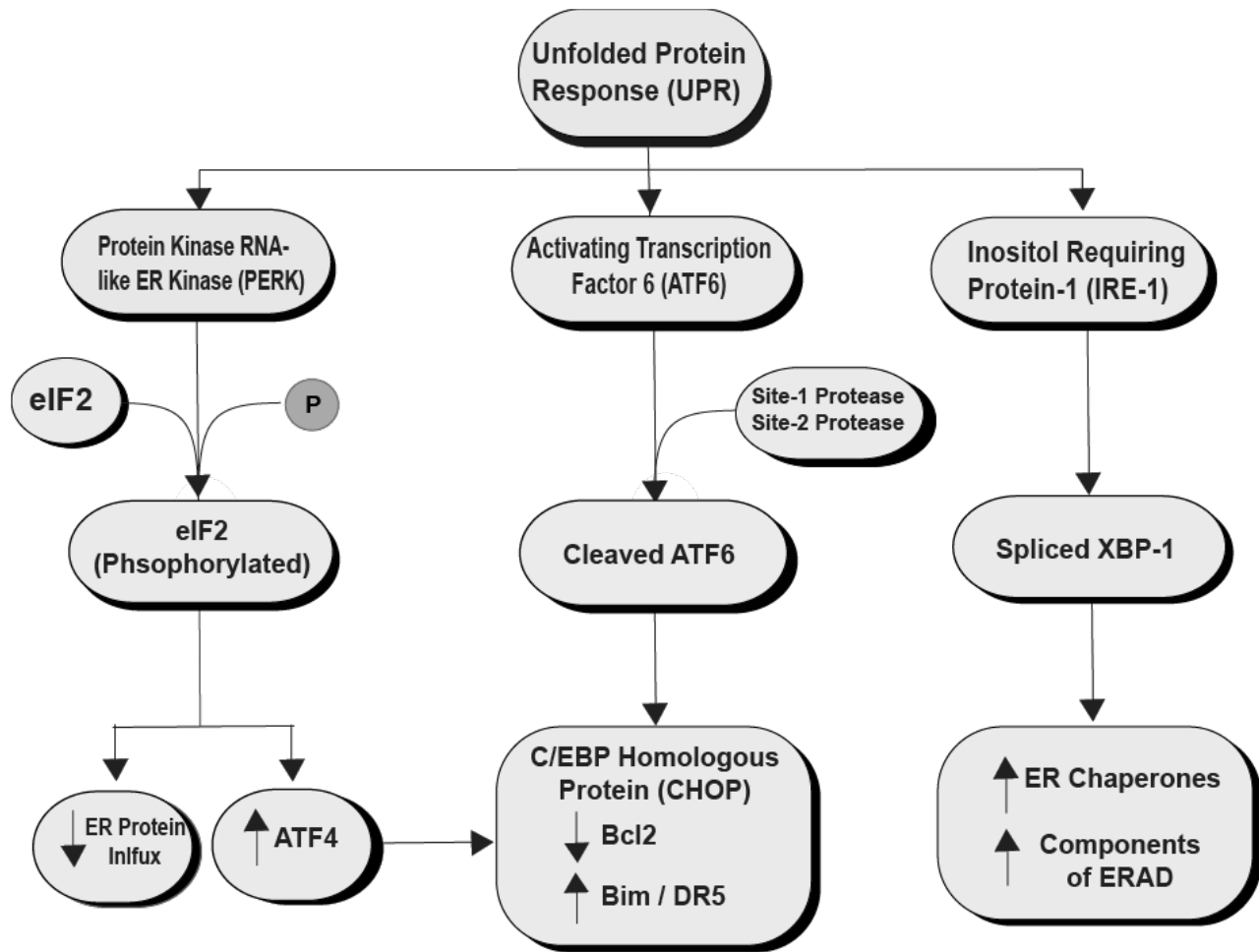


Figure 4. Pathways involved in the UPR.

Mitogen-activated protein kinases (MAPKs) such as the extracellular signal-regulated kinases (ERK1/2 or p42/44MAPK), the c-Jun N-terminal kinases (JNK1/2), and p38MAPK have been shown to be activated in response to ROS (Matsuzawa & Ichijo, 2008; Robinson & Cobb, 1997). The ERK1/2 cascade is activated in response to mitogenic and survival stimuli, whereas JNK1/2 and p38MAPK pathways are stimulated in response to cellular stresses including oxidative agents, hypoxia, UV radiation, and pro-inflammatory cytokines (Ichijo, 1999; Ip & Davis, 1998). Previous studies have shown that renal epithelial cell exposure to RCM results in activation of the intrinsic apoptotic pathway (Romano et al., 2008). An extensive study

performed by Quintavalle et al. demonstrated the role of stress kinases in the activation of this pathway. MDCK cells were exposed to 50, 100, or 200 mg I/mL iobitridol, iopamidol, or iodixanol for 3 hours to determine the effect of RCM on stress kinases. Each of the tested RCM induced a dose-dependent increase in phosphorylated JNK and p38MAPK within 1 hour, indicating that exposure to RCM does induce activation of the pro-apoptotic stress kinases. The role of JNK and p38MAPK were verified in two methods: pretreating the MDCK cells with the p38 inhibitor SB203580 or transfecting MDCK cells with kinase-dead mutants for p38 or JNK. MDCK cells pretreated with SB203580 or transfected with kinase-dead mutants were completely protected from apoptotic effects of all three RCM verifying the role of stress kinases in CI-AKI (Quintavalle et al., 2011). Another study confirming Quintavalle's findings demonstrated that pretreating HK-2 cells with JNK inhibitor SP600125 or p38 inhibitor SP283580 significantly decreased cleaved caspase-3 activation and increased pro-survival protein bcl-2 after exposure to 200 mg I/mL iopamidol (X. He et al., 2016). A more recent study on LLC-PK1 cells determined that 25 mg I/mL of iodixanol will induce increases in activated p38MAPK, JNK, and ERK after 24 hours of exposure (Lee et al., 2018).

Additional kinases important to cellular survival that are affected by RCM exposure include protein kinase B (Akt), PTEN-induced putative kinase (PINK1), Rho-associated protein kinase (ROCK), Janus kinases (JAK) and signal transducer and activator of transcription proteins (STATs). A study performed by Xie et al. on the effects of ioversol on HK-2 cells indicated that a 30 minute exposure to 100 mg/ml of ioversol significantly decreases the presence of phosphorylated Akt while simultaneously inducing caspase-3 cleavage and apoptosis (Xie et al., 2017). This discovery demonstrates that the phosphoinositide-3 kinase (PI3)/Akt pathway may play a role in cellular fate after exposure to RCM. Renal tissues extracted from male Sprague-

Dawley rats that were exposed to 12.25 g I/kg iohexol demonstrated a significant increase of PINK1 (X. Yang et al., 2018). Activation of PINK1 indicates an increase in mitophagy resulting in decreased ATP production and energy failure. ROCK plays an important role in various cellular processes including: cell adhesion, migration, proliferation, cytokine activation, inflammatory cell migration, smooth muscle cell contraction and cell cycle regulation. Inhibition of Rho-ROCK pathways has been shown to diminish CI-AKI *in vivo* (Su et al., 2014; Wang et al., 2018); however, the relationship of CI-AKI and ROCK has not been explored *in vitro*. The role of JAK-STAT pathway was determined in a study performed by Yokomaku et al. Pretreating male Sprague-Dawley rats or LLC-PK1 cells with asialoerythropoietin or erythropoietin activated JAK2 and STAT5 and attenuated ioversol-induced nephropathy or cellular injury indicating that the JAK-STAT pathway may play a role in CI-AKI (Yokomaku et al., 2008).

Calcium overload within renal parenchyma is also thought to play a role in CI-AKI via ROS overproduction, p38 MAPK activation, and endothelin activation and release (Duan et al., 2000; Humes et al., 1987; Jin et al., 2015; Schick, Bangert, Kubler, & Haller, 2002; D. Yang & Yang, 2013). However, the initial source of intracellular calcium overload has not been fully elucidated and could result from ER or mitochondrial dysfunction, inhibition of the Na/K-ATPase, or changes in function of the Na/Ca exchanger system (Krebs, Agellon, & Michalak, 2015; D. Yang & Yang, 2013; D. Yang, Yang, Jia, & Ding, 2013).

INTERVENTIONS FOR CYTOTOXICITY BY HYDRATION, DRUGS, AND NATURAL PRODUCTS

Adequate hydration is the gold standard for prevention of CI-AKI. The rationale is that forced or adequate hydration induces an expansion of intravascular volume, suppression of renin-angiotensin cascade, reduction of renal vasoconstriction and hypoperfusion, and increases

urine output (Andreucci, Faga, et al., 2014). Higher urine output is associated with a lower incidence of CI-AKI due to the decreased time of tubular RCM exposure (Solomon & Dauerman, 2010). Unfortunately, high infusion rates or increased total extracellular volumes can result in a volume overload and initiate pulmonary edema in patients with preexisting cardiac impairment (S. Q. Chen et al., 2018). Due to the considerable dissent in the medical community pertaining to acceptable preventative measures for CI-AKI, substantial research has gone into finding a potential nephroprotective agent.

The most explored strategy in the prevention of CI-AKI is the use of antioxidants to decrease contrast-induced oxidative stress. Common antioxidants have been studied including N-acetylcysteine (NAC), ascorbic acid, and α - γ -tocopherol. *In vitro* studies have provided consistent results for protection by NAC. A study performed by Romano et al. demonstrated the protective effects of NAC on LLC-PK1, MDCK, and human embryonic kidney cells (HEK-293) against IOCM and LOCM. At a concentration of 200 mg I/mL of iobitridol and iodixanol and an incubation time of 3 hours, pre-treatment with NAC protected the three cell lines from RCM-induced apoptosis in a dose dependent manner (Romano et al., 2008). Yang et al. demonstrated that NRK-52E cells pretreated with low concentration NAC (10 mmol/L) before being exposed to 50, 100, and 150 mg I/mL of iopromide for 4 hours significantly decreased early stage apoptosis as seen by Annexin V and propidium iodide (PI) staining (Y. Yang et al., 2014). The Romano et al. study mentioned above also examined the protective effects of ascorbic acid (vitamin C) *in vitro*. The authors demonstrated that a 2 hour pretreatment with ascorbic acid prevented high concentration IOCM- and LOCM-induced apoptosis in a dose-dependent fashion; however, NAC was more effective than ascorbic acid at preventing RCM-induced cytotoxicity

(Romano et al., 2008). Unfortunately, the protective effects of α -/ γ -tocopherol on CI-AKI have not been studied *in vitro*.

Although certain antioxidants have shown to be protective against CI-AKI *in vitro*, the results from a clinical standpoint are inconclusive. Numerous clinical studies have shown NAC to be a potentially effective strategy for the prevention of CI-AKI (Briguori et al., 2007; Briguori et al., 2004; Tepel et al., 2000); other studies have concluded that NAC alone or in combination with ascorbic acid was not beneficial to patients (Palli et al., 2017; Yeganehkah et al., 2014). Further studies are needed to evaluate the long-term clinical benefits in patients as a study in over 5000 patients concluded that acetylcysteine was not beneficial when evaluating outcomes 90 days after angiography in high renal risk patients (Weisbord et al., 2018). Antioxidant vitamins α -/ γ -tocopherol (Vitamin E) have also been shown to be useful in the prevention of CI-AKI in a clinical setting (Briguori et al., 2007; Spargias et al., 2004; Tasanarong, Vohakiat, Hutayanon, & Piyayotai, 2013). A study performed by Kongkham et al. on male Sprague-Dawley rats demonstrated that pretreatment with 250 or 500 mg Vitamin E prior to induction of CI-AKI with 1.6 g I/kg iopromide significantly decreased tubular necrosis, PT cell congestion, and interstitial edema while simultaneously increasing total antioxidant capacity and MnSOD activity when compared to non-pretreated rats (Kongkham, Sriwong, & Tasanarong, 2013).

HMG-CoA reductase inhibitors, or statins, are a class of lipid lowering medications specifically used in the treatment of cardiovascular disease. Statins are thought to protect against RCM cytotoxicity by increasing heme oxygenase-1 production and diminishing the activity of NADPH oxidase, resulting in the reduction of ROS formation and oxidative stress induced by RCM (Grosser et al., 2004; Stoll, McCormick, Denning, & Weintraub, 2004). A sole *in vitro* study performed by Quintavalle et al. on the nephroprotective effects of atorvastatin determined

that MDCK and HK-2 cells pretreated with 0.2 μ M atorvastatin for a minimum of 6 hours induced a significant increase in cell viability and subsequent decrease in RCM-induced apoptosis after a 3 hour exposure to 200 mg I/mL iodixanol (Quintavalle et al., 2012). This class of pleiotropic drugs may also be an effective pretreatment in reducing the incidence of CI-AKI as seen by various clinical studies (Jo et al., 2008; Toso et al., 2010; Tropeano et al., 2016).

Pharmacologic agents used primarily for the treatment of hypertension such as nebivolol, ACEIs, and ARBs have garnered some interest in the prevention of CI-AKI. Nebivolol is a third generation β_1 -receptor antagonist that may protect the kidney via its antioxidant and NO-mediated vasodilating properties (Toprak et al., 2008). Toprak et al. determined the efficacy of nebivolol in preventing CI-AKI initially in female Wistar albino rats pretreated with 2 mg/kg of nebivolol once daily for 5 consecutive days prior to administration of 6 ml/kg of diatrizoic acid on the fourth day. Pretreatment with nebivolol resulted in a reduction of tubular necrosis, medullary congestion, and tubular casts, as well as an increase renal NO levels in rats when compared to rats that did not receive nebivolol (Toprak et al., 2008). A more recent study followed the Toprak et al. study design and determined that pretreatment with nebivolol prior to administration of RCM significantly reduced advanced oxidation protein products and malondialdehyde in serum and kidney tissue and increased total serum NO concentration (Koc et al., 2011). The role of the renin-angiotensin-aldosterone system (RAAS) and RAAS-blocking drugs in CI-AKI is controversial. This is due to experimental data suggesting that ACEIs or ARBs protect the kidneys from RCM-induced nephrotoxicity while other claims that RAAS-blocking drugs are nephrotoxic and worsen CI-AKI (Ikeda et al., 2006; Patel, King, & Jovin, 2011; Rosenstock et al., 2008). A large prospective study performed by Holscher et al. evaluated CI-AKI predictors and long-term outcomes of high-risk patients. The authors noted that

decreased eGFR, the use of ACEIs, and post-procedural hemodialysis were independently associated with increased incidence of CI-AKI (Holscher et al., 2008). The overall lack of *in vitro* experimentation pertaining to high blood pressure medications is troubling when compared to the amount of clinical data that has been collected. This is an area where more research is necessary to make an accurate prediction of the possible mechanisms involved.

The administration of naturally derived compounds in the prevention of CI-AKI has shown considerable promise in recent years. Polyphenolic compounds such as resveratrol, salvianolic acid B, epigallocatechin gallate (EGCG), flavonoids compound found in *Artemisia argyi*, the xanthone compound α -mangostin all demonstrated protective effects against CI-AKI *in vitro*. Resveratrol, a compound found in grape skins, significantly reduced HK-2 cytotoxicity induced by ioxithalamate after 48 hour exposure (Huang et al., 2016). Salvianolic acid B, derived from the traditional Chinese medicine Danshen, decreased renal epithelial damage in male Sprague-Dawley rats exposed to iohexol (Tongqiang et al., 2016). In a similar fashion to salvianolic acid B, EGCG, the major antioxidant component of green tea, reduced the damage induced by iopromide in male Sprague-Dawley rats (Z. Gao et al., 2016). A study performed by Lee et al. demonstrated that the flavonoid components of *Artemisia argyi*, also called mugwort, completely prevented the cytotoxic effects induced by iodixanol on LLC-PK1 cells (Lee et al., 2018). A separate study performed by Lee et al. showed that non-toxic concentrations of α -mangostin, found in mangosteen, improved the viability of iodixanol treated LLC-PK1 cells by 90.42% against contrast-induced apoptotic damage (Lee et al., 2016). It is apparent that the nephroprotective effects of certain naturally derived compounds can prevent contrast-induced cytotoxicity both *in vitro* and *in vivo*.

CONCLUSIONS

RCM are non-biologically active compounds necessary for a multitude of diagnostic imaging procedures. Modern RCM induce severe and prolonged vasoconstriction within the renal medulla and are directly toxic to the extremely metabolically-active renal epithelium such as PT cells and the TAL. Exposure to RCM and the consequential epithelial damage results in an increase in ROS and oxidative stress, vacuolization of tubular cells, damage to the mitochondria in the form of decreased respiration and ATP production, perturbations in the protein folding capacity of the ER resulting in activation of the UPR and ER stress, and decreased activity of survival kinases and activation of pro-apoptotic stress kinases. Current measures to ensure the prevention of CI-AKI are lacking and considerable research needs to be invested into *in vitro* studies to determine the source of direct RCM induced cytotoxicity.

CHAPTER 2: GENERAL METHODS, MATERIALS, AND STATEMENT OF HYPOTHESIS

THE HK-2 CELL MODEL

To determine the direct cytotoxicity of DA, a system that is devoid of the renal hemodynamic and inflammatory responses to RCM is necessary. Thanks to doctoral work previously done in our laboratory (Murphy et al., 2017), we had the advantage of having a well-documented *in vitro* model focused on nephrotoxicity to use for my dissertation research. Human kidney 2 (HK-2) cells are an immortalized, noncancerous, human epithelial proximal tubule cell line that maintains biochemical properties and activity similar to human proximal tubules *in situ* (Gunness et al., 2010; Paolicchi et al., 2003; Ryan et al., 1994). HK-2 cells retain functioning organic ion transporters (OAT) 1 and 3, which have been reported to transport DA into proximal tubule cells (Mudge, Berndt, Saunders, & Beattie, 1971) and have been used as a widely accepted model for CI-AKI studies (Haeussler, Riedel, & Keller, 2004; Zager, Johnson, & Hanson, 2003).

HK-2 cells were purchased from the American Type Culture Collection (ATCC, Manassas, VA, CRL-2190) and were cultured according to ATCC guidelines. Cells were grown according to ATCC recommended conditions of keratinocyte-free media with added bovine pituitary extract (50 µg/mL) and recombinant epithelial growth factor (5 ng/mL) purchased from Fisher Scientific (Gibco, Carlsbad, CA, Item No. 17005-042). Cells were grown in a warm, humidified incubator at 37°C with 5% CO₂.

EXPERIMENTAL PROTOCOL

For all experiments, HK-2 cells were plated into T75 flasks, 6 well plates, 96 well plates, or XFe and XFp Culture Miniplates at a cellular density of 1.0×10^6 , 5×10^5 , 37,000, and 1.75×10^5

cells/mL, respectively, and allowed to equilibrate for 48 hr in a warm, humidified incubator set to 37°C with 5% CO₂. Media was subsequently replaced, and cells were treated with a final concentration of 0, 2, 5, 10, 15, 18, 23, 28, or 30 mg I/mL DA for 2, 8, or 24 hr. Due to the fact that preparations of RCM vary based on iodine concentration, manufacturer, and viscosity, units of RCM are conventionally expressed as mg I/mL to maintain iodine dose and bolus compaction in a clinical setting (Faggioni & Gabelloni, 2016). Vehicle control was an equal volume of PBS. The concentrations used are levels of DA that are found within the plasma of a healthy 75 kg man after intravenous administration, depending on procedure. A literature review indicates that the concentrations used in this study are far less than what is currently being used in other mechanistic studies. Some studies use concentrations as high as 150 mg I/mL to induce direct cytotoxicity (Jeong et al., 2018; Y. Yang et al., 2014). Exposing HK-2 cells to a concentration closer to what proximal tubule cells experience *in situ* following an imaging procedure better represents the renal damage observed in a clinical setting.

HK-2 cells were exposed to clinically relevant concentrations of DA for 2, 8, or 24 hr. These time points were decided upon based on the half-life of DA. Theoretically, following administration of RCM, the tubular epithelium of a patient with a GFR > 60 mL/min is exposed to RCM for approximately 8 hr; however, as the viscosity of RCM rises the amount of time the kidney could experience a DA-induced insult can increase for up to 24 hr. Following the exposure period, cells were either collected for trypan blue exclusion, isolation of cellular fractions, protein expression analysis, SOD activity assays, and calpain activity assays or used for MTT assays or Agilent Seahorse cellular energy assays.

GENERAL PROTOCOL FOR WESTERN BLOTTING AND OXYBLOT®

Following the DA exposure period, cells were collected, lysed, and protein levels were determined using the Bradford protein assay (discussed below) (Bradford, 1976). Western blots were performed as follows: 40 µg aliquots of cell lysate were diluted to 25 µl with double distilled H₂O (denoted from this point on as H₂O) followed by the addition of 25 µl reducing sample buffer (RSB). In scenarios where the volume of cell lysate was greater than 25 µL prior to dilution with H₂O, the sample aliquots were placed into microcentrifuge tubes and lyophilized in a vacuum at -107°C. The lyophilized samples were reconstituted in 25 µL H₂O and 25 µL RSB. The samples were then denatured in boiling water for 5 min. After the denaturation step, samples were separated via gel electrophoresis on a 12.5% polyacrylamide gel and transferred to a 0.45 µM nitrocellulose membrane (Bio-Rad; Hercules, CA, Item No. 1620115). MemCode® staining was used to verify transfer of equal protein loading and standardize the densitometry to total protein in each of the lanes. Protein staining was used as an alternative to standard housekeeping proteins such as GAPDH or actin due to more reliable results in toxicological studies (Zhang et al., 2019).

Membranes were then blocked using 1% bovine serum albumin (BSA) or 5% milk dissolved in TBST (10 mM Tris-HCl, 150 mM NaCl, 0.1% Tween-20; pH 8.0) or PBST (8mM Na₂HPO₄, 0.15M NaCl, 2mM KH₂PO₄, 3mM KCl, 0.1% Tween-20; pH 8.0) for 1 hr. All of the antibodies used in the current work can be found in Table 3. The membrane was then washed with TBST or PBST three times for ten min each followed by the addition of secondary antibody. After another round of three washes, the membrane was developed using Amersham ECL Western Blotting Detection Agent (GE Healthcare Life Sciences, Marlborough, MA, Item

No. RPN2232). A BioRad chemic-doc system was used to capture the gel image and used for densitometry analysis (version 4.0.1, Bio-Rad, Hercules, CA, Catalog No. 170-9690).

The OxyBlot® (EMD Millipore; Burlington, MA, Item No. S7150) procedure requires a derivatization step. Protein carbonyls within each sample are derivatized to 2,4-dinitrophenylhydrazine (DNPH) and can then be measured using an antibody that recognizes DNPH.

Table 3. Primary and secondary antibodies used in current work.

	Antibody	Product Number	Manufacturer
Primary Antibodies	GRP78	ab21685	Abcam Inc; Cambridge, MA
	CHOP	5554	Cell Signaling Technology; Danvers, MA
	MnSOD	ab13533	Abcam Inc; Cambridge, MA
	TNF α	ab66579	Abcam Inc; Cambridge, MA
	NOX4	ab60940	Abcam Inc; Cambridge, MA
	4HNE	393207	Calbiochem; Merck, Darmstadt, Germany
	OxyBlot	S7150	EMD Millipore; Burlington, MA
	LC3B	ab48394	Abcam Inc; Cambridge, MA
	Cytochrome c	sc-7159	Santa Cruz Biotechnology; Santa Cruz, CA
	Caspase 3	9662	Cell Signaling Technology; Danvers, MA
	Caspase 4	4450	Cell Signaling Technology; Danvers, MA
Caspase 12	2202	Cell Signaling Technology; Danvers, MA	
Secondary Antibody	Goat Anti-Rabbit HRP	7074	Cell Signaling Technology; Danvers, MA

Selected abbreviations: GRP78 (glucose-regulated protein 78), CHOP (C/EBP homologous protein), MnSOD (manganese superoxide dismutase), TNF α (tumor necrosis factor alpha), NOX4 (NADPH oxidase 4), 4HNE (4-hydroxynonenal), LC3B (microtubule-associated proteins 1A/1B light chain 3B)

Table 3. Primary and secondary antibodies used in current work.

SEAHORSE XFe ASSAYS

The Agilent Seahorse XFe analyzer allows for real-time measurements of cellular metabolic function in cultured cells. Oxygen Consumption Rate (OCR) and Extracellular Acidification Rate (ECAR) are measured to interrogate key cellular functions such as mitochondrial respiration and glycolysis. Mitochondrial function and glycolysis were measured

using Agilent cell mito stress tests, cell glycolysis stress tests, mito fuel flex tests, and real-time ATP rate assays following optimization of cell number per well.

HK-2 cells were cultured in XFe Culture Miniplates (175,000 cells/mL) (Agilent Technologies, Item No. 101085-004) and allowed to grow for 48 hr followed by treatment with vehicle or DA. Prior to the assay, cells were washed with assay media (Agilent Technologies, Santa Clara, CA, Item No. 103575-100) supplemented with 1 mM glucose (Agilent Technologies, Item No. 103577-100), 1 mM pyruvate (Agilent Technologies, Item No. 103578-100), and 2 mM glutamine (Agilent Technologies, Santa Clara, CA, Item No. 103579-100) and equilibrated in 175 or 180 μ L pre-warmed assay media at 37°C devoid of CO₂ for 45 min.

In each assay, three basal OCR/ECAR measurements were taken at three minute intervals using the Seahorse XFe instrument system. Following basal measurements, various probes were injected and additional OCR and ECAR measurements were taken. Oligomycin, an ATP-synthase inhibitor, was used to stimulate glycolysis and the final step of the electron transport chain. Maximal respiration was stimulated by the addition of carbonyl cyanide-4-(trifluoromethoxy)phenylhydrazone (FCCP), an uncoupler of mitochondrial oxidative phosphorylation that moves protons across the mitochondrial inner membrane. The complex I and complex III inhibitors rotenone and antimycin-A, respectively, were used to completely inhibit mitochondrial respiration. The hexokinase inhibitor, 2-deoxyglucose, was used as an inhibitor of glycolysis. The cell mitochondrial stress test (Agilent Technologies, Item No. 103015-100), initially inhibits ATP synthase with an injection of oligomycin (0.5 μ M), FCCP (0.5 μ M), followed by complete inhibition of the electron transport chain by injection of a mixture of rotenone/antimycin-A (0.5 μ M) and mitochondrial function was assessed by continuous measurement of OCR (Figure 5). Preliminary studies for FCCP indicated a final

concentration of 0.5 μM was optimal. The cell glycolysis stress test (Agilent Technologies, Item No.103020-100), utilizes glucose (10 mM), oligomycin (1 μM), and 2-DG (50 mM) followed by continuous OCR and ECAR measurements to assess parameters of glycolysis. The real-time ATP rate assay (Agilent Technologies, Item No. 103592-100), uses serial injections of oligomycin (1.5 μM) and a mixture of rotenone/antimycin-A (0.5 μM) followed by continuous OCR and ECAR measurements to assess total ATP, mitochondrial-linked ATP, and glycolysis-linked ATP production. The mito fuel flex test (Agilent Technologies, Item No. 103260-100), utilizes UK5099, BPTES, and Etomoxir injections followed by continuous OCR measurements to determine mitochondrial fuel source oxidation. Following each assay, cells were washed with 200 μL PBS and lysed. Total number of cells were measured using the CyQUANT Cell Proliferation Kit (Invitrogen, Carlsbad, CA, Item No. C7026). Results were normalized to number of cells and analyzed using Wave Software (Agilent Technologies, Wave for Desktop, Version 2.5.0.6).

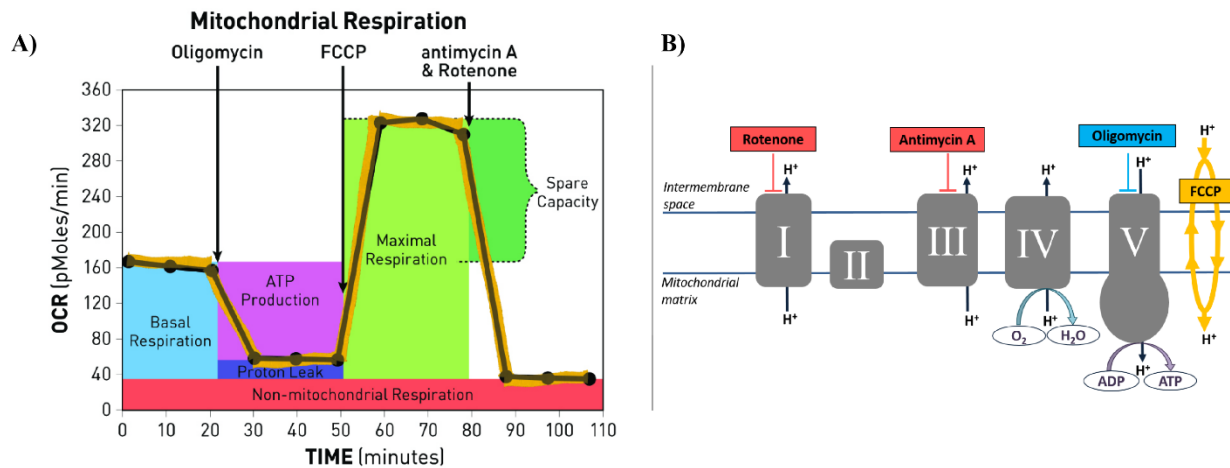


Figure 5. Agilent Seahorse XF cell mito stress test profile and electron transport chain. Key parameters of mitochondrial function shown by the Agilent Seahorse cell mito stress test profile (A). Effects of the cell mito stress test modulators on the electron transport chain (B).

https://www.agilent.com/cs/library/usermanuals/public/XF_Cell_Mito_Stress_Test_Kit_User_Guide.pdf

CELL AND PROTEIN NORMALIZATION

Protein concentration in cell lysates, mitochondrial fractions, and SOD activity assays were determined using the Bradford assay (Bradford, 1976). A 5 or 11 μL aliquot of cell lysate or mitochondrial lysate was diluted with 45 or 11 μL ddH₂O, respectively. An aliquot of 16 μL of lysate mixture was then mixed with 784 μL Coomassie Blue, and a 200 μL aliquot was pipetted into a 96-well plate in triplicate. Protein concentration was then determined by comparing the absorbance of the samples to the absorbances of a standard curve using 100, 200, 400, and 600 mg/mL BSA in H₂O. Western blots, OxyBlots, and SOD activity assays were normalized using constant loading concentrations and volumes.

Agilent Seahorse and calpain activity assays were normalized using CyQUANT® Direct Cell Proliferation Assay (ThermoFisher Scientific). Immediately following the completion of a specific Seahorse assay, the media was removed via aspiration and the Culture Miniplate was stored in a -80°C freezer overnight. The CyQUANT assay utilizes CyQUANT GR dye which produces a large fluorescence enhancement upon binding to cellular nucleic acids that can be measured using standard fluorescein excitation (485 nm) and emission (530 nm) wavelengths. The fluorescence emission of the dye-nucleic acid complexes correlated linearly with cell number over a large range using a wide variety of cell types (Jones et al., 2001).

STATISTICAL ANALYSIS

All values are reported as mean \pm SEM with at least 3 independent experiments conducted from at least 2 biological replicates. Differences between groups were determined with a one-way or two-way ANOVA followed by a Holm–Sidak post-hoc test (GraphPad Prism, GraphPad Software Inc., San Diego, CA). Significant differences were assessed using $\alpha = 0.05$.

STATEMENT OF HYPOTHESIS

Previously published studies have demonstrated that DA induces direct toxicity to proximal tubule epithelial cells (Huang et al., 2016; P. A. Peng et al., 2015). The purpose of my dissertation was to investigate the initial mechanisms of toxicity at clinically relevant DA concentrations which could provide a foundation for future studies to explore potential methods to mitigate or prevent CI-AKI. In order to determine these mechanisms, the following hypotheses were tested: exposure to DA decreases mitochondrial and cell viability of HK-2 cells at clinically relevant concentrations; the mechanism of this toxicity is caused by calcium dysregulation, mitochondrial degeneration, and oxidative stress; decreasing intracellular calcium mitigates DA induced cytotoxicity (Figure 6).

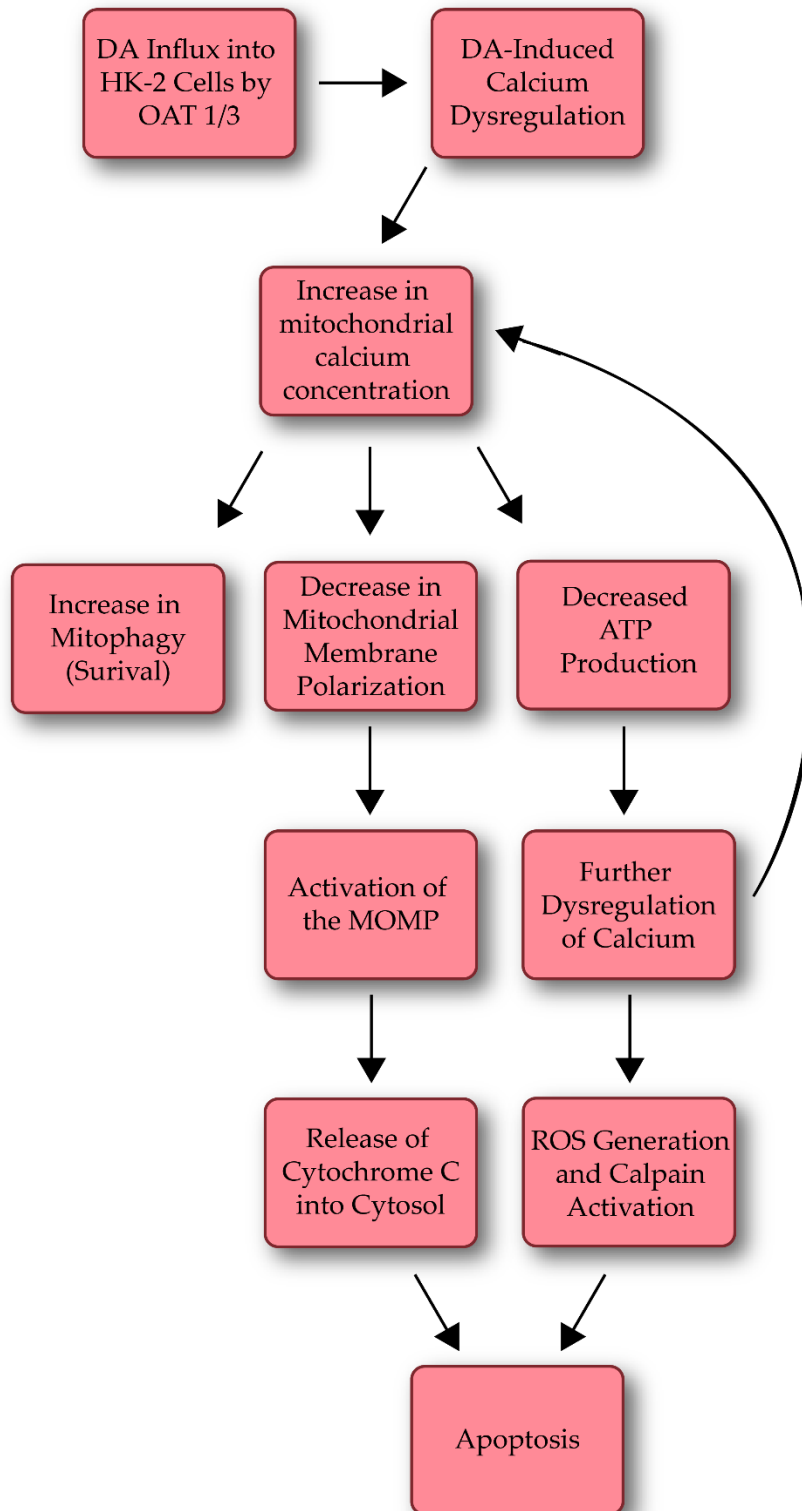


Figure 6. Hypothesized sequence of events following exposure of HK-2 cells to DA.

CHAPTER 3: RADIOCONTRAST AGENT DIATRIZOIC ACID INDUCES MITOPHAGY AND OXIDATIVE STRESS VIA CALCIUM DYSREGULATION

A portion of this chapter was submitted as a manuscript to the *International Journal of Molecular Sciences* in the Special Nephrotoxicity Issue.

Ward, D. B., Brown, K. C., and M. A. Valentovic (2019).

“Radiocontrast Agent Diatrizoic Acid Induces Mitophagy and Oxidative Stress Via Calcium Dysregulation.”

Reprinting for dissertation is part of the author’s rights and permission is not required from the Multidisciplinary Digital Publishing Institute (MDPI), the copyright holder.

Dakota B. Ward*, Kathleen C. Brown*, Monica A. Valentovic*¹

*Department of Biomedical Sciences, Joan C. Edwards School of Medicine, Marshall University, Huntington, WV 25755

¹Correspondence should be addressed to: Department of Biomedical Sciences; 1 John Marshall Drive, Joan C. Edwards School of Medicine, Marshall University, Huntington, WV, 25755.

Phone (307-696-7332) Fax (304-696-7391) Email: valentov@marshall.edu

ABSTRACT

Contrast-Induced Acute Kidney Injury (CI-AKI) is the third most common cause of hospital associated kidney damage. Potential mechanisms of CI-AKI may involve diminished renal hemodynamics, inflammatory responses, and direct cytotoxicity. The hypothesis for this study is that diatrizoic acid (DA) induces direct cytotoxicity to human proximal tubule (HK-2) cells via calcium dysregulation, mitochondrial dysfunction, and oxidative stress. HK-2 cells were exposed to 0-30 mg I/mL DA or vehicle for 2-24 h. MTT conversion and trypan blue exclusion indicated a decrease in mitochondrial and cell viability within 2 and 24 h, respectively. Mitochondrial dysfunction was apparent within 8 h post exposure to 15 mg I/mL DA as shown by cell mito and glycolysis stress tests. Mitophagy was increased at 8 h by 15 mg I/mL DA as confirmed by elevated LC3BII/I expression ratio. HK-2 cells pretreated with calcium level modulators BAPTA-AM, EGTA, or 2-aminophenyl borinate abrogated DA-induced mitochondrial damage. DA increased oxidative stress biomarkers of protein carbonylation and 4-hydroxynonenol (4-HNE) adduct formation. Caspase 3 and 12 activation was induced by DA compared to vehicle at 24 h. These studies indicate that clinically relevant concentrations of DA impair HK-2 cells by dysregulating calcium, inducing mitochondrial turnover and oxidative stress, and activating apoptosis.

INTRODUCTION

The use of iodinated radiocontrast media (RCM) to visualize internal structures during diagnostic procedures has increased exponentially since their first use in 1928. Exposure to RCM may lead to contrast-induced acute kidney injury (CI-AKI) which occurs in up to 30% of patients and is the third leading cause of iatrogenic acute renal failure accounting for 10-25% of all AKI cases (Fahling, Seeliger, Patzak, & Persson, 2017). Following X-ray based imaging procedures

such as percutaneous coronary intervention and cardiac angiography, renal dysfunction can range from non-symptomatic increases in serum creatinine (SCr) to severe and permanent renal damage resulting in the need for dialysis (Brown et al., 2016). The renal pathogenesis of CI-AKI is complex and not completely understood. Intravenous administration of RCM induces transient vasodilation of renal vasculature followed by severe, sustained vasoconstriction resulting in decreased oxygen supply and oxidative damage to the outer renal medulla (Z. Z. Liu et al., 2012; Persson et al., 2005). Aside from the renal ischemia, exposure to RCM has been shown to be directly toxic to renal parenchyma (Huang et al., 2016; Itoh et al., 2006; Jeong et al., 2018); however, the exact mechanisms of direct cytotoxicity have not been fully elucidated.

Numerous studies using very high concentrations of RCM have been performed to evaluate direct toxicity of RCM within the proximal tubule (PT). Commonly reported responses to the interaction between very high concentrations RCM and the PT *in vitro* are vacuolization of the PT cells, increased production of ROS and induction of oxidative stress, mitochondrial dysfunction and the ensuing decline in ATP production and energy failure, activation of the unfolded protein response (UPR) and endoplasmic reticulum (ER) stress, and alterations in activity of stress kinases (Andersen et al., 1994; Andersen et al., 1995; Michael et al., 2014; Tervahartiala et al., 1997; Tervahartiala et al., 1991). Although there has been substantial knowledge obtained from these studies, the initial source of cellular damage remains elusive. This may be, in part, due to the clear majority of mechanistic studies using concentrations of RCM far higher than what PT cells experience in the healthy kidney. Studies commonly use 100-200 mg I/mL RCM *in vitro*, equating to approximately 5-100 times concentrations found in circulating plasma (Ho, Nelson, & Delong, 2007; Thomsen & Morcos, 2000). It is possible that

exposing cells to concentrations of RCM of this magnitude are inducing changes in cellular homeostasis that would not occur at clinically relevant concentrations of RCM.

The purpose of this study was to explore the various mechanisms of toxicity associated with the first generation RCM diatrizoic acid (DA) in a human kidney (HK-2) cell line. This model was chosen as these cells are adult, non-cancerous, immortalized human epithelial cells that maintain biochemical properties and activities similar to *in vivo* proximal tubule cells (Gunness et al., 2010; Paolicchi et al., 2003; Ryan et al., 1994). Additionally, HK-2 cells maintain organic ion transporters (OAT) 1 and 3, which have been reported to transport DA into proximal tubule cells (Mudge et al., 1971). The present study was undertaken to demonstrate that exposure of HK-2 cells to clinically relevant DA concentrations induce mitochondrial dysfunction, cytokine release and downstream activity, activate the UPR and ER stress, induce oxidative stress. This study also determines the role of calcium homeostasis in RCM-induced PT cytotoxicity.

METHODS

Chemicals and Reagents

DA (S4506-50G), MTT (M2128-10G, and SOD activity kits (19160) were purchased from Sigma Aldrich (St. Louis, MO) and were used for all studies. The vehicle used for cell treatments was phosphate buffered saline (PBS) purchased from Fisher Scientific (Gibco, Pittsburg, PA, Item No. 14175-095). All other chemicals were of the highest quality and procured from Sigma Aldrich or Fisher Scientific Inc. Antibodies were purchased as indicated in the sections below. The OxyBlot™ Protein Oxidation Detection Kit was purchased from EMD Millipore (Burlington, MA, Item No. S7150).

Cell Line and Diatrizoic Acid (DA) Treatment

Non-cancerous human immortalized kidney epithelial cells (HK-2) were purchased from the American Type Culture Collection (ATCC, Manassas, VA, Item No. CRL-2190) and were cultured according to ATCC guidelines. Cells were grown in keratinocyte-free media with added bovine pituitary extract (50 µg/mL) and recombinant epithelial growth factor (5 ng/mL) purchased from Fisher Scientific (Gibco, Carlsbad, CA, Item No. 17005-042). Cells were grown in a warm, humidified incubator set to 37°C with 5% CO₂. HK-2 cells were plated into six-well cell culture plates (Corning, Sigma Aldrich Item No. CLS3516) at a cellular density of 750,000 cells/mL and allowed to grow for 48 hr. Media was subsequently replaced and cells were treated with a final concentration of 0, 2, 5, 10, 15, 18, 23, 28, or 30 mg I/mL DA for 2, 8, or 24 hr prior to cell lysate collection. Vehicle control was an equal volume of PBS. Following the treatment period, media was removed via aspiration and cells were collected using Trypsin-EDTA (0.25%) (Gibco, Carlsbad, CA, Item No. 25200-072) for sample analysis.

Mitochondrial and Cell Viability

HK-2 cells were plated into 96-well cell culture plates (Cyto One Scientific, Ocala, FL, Item No. CC7682-7596) at a cellular density of 37,500 cells/mL and allowed to grow for 48 hr. Following the equilibration period, media was replaced, and cells were treated with a final concentration of 0, 2, 5, 10, 15, 18, 23, 28, or 30 mg I/mL DA for 2, 8, or 24 hr. Vehicle control was an equal volume of PBS. Mitochondrial viability was assessed using the MTT assay (Humphrey, Cole, Pendergrass, & Kiningham, 2005). The MTT assay relies on the conversion of tetrazolium dye 3-(4,5-dimethylthiazol-2-yl)-2,5-diphenyltetrazolium bromide (MTT) (Sigma Aldrich, Item No. M5655-5X1G) to formazan by mitochondrial oxidoreductases.

Trypan blue exclusion was used as a confirmation that the DA mediated decline in MTT reduction was due to a decrease in mitochondrial viability and not an interaction between DA and mitochondrial reductase enzymes. The trypan blue exclusion assay was run using the Countess II FL cell counter (Thermo Fisher Scientific Inc.) An aliquot of collected cells were diluted 1:1 with 40% w/v trypan blue solution (Sigma Aldrich, Item No. T6146). The solution was lightly mixed via pipetting and a 10 μ L aliquot was transferred to the Cell Countess II FL reusable glass slide prior to inserting the slide into the instruments sample port. The Cell Countess II FL measures total cells, living cells, and dead cells as a measure of overall cell viability.

Mitochondrial Isolation

Mitochondria were isolated from HK-2 cells collected with trypsin-EDTA using a Mitochondrial Isolation Kit for Cultured Cells (Thermo Scientific, Item No. 89874) and differential centrifugation. Mitochondria were isolated according to the manufacturer's directions, with the exception of added protease inhibitor (Thermo Scientific, Item No. 78430) to prevent proteolytic degradation during isolation. Briefly, cells were centrifuged at 2000xg for 10 min at 4°C and resuspended in 800 μ L of Reagent A with added protease inhibitor (10 μ L/mL). Samples were vortexed for five sec at maximum speed and then incubated on ice for 5 min. Following addition of 10 μ L of Reagent B, samples were incubated on ice and vortexed for 5 sec at maximum speed every min for 10 min. Next, 800 μ L of Reagent C with added protease inhibitor (10 μ L/mL) was added, inverted multiple times to mix, and the samples were centrifuged at 700xg for 20 min at 4°C. The supernatant was transferred to new microcentrifuge tubes and centrifuged at 12,000xg for 15 min at 4°C. The supernatant (cytosolic fraction) was transferred to a new microcentrifuge tube and the pellet (mitochondrial fraction) was

resuspended in 100 μ L cell lysis buffer. The cellular and mitochondrial fractions were then placed in a -80°C freezer prior to protein quantification via Bradford assay.

Oxyblot and Western Blot

Western blot analysis was conducted to assess the expression of glucose-regulated protein (GRP78), C/EPB homologous protein (CHOP), 4-hydroxynonenal (4-HNE), manganese superoxide dismutase (MnSOD), NADPH oxidase 4 (NOX4), tumor necrosis factor- α (TNF- α), cytochrome c, caspase 3, caspase 4, and caspase 12. Protein concentration was determined using the Bradford assay (Bradford, 1976). An aliquot of sample containing 40 μ g of protein were placed in microcentrifuge tubes and denatured by placing in boiling water for 5 min followed by separation on a 12.5% polyacrylamide gel via electrophoresis and transferred onto a 0.45 μ M nitrocellulose membrane (Bio-Rad, Hercules, CA, Item No. 1620115). Successful transfer and protein loading were verified using MemCode Reversible Protein Stain Kit (Pierce Biotechnology, Rockford, IL, Item No. PI-24580). Membranes were blocked at room temperature using 5% w/v milk/TBST solution (10 mM Tris-HCl, 150 mM NaCl, 0.1% Tween-20; pH 8.0), 1% Bovine Serum Albumin (BSA)/TBST, or 5% BSA/TBST solution for 1 hr. Membranes were next incubated with continual shaking overnight at 4°C with primary antibodies: GRP78 (1:1000 dilution, Abcam Inc; Cambridge, MA, Item No. ab21685), CHOP (1:1000, Cell Signaling Technology; Danvers, MA, Item No 5554), MnSOD (1:5000, Abcam Inc; Cambridge, MA, Item No. ab13533), TNF α (1:1000, Abcam Inc; Cambridge, MA, Item No. ab66579), NOX4 (1:1000 Abcam Inc; Cambridge, MA, Item No. ab60940), LC3B (1:1000, Abcam Inc; Cambridge, MA, Item No. ab48394), 4-HNE (1:1000 dilution, Calbiochem; Merck, Darmstadt, Germany, Item No. 393207) cytochrome c (1:1000, Santa Cruz Biotechnology, Santa Cruz, CA, Item No. sc-7159), caspase 3 (1:1000, Cell Signaling Technology; Danvers, MA, Item

No. 9662), caspase 4 (1:1000, Cell Signaling Technology; Danvers, MA, Item No. 4450), and caspase 12 (1:1000, Cell Signaling Technology; Danvers, MA, Item No. 2202) in blocking solution. The membranes were washed three times with TBST or PBST for 10 min each followed by incubation with goat anti-rabbit HRP-linked secondary antibodies diluted to 1:2000 in blocking solution for 1.0 to 1.5 hr. Membranes were washed again with TBST or PBST and then developed using Amersham ECL Western Blotting Detection Agent (GE Healthcare Life Sciences, Marlborough, MA, Item No. RPN2232). A BioRad chemi-doc system was used to capture the gel image and used for densitometry analysis (version 4.0.1, Catalog No. 170-9690, BioRad, Hercules, CA).

Aside from 4-HNE protein adduct formation, protein carbonylation is also a marker of oxidative stress. The accumulation of carbonyl groups introduced into cellular proteins was measured using the Oxyblot Protein Oxidation Detection Kit (EMD Millipore, Burlington, MA, Item No. S7150). A 15 μ g aliquot of sample was derivatized as previously described (Terneus et al., 2007). Protein carbonyl moieties on cellular proteins generated by oxidative stress are derivatized in the presence of 2,4-dinitrophenylhydrazine (DNPH) to stable 2,4-dinitrophenylhydrazone groups. The 2,4-dinitrophenylhydrazone groups are recognized by the primary antibody (1:150 dilution in 1% BSA/PBST). A Bio-Rad chemi-doc system was used to capture the gel image and used for densitometry analysis (version 4.0.1, Bio-Rad, Hercules, CA, Catalog No. 170-9690).

Seahorse XF Assays

The Agilent Seahorse XFe analyzer allows for real-time measurements of cellular metabolic function in cultured cells. Oxygen Consumption Rate (OCR) and Extracellular Acidification Rate (ECAR) are measured to interrogate key cellular functions such as

mitochondrial respiration and glycolysis. Mitochondrial function and glycolysis were measured using Agilent cell mito stress tests, cell glycolysis stress tests, mito fuel flex tests, and real-time ATP rate assays following optimization of cell number per well.

HK-2 cells were cultured in XFe Culture Miniplates (175,000 cells/mL) (Agilent Technologies, Item No. 101085-004) and allowed to grow for 48 hr followed by treatment with vehicle or 5, 15, 18, 23, 28, or 30 mg I/mL DA. Prior to the assay, cells were washed with assay media (Agilent Technologies, Item No. 103575-100) supplemented with 1 mM glucose (Agilent Technologies, Item No. 103577-100), 1 mM pyruvate (Agilent Technologies, Item No. 103578-100), and 2 mM glutamine (Agilent Technologies, Santa Clara, CA, Item No. 103579-100) and equilibrated in 175 or 180 μ L pre-warmed assay media at 37°C with no CO₂ for 45 min.

TNF α in Cell Media and Cell Lysate

TNF-alpha is expressed on the surface of renal proximal tubular cells and is activated as part of the inflammatory response within the kidney. TNF α concentrations were measured in cell culture media using an ELISA assay kit (Abcam, Cambridge, MA, USA, Item No. ab181421) per the manufacturer's instructions. Briefly, 50 μ L of collected media and a capture/detector antibody cocktail were added to precoated wells and incubated for 1 hr, shaking at 400 rpm. Following the immunocapture incubation period, the wells were washed and 3,3',5,5'-tetramethylbenzidine (TMB) substrate was added, producing a color change based on the amount of bound TNF α , which was then read at 450 nm. The TNF α concentration was determined using a standard curve. TNF α expression in DA treated cell lysate was determined using Western blot as described above. Each lane was loaded with 40 μ g of protein; membranes were probed using a rabbit-polyclonal HRP-linked antibody for TNF α diluted to 1:1000 in 5% BSA/TBST (Abcam, Item No. ab66579). TNF α was normalized to protein and compared relative to control.

SOD Activity Assay

SOD activity was determined using a Fluka designed spectrophotometric kit purchased from Sigma (St. Louis, MO, Item No. 19160). Cu/Zn-SOD was inhibited by incubating the sample (40 $\mu\text{g}/\mu\text{L}$ cell lysate) at room temperature with sodium diethyldithiocarbamate (DDTC) at a final concentration of 25 mM. The difference between total SOD and MnSOD activity was calculated as a measure of Cu/ZnSOD activity. The assay was completed according to manufacturer's recommendations.

Calcium Assays

MTT assays and cellular fractions were isolated for protein expression following pretreatment with various calcium modulators to analyze the influence of intracellular calcium concentration on mitochondrial viability, mitophagy, and apoptosis. HK-2 cells were pretreated with 10 μM of the intracellular calcium chelator, 1, 2-bis (*o*-aminophenoxy) ethane-*N,N,N',N'*-tetra-acetic acid (BAPTA-AM) (Sigma-Aldrich, Item No. A1076-25MG), 1 mM of extracellular calcium chelator, ethyleneglycol-bis(β -aminoethyl)-*N,N,N',N'*-tetra-acetic acid (EGTA) (Sigma-Aldrich, Item No. E3889-25G), 10 μM of the inositol trisphosphate receptor antagonist, 2-aminoethoxydiphenyl borinate (2-APB) (Sigma-Aldrich, Item No. D9754), or 10 μM of the calpain inhibitor, calpeptin (Sigma-Aldrich, Item No. C8999), for 45 min prior to the addition of DA. HK-2 cells were then incubated for 24 hr with varying concentrations of DA as described above. The calpain activity assay kit was purchased from AnaSpec Inc. (Fremont, CA, Item No. AS-72149) was used to determine the role of calcium in mitophagy and apoptosis. The calpain activity assay was performed in a 96-well plate according to manufacturer's instructions.

Statistical Analysis

Values represent mean \pm SEM with at least 3 independent experiments conducted. Differences between groups were determined with a one-way ANOVA followed by a Holm–Sidak post-hoc test with $\alpha < 0.05$ (GraphPad Prism, GraphPad Software Inc., San Diego, CA).

RESULTS

DA Effects on Mitochondrial and Cell Viability

Conversion of MTT, (3-(4,5-dimethylthiazol-2-yl)-2,5-diphenyltetrazolium bromide), to its insoluble formazan dye counterpart was used as an indicator of mitochondrial viability. DA exposure induced concentration and time dependent changes in MTT (Figure 7). Exposure to DA substantially reduced mitochondrial viability within 2 hr ($p < 0.001$) beginning with the 15 mg I/mL DA when compared to vehicle control. MTT values were diminished at all DA concentrations at 8 hr and 24 hr ($p < 0.001$) when compared to vehicle control (Figure 7). A concentration-dependent decrease in mitochondrial viability was evident at 8 hr and 24 hr when compared to other treatment groups ($p < 0.05$) (Figure 7). A time-dependent decrease in mitochondrial viability was also evident between the 2 hr and 24 hr treatment groups at 23-30 mg I/mL ($p < 0.01$) (Figure 7).

Trypan blue exclusion was used as an indicator of cell viability, as well as confirmation that the DA mediated decline in MTT reduction was not due to a decrease in the overall number of viable cells. Unlike the MTT assay, there was no significant decrease in cell viability until 24 hr exposure to concentrations of 23 mg I/mL DA or higher ($p < 0.05$) (Figure 8). DA final concentrations of 28 and 30 mg I/mL showed an additional decline in cell viability at 24 hr when compared to other treatment groups ($p < 0.05$) (Figure 8). A time-dependent decrease in cell viability was also evident when compared to other time points ($p < 0.01$) (Figure 8).

Concentrations of DA of 15 mg I/mL and 23 mg I/mL decreased the conversion of MTT to formazan within 2 hr and trypan blue exclusion within 24 hr of DA exposure when compared to vehicle control, respectively, suggesting that our model is appropriate to explore the cellular mechanisms of DA-induced cytotoxicity in HK-2 cells.

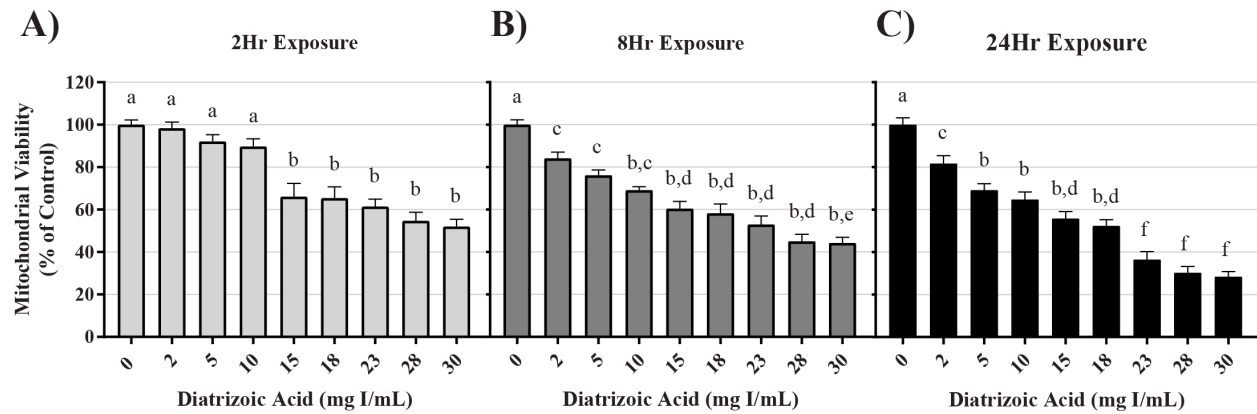


Figure 7. Diatrizoic acid cytotoxic effects on mitochondrial viability in HK-2 cells using MTT. DA diminished mitochondrial viability at 2 hr (A), 8 hr (B), and 24 hr (C). Different superscripts (a-f) indicate a statistical difference between groups across all time points. Statistical difference between time and concentration of each group was determined using Holm-sidak post-hoc test following two-way ANOVA. Values represent mean \pm SEM for three independent experiments of at least 4 biological replicants.

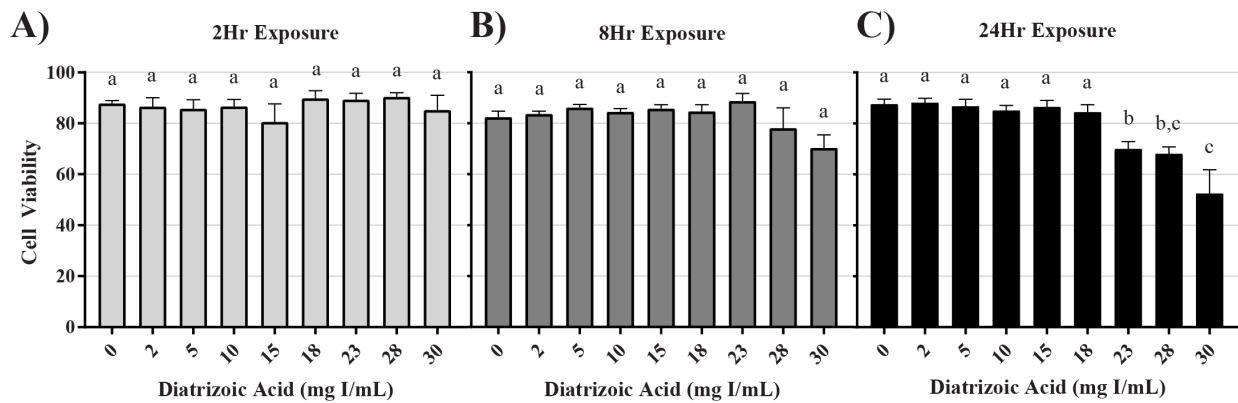


Figure 8. Diatrizoic acid cytotoxic effects on cell viability in HK-2 cells using Trypan Blue Exclusion. DA diminished cell viability at 24 hr (C) but not at 2 hr (A) or 8 hr (B). Different superscripts (a, b, c) indicate a statistical difference between groups across all time points. Statistical difference between time and concentration of each group was determined using Holm-sidak post-hoc test following two-way ANOVA. Values represent mean \pm SEM for three independent experiments of at least 4 biological replicants.

DA Effects on Mitochondrial Function and Energy Utilization

Mitochondrial function following exposure to DA was assessed using an Agilent Seahorse XFe instrument. In an attempt to more accurately understand the effects of DA on mitochondrial function, various XFe assays were utilized including: cell mito stress test, cell glycolysis stress test, mito fuel flex test, and real-time ATP rate assay. In the cell mitochondrial stress test, oxygen consumption rate (OCR) following serial injection of various probes is used as an indicator of mitochondrial function. Oligomycin, an ATP synthase inhibitor, probes for ATP linked oxygen consumption; FCCP, an oxidative phosphorylation uncoupling agent, induces maximum oxygen consumption and the resultant OCR can be used to calculate spare respiratory capacity. The final injection, a mixture of rotenone and antimycin-A, inhibits complex I and complex III resulting in complete inhibition of mitochondrial respiration and determination of the non-mitochondrial oxygen consumption.

Statistically significant decreases in basal OCR, maximal OCR, spare respiratory capacity, and ATP production were evident at 8 and 24 hr (Figure 9). OCR was decreased at 18 mg I/mL for basal OCR ($p < 0.05$), 15 mg I/mL for maximal OCR and spare respiratory capacity ($p < 0.01$), and 23 mg I/mL for ATP production ($p < 0.05$) when compared to vehicle control at 8 hr; however, OCR linked to proton leak and non-mitochondrial oxygen consumption did not change (Figure 9). Basal OCR, maximal OCR, spare respiratory capacity, and ATP production were all significantly decreased at 15 mg I/mL ($p < 0.001$) within 24 hr when compared to vehicle control (Figure 9). Similar to the 8 hr timepoint, there was no change in non-mitochondrial oxygen consumption, although, there was an increase in OCR linked to proton leak at 30 mg I/mL ($p < 0.05$) when compared to vehicle control at 24 hr (Figure 9).

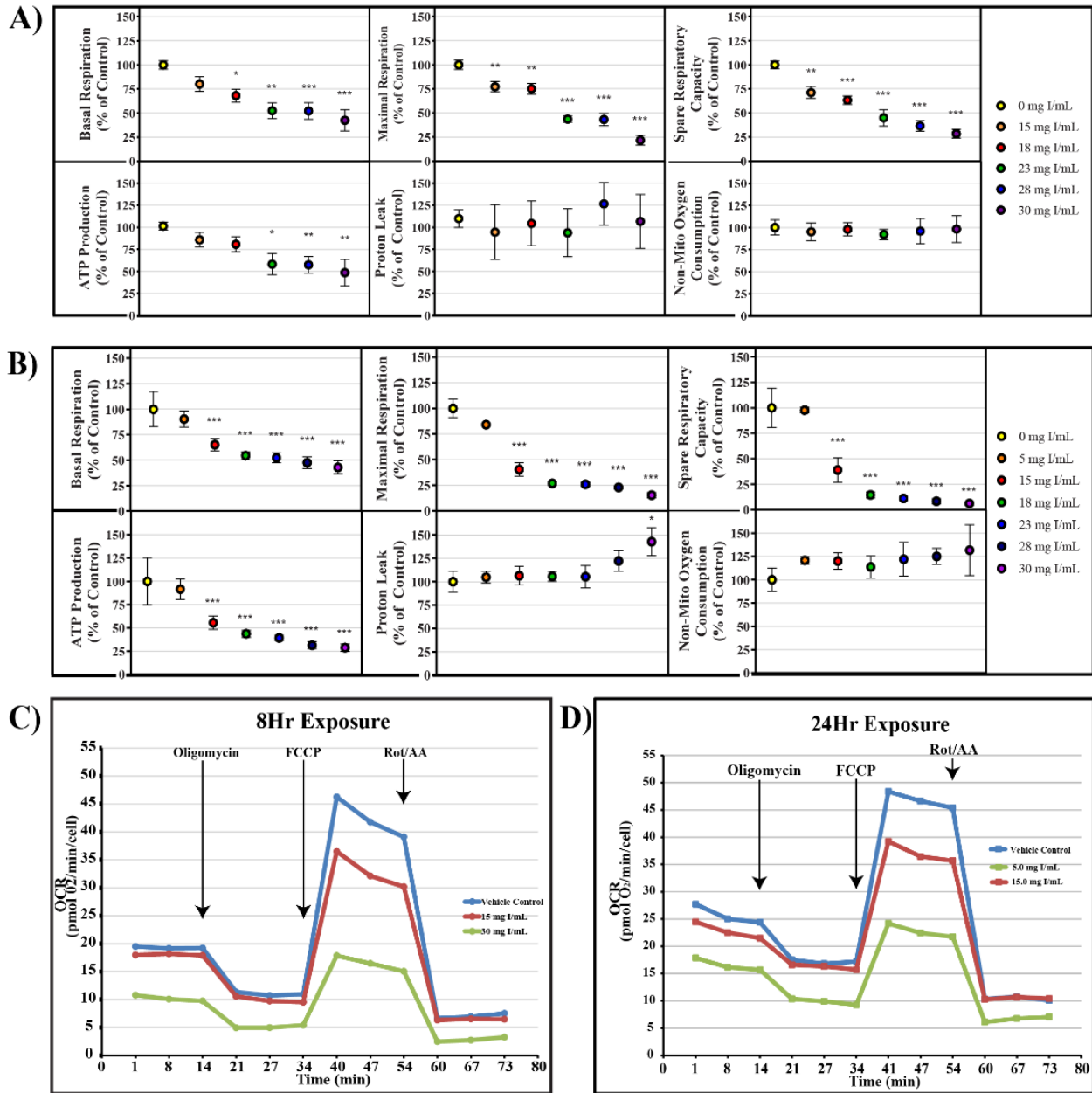


Figure 9. Diatrizoic acid effects on various parameters of mitochondrial respiration in HK-2 cells. DA diminished key parameters of mitochondrial respiration following 8 hr (A) and 24 hr (B) exposure. Representative time course profile of OCR of a Seahorse cell mito stress test following exposure to DA for 8Hr (C) and 24 hr (D). Statistical difference from 0 mg I/mL DA depicted by an asterisk (* $p < 0.05$, ** $p < 0.01$, *** $p < 0.001$). Values represent mean \pm SEM for three independent experiments of at least four biological replicants

The cell glycolysis stress test utilizes extracellular acidification rate (ECAR) as an indicator of various parameters of glycolysis. HK-2 cells were starved of glucose and pyruvate

for 40 min prior to glucose saturation and measurement of basal glycolysis. The ATP synthase inhibitor oligomycin was then injected to drive glycolysis to maximum capacity from which glycolytic capacity and glycolytic reserve can be calculated. ECAR linked to non-glycolytic acidification is determined by the addition of the hexokinase inhibitor, 2-deoxyglucose. Whereas decreases in OCR are evident at 15 mg I/mL at both 8 and 24 hr, statistically significant decreases in glycolysis and glycolytic capacity as shown by ECAR were not apparent until 28 mg I/mL at 8 hr ($p < 0.05$) and 23 mg I/mL at 24 hr ($p < 0.05$) (Figure 10). Glycolytic reserve and non-glycolytic acidification were unchanged for all concentrations at both time points (Figure 10).

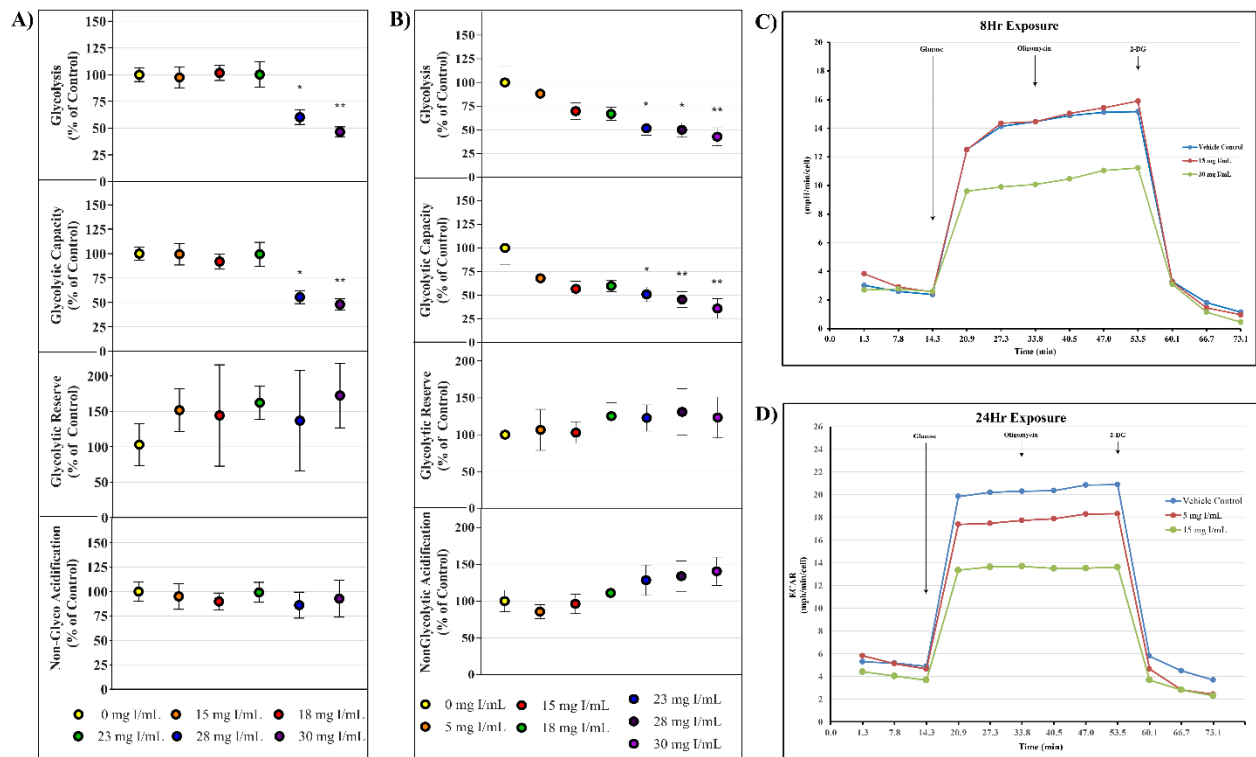


Figure 10. Diatrizoic acid effects on various parameters of glycolysis in HK-2 cells. DA diminished key parameters of glycolysis following 8 hr (A) and 24 hr (B) exposure. Representative time course profile of ECAR of a Seahorse cell glycolytic stress test following exposure to DA for 8 hr (C) and 24 hr (D). Statistical difference from 0 mg I/mL DA depicted by an asterisk (* $p < 0.05$, ** $p < 0.01$). Values represent mean \pm SEM for three independent experiments of at least four biological replicants.

The initial studies examining mitochondrial function indicated DA impaired mitochondrial function prior to alterations in cell viability (Figure 8). Additional independent studies were conducted to probe alterations in mitochondrial function and energy production. The real-time ATP rate assay was used to evaluate DA changes in mitochondrial and glycolytic pathway production of ATP. The real-time ATP assays utilize serial injections of oligomycin and rotenone/antimycin-A to determine ATP production within the cell. OCR, ECAR, and proton efflux rate (PER) measurements are used to calculate total ATP production, glycolytic ATP production, and mitochondrial ATP production. Exposure to DA for 24 hr induced a significant decrease in total and mitochondrial ATP production at 18 mg I/mL ($p < 0.05$) but the slight decrease in glycolytic ATP production was not significant (Figure 11). The findings suggest that the decline in total ATP production, therefore, can be attributed to the decrease in mitochondrial ATP production.

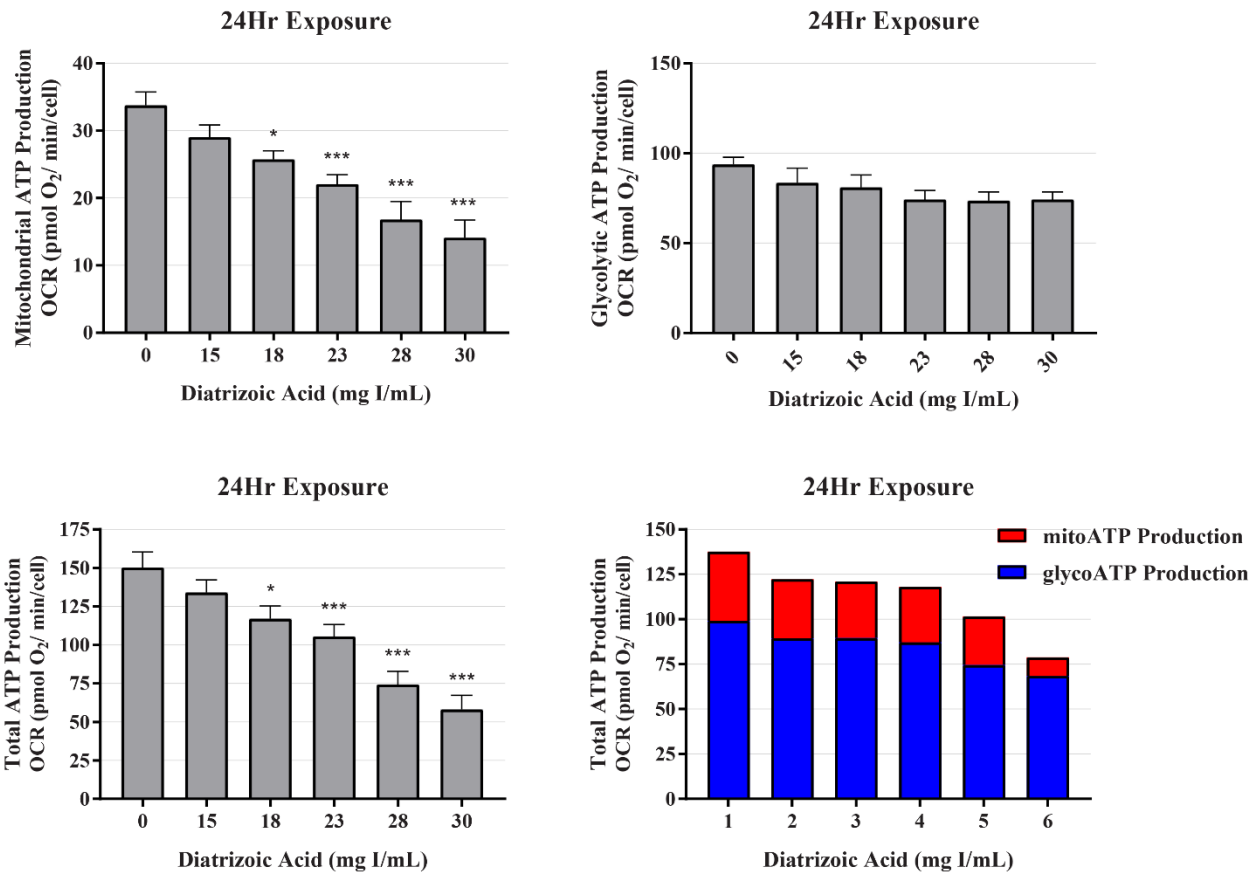


Figure 11. Diatrizoic acid effects on mitochondrial, glycolytic, and total ATP production. DA diminished ATP production linked to mitochondrial respiration (A) and total ATP production (C) but not glycolytic ATP production (B) following 24 hr exposure. Representative graph of ATP production of the real-time ATP rate assay following exposure to DA for 24 hr (D). Statistical difference from 0 mg I/mL DA depicted by an asterisk (* $p < 0.05$, *** $p < 0.001$). Values represent mean \pm SEM for three independent experiments of at least four biological replicants.

The mito fuel flex test measures OCR following inhibition of the three major mitochondrial fuel sources (glucose, glutamine, and fatty acid oxidation) to determine the mitochondrial dependency and flexibility on each fuel source. The mitochondrial dependency on a specific fuel source is determined by first injecting an inhibitor of the pathway in question followed by inhibition of the other two pathways. The flexibility of the mitochondria to adjust to changes in fuel sources is calculated by subtracting the dependency of a fuel source from the mitochondrial capacity of that fuel source. Capacity is determined by first inhibiting the other

fuel pathways followed by the pathway in question. In response to exposure to DA for 8 hr, there was no significant change in the dependency of glutamine, glucose, or fatty acid oxidation (Figure 12). The flexibility to glutamine and glucose oxidation was unchanged as well (Figure 12). These results suggest that DA does not inflict damage to the fuel transport or oxidation machinery within the mitochondria.

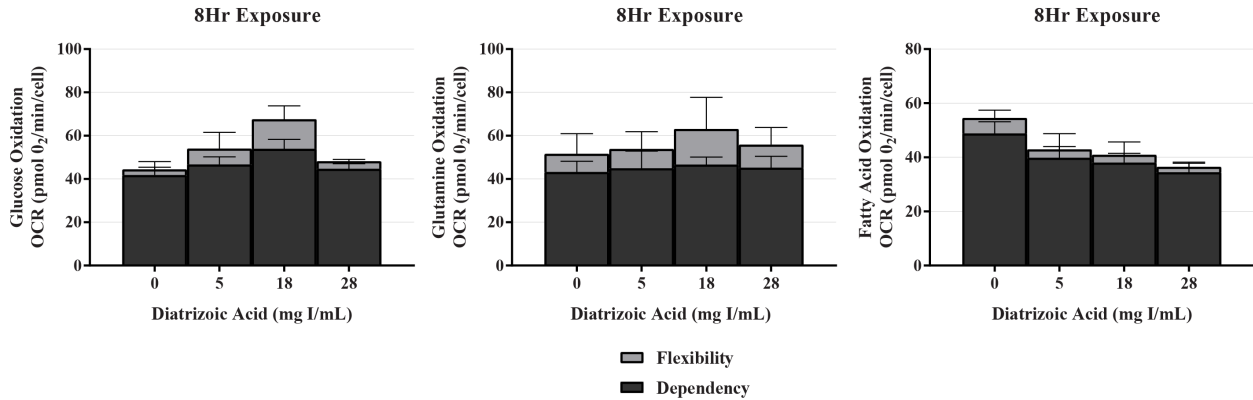


Figure 12. Diatrizoic acid effects on mitochondrial fuel oxidation in HK-2 cells. DA does not affect mitochondrially-linked oxidation of glucose (A), glutamine (B), and fatty acids (C) in response to 8 hr exposure. Values represent mean \pm SEM for three independent experiments of at least four biological replicants.

DA Effects on Mitophagy

A decrease in mitochondrial function in the absence of damage to mitochondrial fuel oxidation can be explained by other means. The global decrease in OCR seen in response to DA could be attributed to a decrease in the total number of active mitochondria. To evaluate the role of exposure to DA on mitochondrial turnover, the expression of microtubule-associated proteins 1A/1B light chain 3B I and II (LC3BI and II) was evaluated. A statistically significant decrease in LC3BI was evident in response to exposure of HK-2 cells to DA within 8 hr at 18 mg I/mL ($p < 0.05$) and at 15 mg I/mL within 24 hr ($p < 0.05$) (Figure 13, Figure 14). An increase in LC3BII expression was not apparent within 8 hr of exposure to DA (Figure 13), however, an increase in LC3BII expression did increase to significance within 24 hr ($p < 0.01$) (Figure 14). The relative

ratio of LC3BII/I was significantly increased ($p < 0.05$, $p < 0.01$) at both time points (Figure 13, Figure 14). These findings suggest that the decrease in OCR observed in the cell mito stress could be due to mitophagy and not damage to the electron transport chain or transport machinery. This conclusion is supported by the results of the mito fuel flex test.

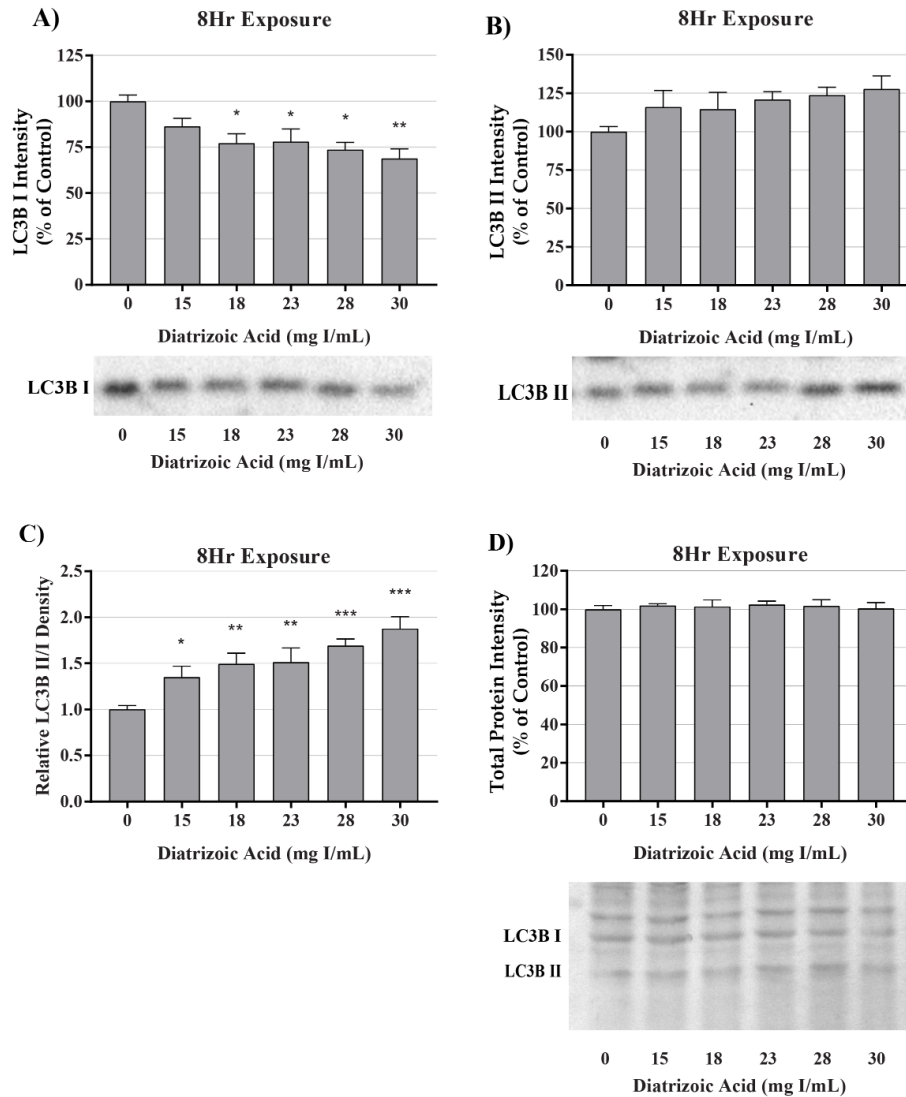


Figure 13. Diatrizoic acid effects on LC3B expression in HK-2 cells following 8 hr exposure. DA induces mitophagy following 8 hr exposure. Representative blots and cumulative densitometry included for LC3BI (A), LC3BII (B) exposure, and LC3BII/LC3B I ratio (C) following 8 hr exposure to DA. Representative blot with Memcode Reversible stain for 40 μ g loaded protein and cumulative protein densitometry depicted for 8 hr (D) exposure. Statistical difference from 0 mg I/mL diatrizoic acid depicted by an asterisk (* $p < 0.05$, ** $p < 0.01$, *** $p < 0.001$). Values represent mean \pm SEM for three independent experiments of two biological replicants.

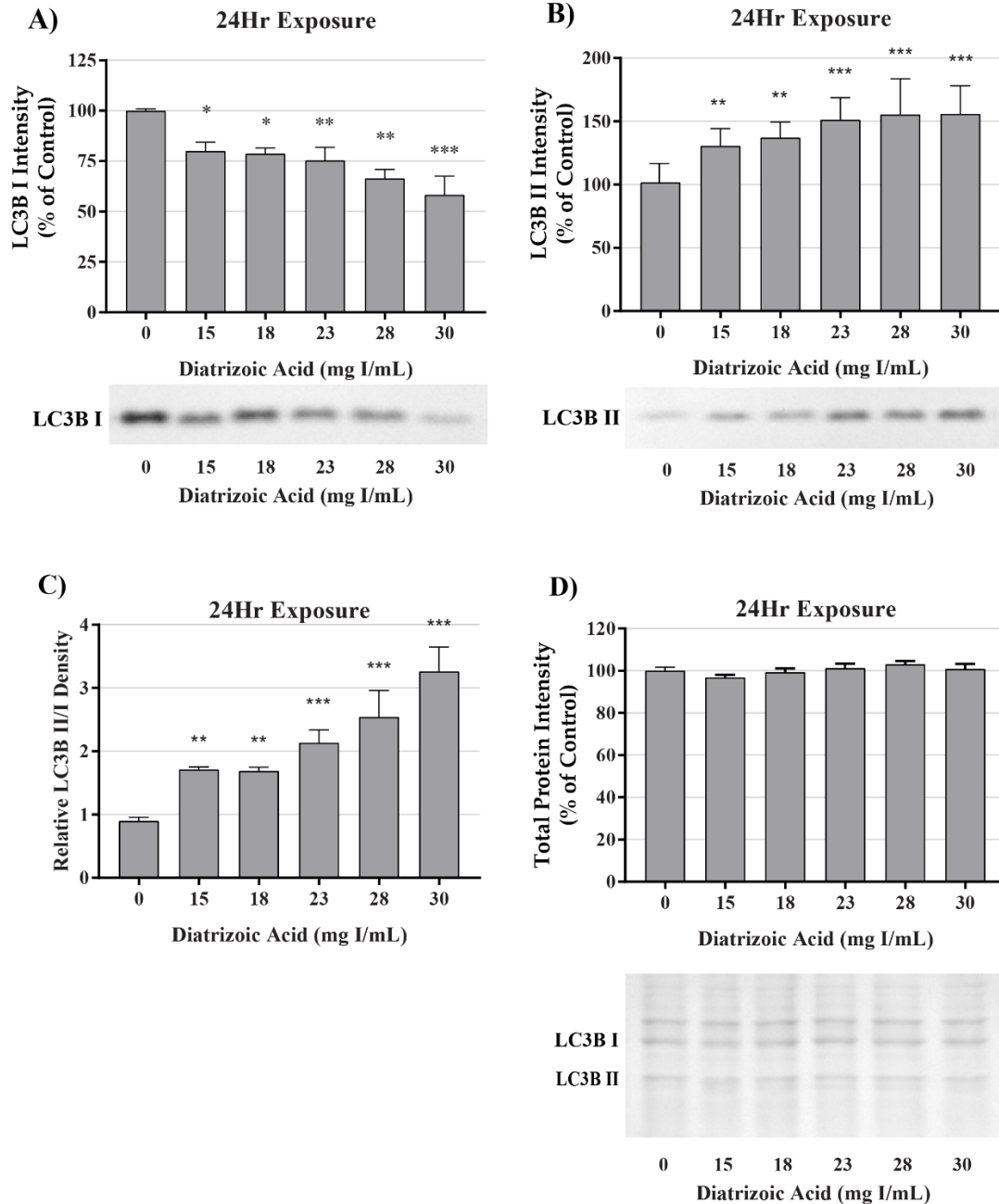


Figure 14. Diatrizoic acid effects on LC3B expression in HK-2 cells following 24 hr exposure. DA induces mitophagy following 24 hr exposure. Representative blots and cumulative densitometry included for LC3BI (A), LC3BII (B) exposure, and LC3BII/LC3BI ratio (C) following 24 hr exposure to DA. Representative blot with Memcode Reversible stain for 40 μ g loaded protein and cumulative protein densitometry depicted for 24 hr (D) exposure. Statistical difference from 0 mg I/mL diatrizoic acid depicted by an asterisk (* $p < 0.05$, ** $p < 0.01$, *** $p < 0.001$). Values represent mean \pm SEM for three independent experiments of two biological replicants.

DA Effects on Endoplasmic Reticulum Stress

Potential mechanisms for DA cytotoxicity to the PT may be mediated by alterations in cell repair and protein folding. To evaluate the role of DA exposure and the induction of the unfolded protein response (UPR) and ER stress, the expression of GRP78, CHOP, and the ER stress specific caspase, caspase-12, were measured via Western blot. No change in GRP78 expression was evident following exposure to DA for 2, 8, and 24 hr (Figure 15). Expression of CHOP, which is increased in response to prolonged activation of the UPR, was not apparent following 8 or 24 hr exposure to DA (Figure 16). Although activation of the UPR and subsequent induction of ER stress was not evident by GRP78 or CHOP expression, there was an increase in caspase 12 at 24 hr (Figure 23) relative to vehicle control ($p < 0.05$). These results suggest that UPR and ER stress do not play a role in DA-induced cytotoxicity and caspase 12 activation is initiated by another pathway.

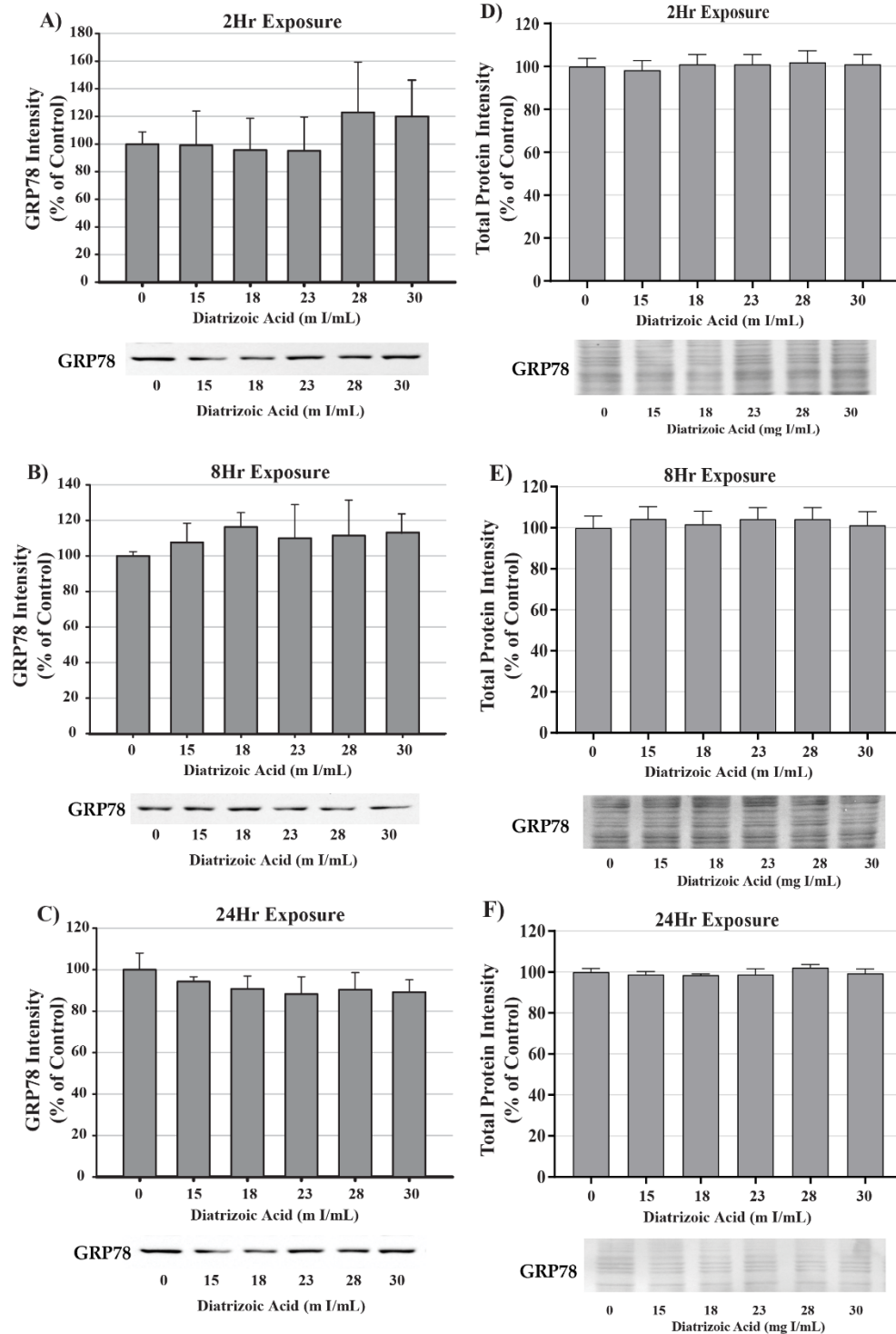


Figure 15. Diatrizoic acid effects on GRP78 expression in HK-2 cells. DA does not activate the UPR. Representative blots and cumulative densitometry included for GRP78 expression following 2 hr (A), 8 hr (B), and 24 hr (C) exposure to DA. Representative blot with Memcode Reversible stain for 40 μ g loaded protein and cumulative protein densitometry depicted for 2 hr (D), 8 hr (E), and 24 hr (F) exposure. Values represent mean \pm SEM for three independent experiments of two biological replicants.

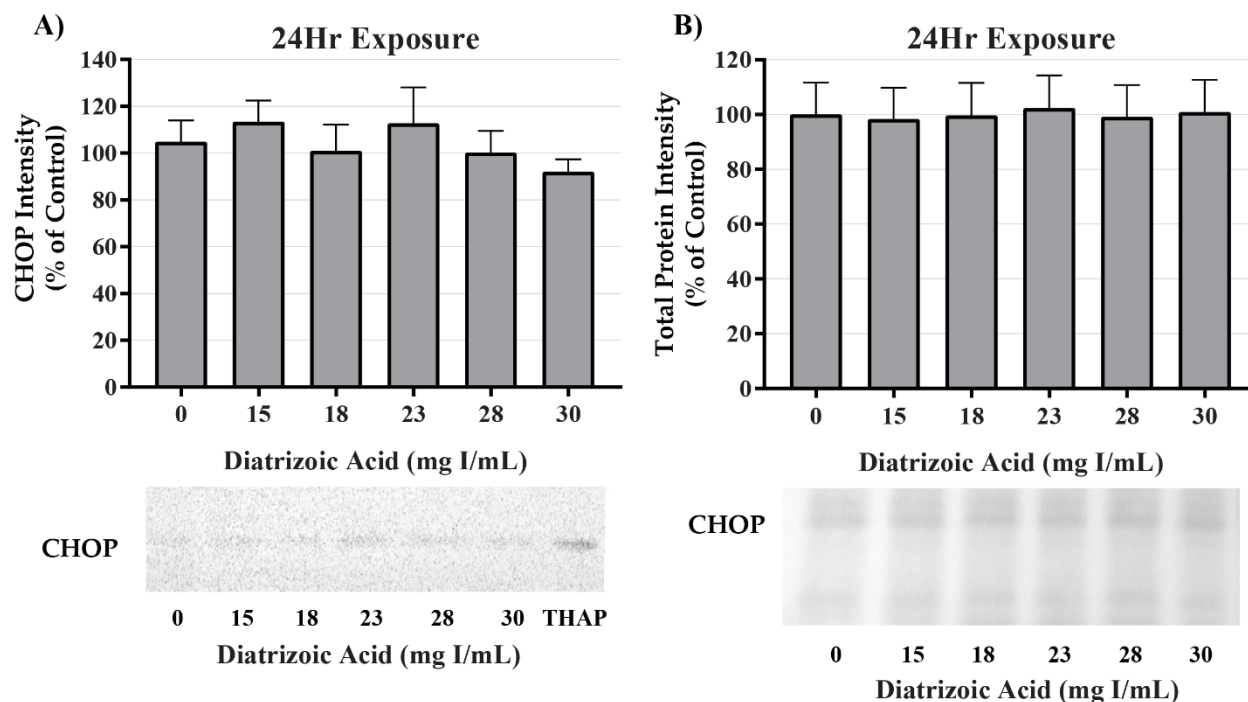


Figure 16. Diatrizoic acid effects on CHOP expression in HK-2 cells. DA does not induce ER stress. Representative blots and cumulative densitometry included for CHOP expression following 24 hr (A) exposure to DA. Representative blot with Memcode Reversible stain for 40 μ g loaded protein and cumulative protein densitometry depicted for 24 hr (B) exposure. Positive control for CHOP expression was thapsigargin, abbreviated THAP. Values represent mean \pm SEM for three independent experiments of two biological replicants.

DA Effects on Oxidative Stress

To evaluate the role of DA exposure and the activation of oxidative stress, protein carbonylation and 4-hydroxynonenal (4-HNE) protein adduct formation were measured via Oxyblot and Western blot, respectively. DA increased oxidative stress as shown by Oxyblot analysis at 24 hr relative to vehicle control in groups treated with 18 mg I/mL DA ($p < 0.05$) (Figure 17). Protein carbonylation was not increased relative to control at 8 hr or at lower concentrations at 24 hr (Figure 17). DA increased oxidative stress as shown by 4-HNE adduct formation at 24 hr relative to vehicle control in groups treated with 18 mg I/mL DA ($p < 0.05$) (Figure 18). 4-HNE protein adduct formation was not increased relative to control at 8 hr or at lower DA concentrations at 24 hr (Figure 18).

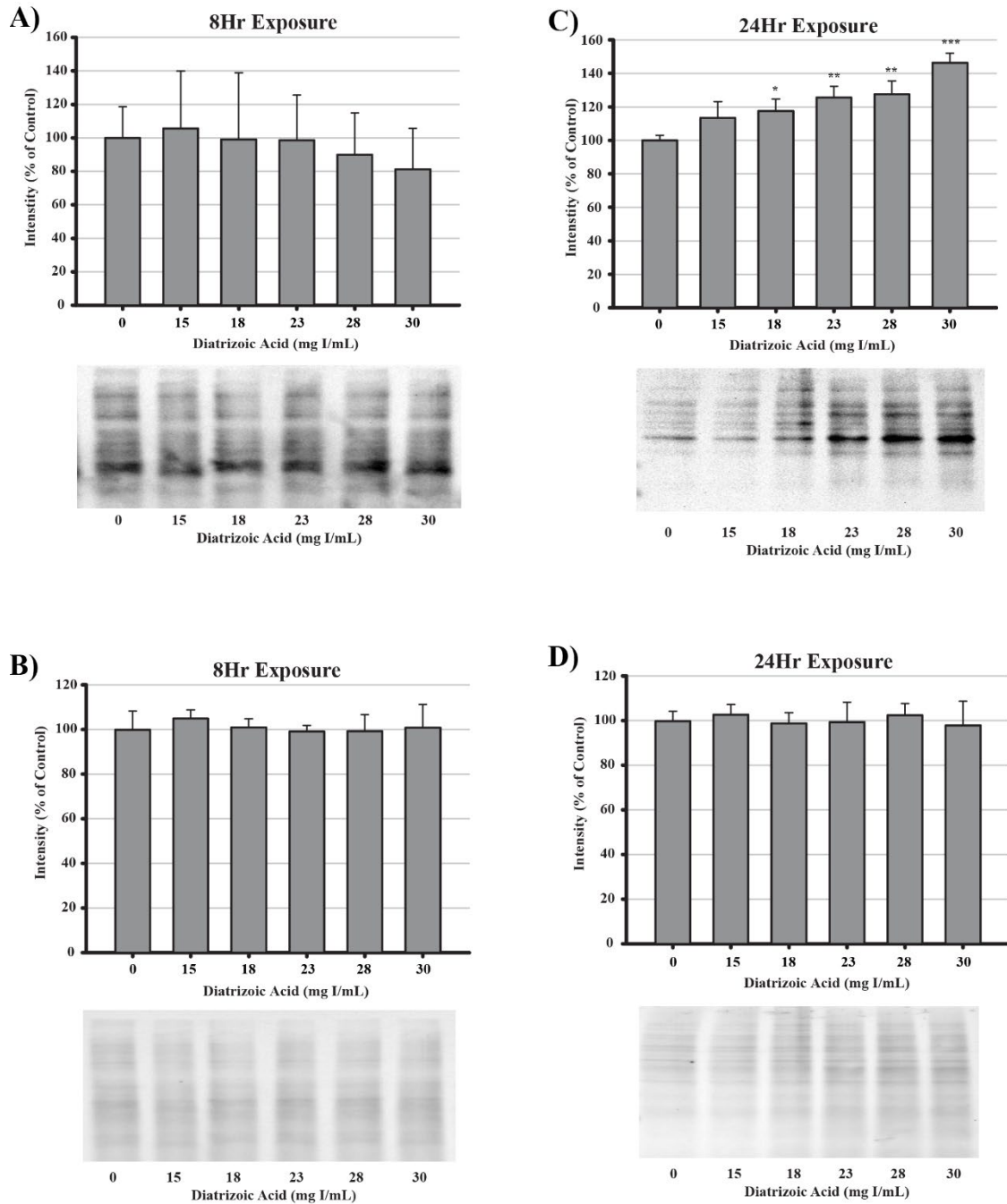


Figure 17. Diatrizoic acid effects on protein carbonylation in HK-2 cells. An increase in protein carbonylation was evident in cell lysate following 24 hr (C) in 18 mg I/mL to 30 mg I/mL DA. Representative blots and cumulative densitometry included for 8 hr (A) and 24 hr (C) exposure to diatrizoic acid. Representative blot with Memcode Reversible stain for 15 μ g loaded protein and cumulative protein densitometry depicted for 8 hr (B) and 24 hr (D) exposure. Statistical difference from 0 mg I/mL diatrizoic acid depicted by an asterisk (* $p < 0.05$, ** $p < 0.01$, *** $p < 0.001$). Values represent mean \pm SEM for three independent experiments of two biological replicants.

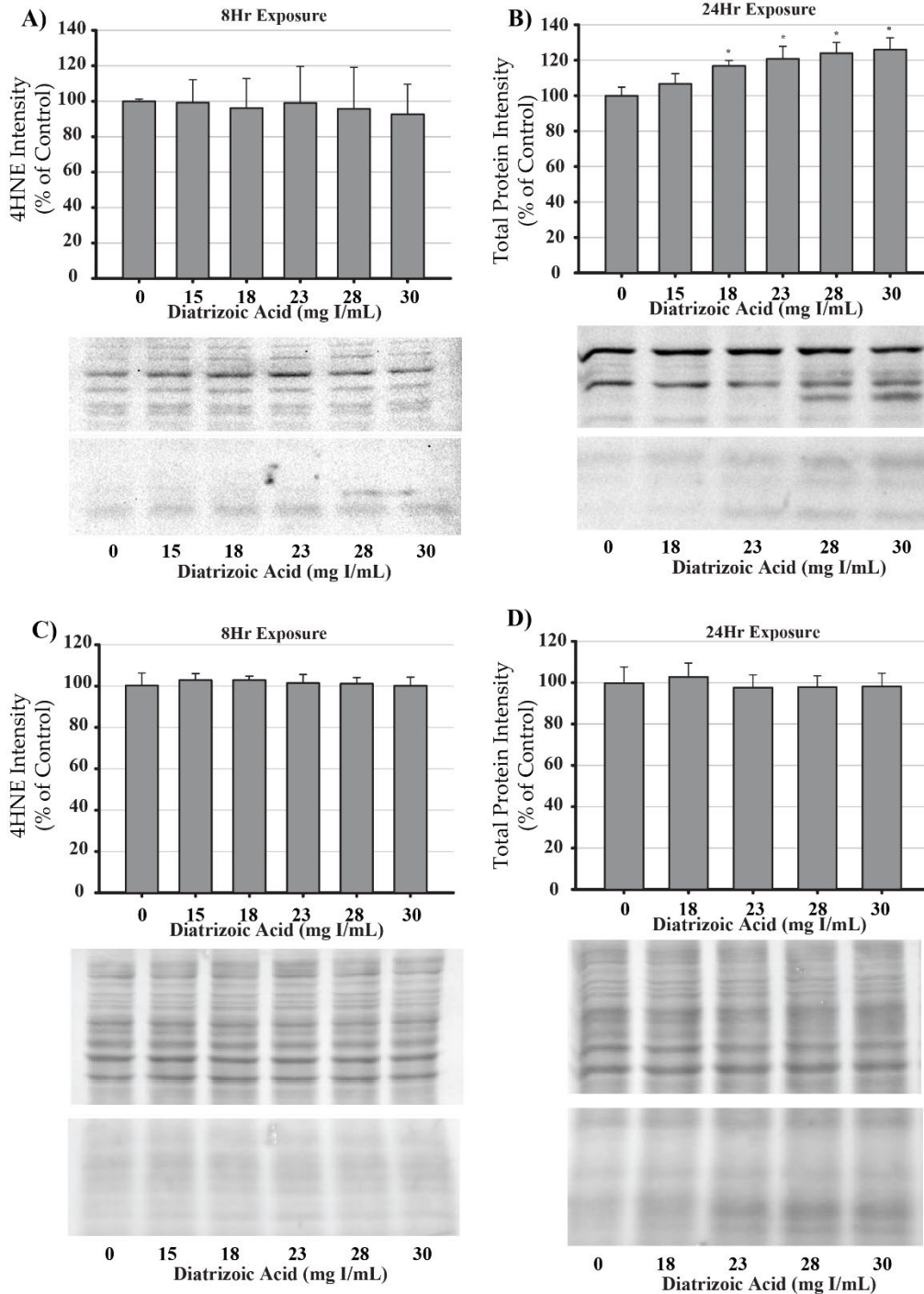


Figure 18. Diatrizoic acid effects on 4-HNE adduct formation in HK-2 cells. An increase in protein adduct formation was evident in cell lysate following 24 hr exposure (C) in 18 mg I/mL to 30 mg I/mL DA. Representative blots and cumulative densitometry included for 8 hr (A) and 24 hr (C) exposure. Representative blot with Memcode Reversible stain for 40 μ g loaded protein and cumulative protein densitometry depicted for 8 hr (B) and 24 hr (D) exposure. Statistical difference from 0 mg I/mL diatrizoic acid depicted by an asterisk (* $p < 0.05$). Values represent mean \pm SEM for three independent experiments of two biological replicants.

Initially, MnSOD expression was measured to determine the effect of DA exposure on antioxidant systems within the mitochondria. In response to DA exposure for 24 hr, there was no noticeable change in MnSOD expression (Figure 19). Due to the fact that levels of expression do not necessarily indicate activity of an enzyme, MnSOD, Cu/ZnSOD, and Total SOD activity were measured to evaluate the effects of DA on cellular antioxidant systems. Total SOD activity was decreased at 24 hr relative to vehicle control in groups treated with 28 and 30 mg I/mL ($p < 0.05$) (Figure 19). MnSOD activity was unchanged in response to exposure to DA at 24 hr (Figure 19), while Cu/ZnSOD activity was significantly reduced in response to 23 mg I/mL DA ($p < 0.05$) relative to vehicle control at 24 hr exposure (Figure 19). Protein carbonylation and 4-HNE adduction were measured in cytosolic and mitochondrial fractions to determine if MnSOD activity within the mitochondria is protecting HK-2 mitochondria from DA-induced ROS generation. Following exposure to 30 mg I/mL DA for 24, protein carbonylation and 4-HNE protein adduction is significantly increased in response to control within the cytosolic fraction but there was no change in either biomarker of oxidative stress in the mitochondrial fraction (Figure 20).

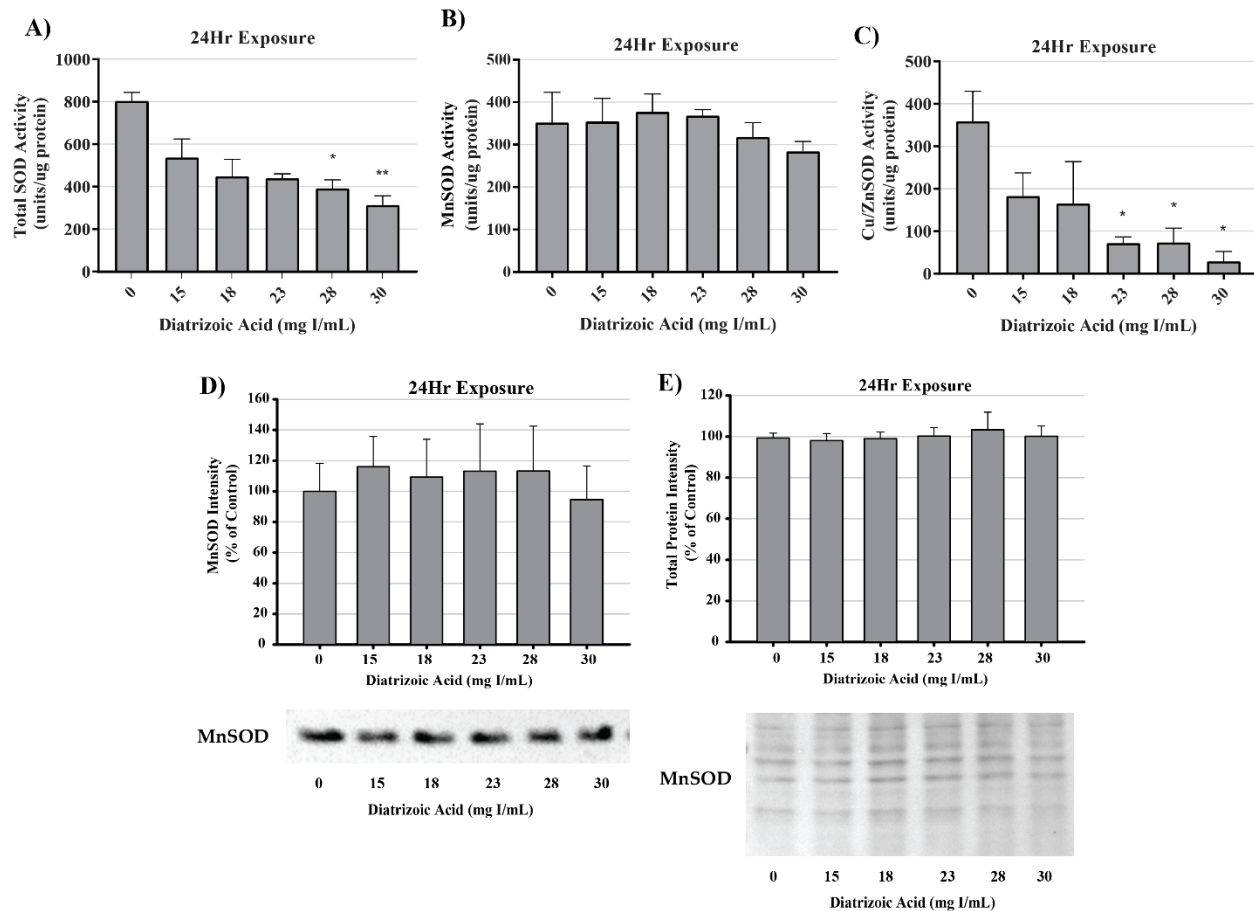


Figure 19. Diatrizoic acid effects on superoxide dismutase expression and activity in cellular fractions of HK-2 cells. A decrease in total SOD activity was evident in groups treated with 28 and 30 mg I/mL at 24 hr (A). No significant change in MnSOD activity was apparent following 24 hr (B) exposure to DA. A decrease in Cu/Zn activity (C) was evident following 24 hr exposure to 23-30 mg I/ml. Exposure to DA did not induce a change in MnSOD expression (D). Representative blots and cumulative densitometry included for 24 hr (D) exposure. Representative blot with Memcode Reversible stain for 40 μ g loaded protein and cumulative protein densitometry depicted for 24 hr (E) exposure. Statistical difference from 0 mg I/mL diatrizoic acid depicted by an asterisk (* $p < 0.05$, ** $p < 0.01$). Values represent mean \pm SEM for three independent experiments of two biological replicants.

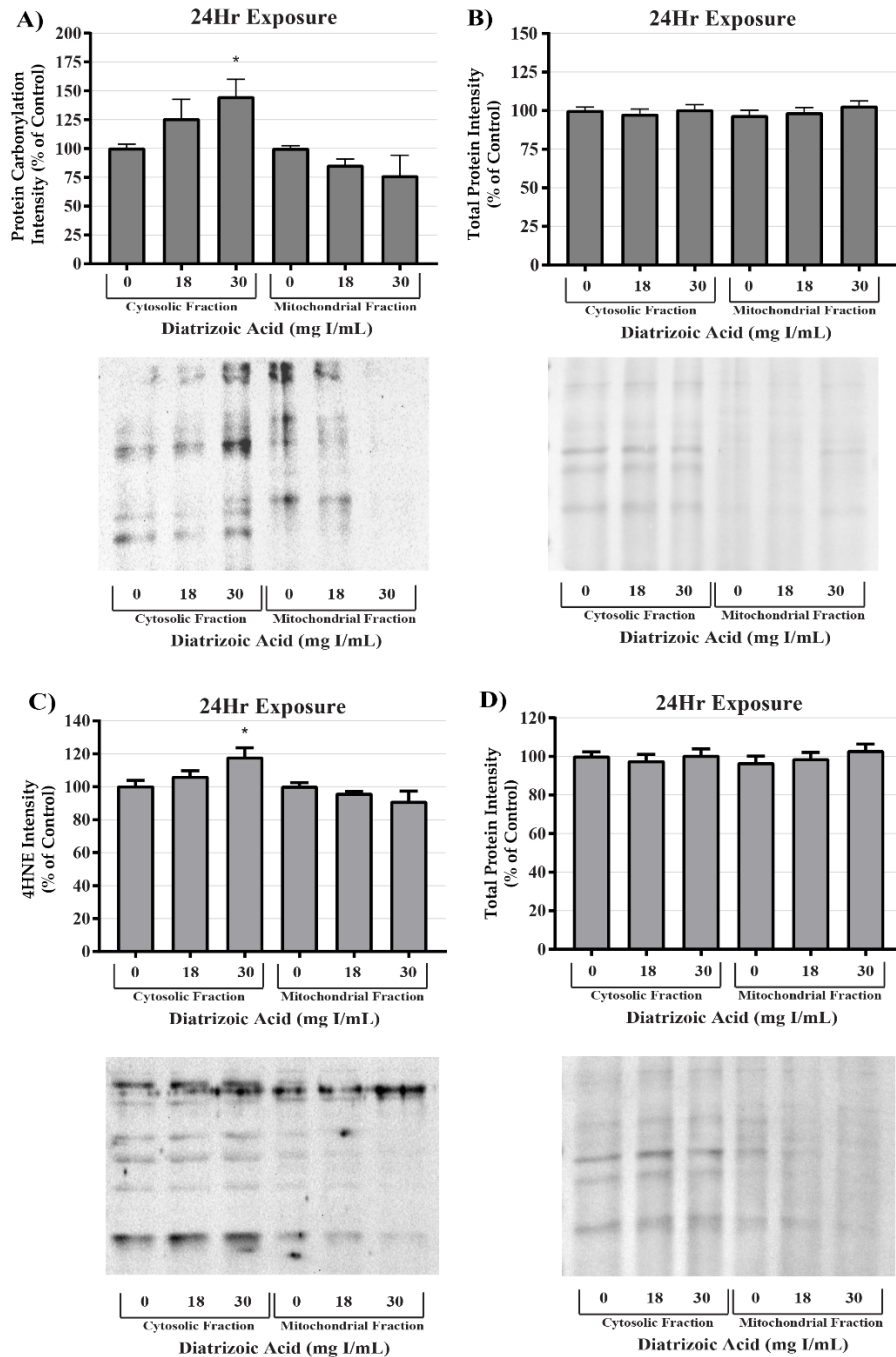


Figure 20. Diatrizoic acid effects on oxidative stress within cellular fractions of HK-2 cells.

DA-induced oxidative stress takes place in the cytosol. Representative blot and cumulative densitometry for expression of Oxyblot (A) and 4-HNE protein adducts (C) in cytosolic and mitochondrial fractions following 24 hr exposure to DA. Representative blots of MemCode reversible staining for 15 and 40 μ g protein loading and cumulative densitometry for Oxyblot (B) and 4-HNE (D). Asterisks (* $p < 0.05$) indicate statistical difference from vehicle control in cytosolic fraction. Values represent mean \pm SEM for three independent experiments of two biological replicants.

To evaluate potential sources for ROS production, TNF α expression was measured in cell lysate and cell media via Western blot and ELISA, respectively. TNF α expression in cell lysate decreased at 24 hr relative to vehicle control in groups treated with 15 and 18 mg I/mL DA ($p < 0.01$) as shown by Western blot (Figure 21). TNF α secretion into the media was increased at 24 hr relative to vehicle control ($p < 0.05$) in groups treated with 15 and 18 mg I/mL as shown by ELISA (Figure 21). NADPH oxidase 4 (NOX4), a ROS generating enzyme linked to TNF- α , expression was also measured. NOX4 expression was unchanged in response to exposure to DA at 24 hr (Figure 21). Although it is apparent that DA exposure elicits an inflammatory response in HK-2 cells, activation of TNF α does not play a role in DA-induced oxidative stress at clinically relevant concentrations. Therefore, the source of ROS overproduction in response to DA is unclear.

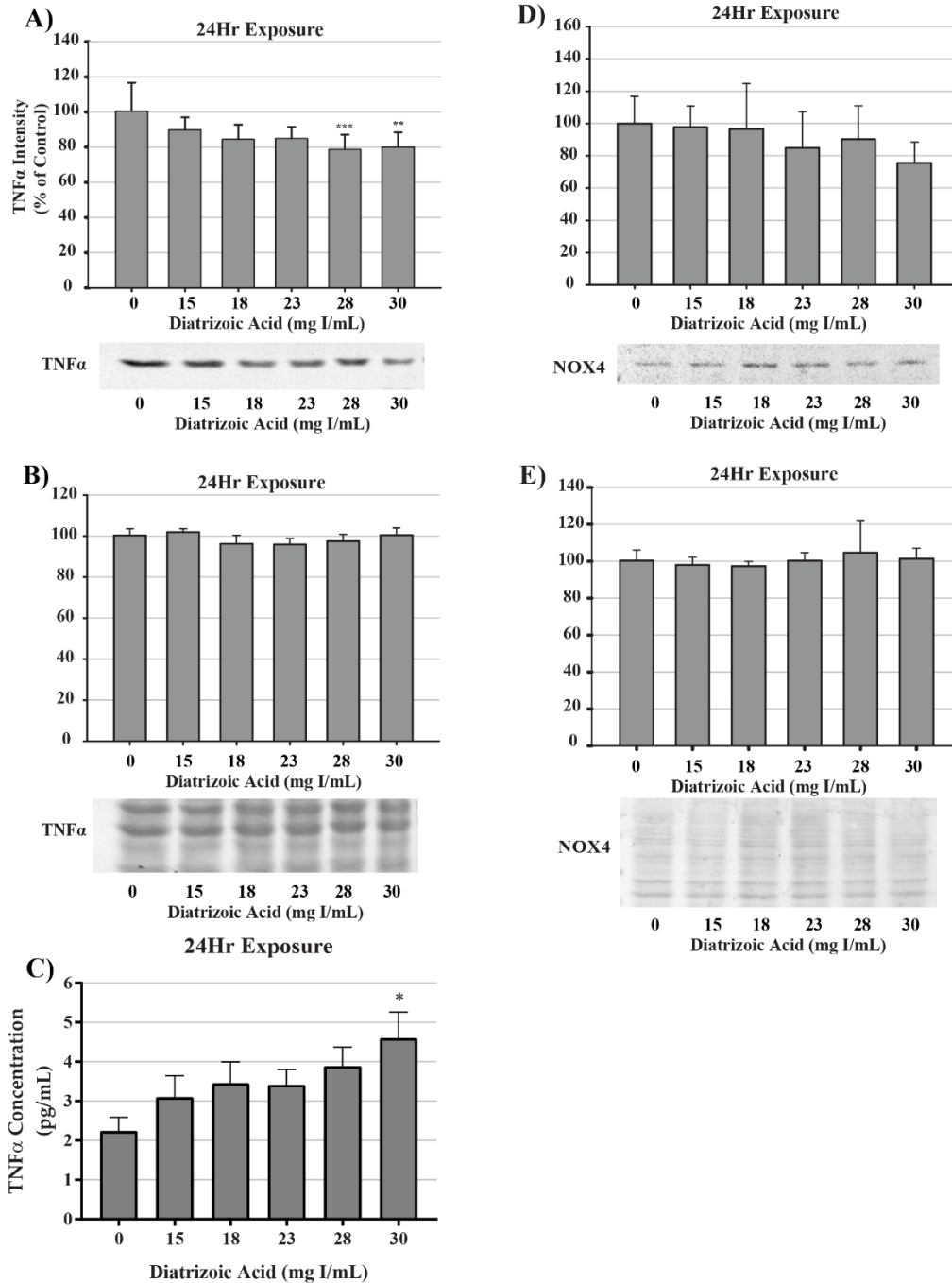


Figure 21. Diatrizoic acid effects on TNF α and NOX4 expression in HK-2 cells. DA induces TNF α activation but does not affect downstream effectors. TNF α expression in cell lysate was decreased in response to 15 and 18 mg I/mL DA at 24 hr (A). An increase in TNF α leakage into the cell media was evident following 24 hr (C) in 15 and 18 mg I/mL DA. No significant change in NOX4 expression was apparent in cell lysate following 24 hr (D) exposure to DA. Representative blot with Memcode Reversible stain for 40 μ g loaded protein and cumulative protein densitometry depicted for TNF α (B) and NOX4 (E) following 24 hr exposure. Statistical difference from 0 mg I/mL diatrizoic acid depicted by an asterisk (* $p < 0.05$). Values represent mean \pm SEM for three independent experiments of two biological replicants.

DA Effects on Mitochondrial Membrane Leakage and Apoptosis Initiation

Alterations in mitochondrial membrane integrity were evident following exposure to DA for 24 hr. DA caused significant cytochrome c leakage from the mitochondrial inner membrane space into the cytosol relative to vehicle control ($p < 0.05$) and the expression of cytochrome c within mitochondrial fractions decreased at 30 mg I/mL relative to control ($p < 0.05$) as shown by Western blot (Figure 22).

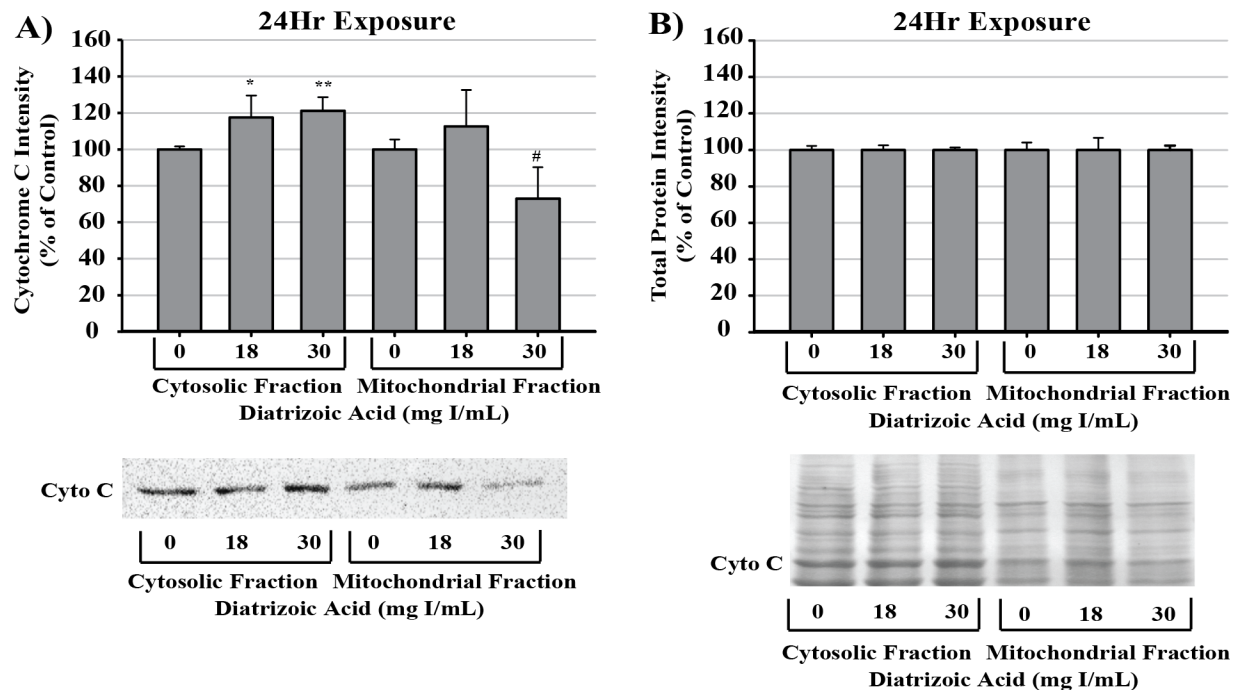


Figure 22. Diatrizoic acid effects on mitochondrial membrane integrity in HK-2 cells. DA diminished mitochondrial membrane integrity. Representative blot and cumulative densitometry for cytochrome c (A) in cytosolic and mitochondrial fractions following 24 hr exposure to DA. Representative blots of MemCode reversible staining for 40 μ g protein loading and cumulative densitometry for cytochrome c (B). Asterisks (* $p < 0.05$, ** $p < 0.01$) indicate statistical difference from vehicle control in cytosolic fraction. Octothorpe (# $p < 0.05$) indicate statistical difference from vehicle control in mitochondrial fraction. Values represent mean \pm SEM for three independent experiments of two biological replicants.

DA increased caspase 3 cleavage and caspase 12 expression relative to vehicle control at 28 and 30 mg I/mL following 24 hr exposure ($p < 0.05$, $p < 0.01$) (Figure 23). Caspase 4

expression and cleavage was unchanged in response to exposure to DA for 24 hr suggesting that the efflux of TNF α into the media was not sufficient to induce activation of caspase 4 (Figure 23).

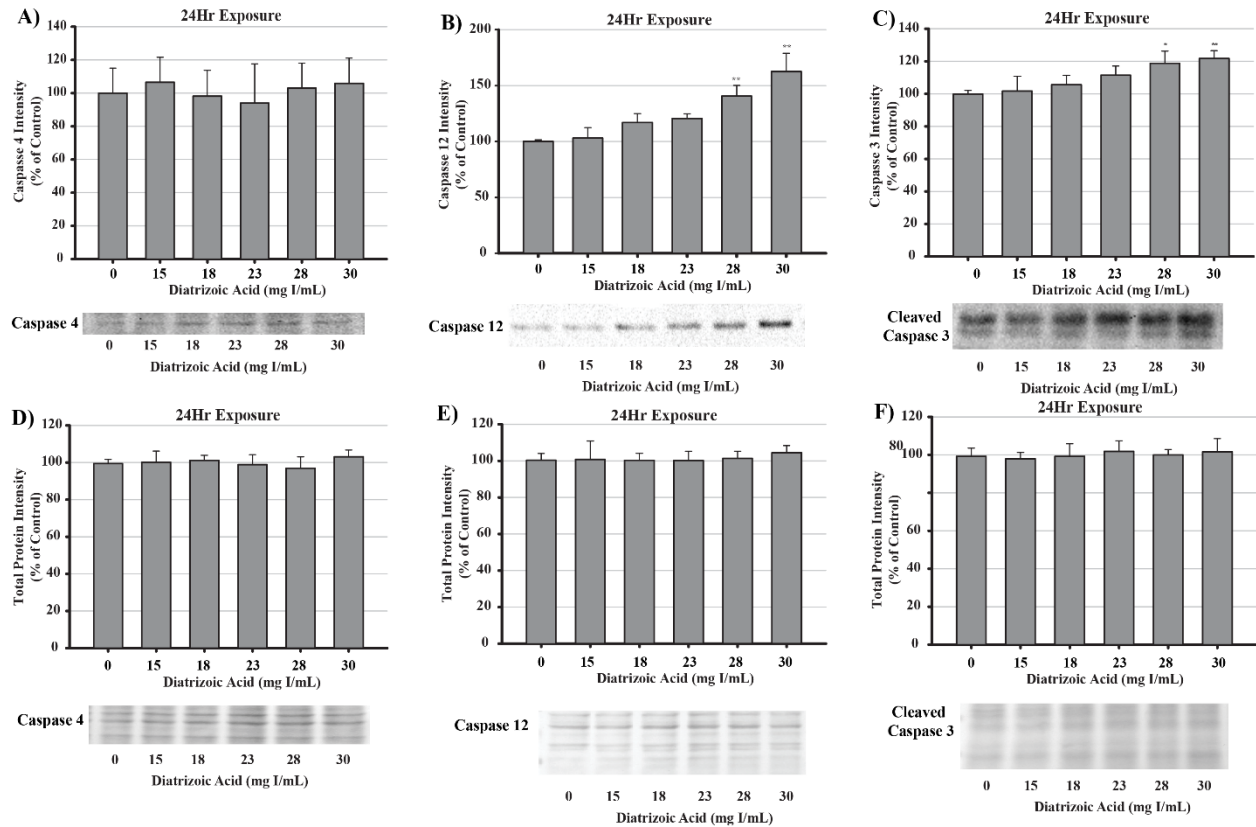


Figure 23. Diatrizoic acid effects on the expression of caspase 4, caspase 12, and caspase 3 in HK-2 cells. DA induces apoptosis via caspase 3 and caspase 12 activation. Representative blot and cumulative densitometry for total caspase 4 (A), caspase 12 (B), and cleaved caspase 3 (C) protein expression following 24 hr exposure to DA. Asterisks (* $p < 0.05$, ** $p < 0.01$) indicate statistical difference from vehicle control. Representative blots of MemCode reversible staining for 40 μg protein loading and cumulative densitometry for caspase 4 (D), caspase 12 (E), and cleaved caspase 3 (F). Values represent mean \pm SEM for three independent experiments of two biological replicants.

DA Effects on Calcium Homeostasis

Mitochondrial viability and calpain activity assays were utilized to determine the role of calcium homeostasis in DA-induced cytotoxicity. MTT assays were performed on HK-2 cells pretreated for 45 min with EGTA, BAPTA-AM, or 2-APB prior to exposure to clinically

relevant concentrations of DA ranging from 15 to 30 mg I/mL. The concentrations of EGTA or BAPTA-AM selected for these studies were not cytotoxic based on the results of the MTT assay. Higher concentrations of BAPTA-AM induced some alterations in the MTT assay and were omitted from any studies with DA. Pretreatment with BAPTA-AM completely protected against DA-induced cytotoxicity within 2, 8, and 24 hr as seen by MTT assays (Figure 24). Within 2 hr, neither EGTA or 2-APB showed any statistically significant protection, however, both showed partial protection within 8 hr at 30 mg I/mL ($p < 0.05$) when compared to the DA group (Figure 24). EGTA and 2-APB provided partial protection from DA-induced cytotoxicity within 24 hr exposure to DA ($p < 0.05$) when compared to the DA group (Figure 24). Calpain activity assays were performed to determine the role of calcium dependent proteases in DA-induced apoptosis. HK-2 cells exposed to 30 mg I/mL for 24 hr experienced a two-fold increase in calpain activity ($p < 0.05$) compared to vehicle control (Figure 25). Pretreatment with 10 μ M BAPTA-AM or 10 μ M calpeptin prior to DA exposure completely inhibited calpain activity (Figure 25).

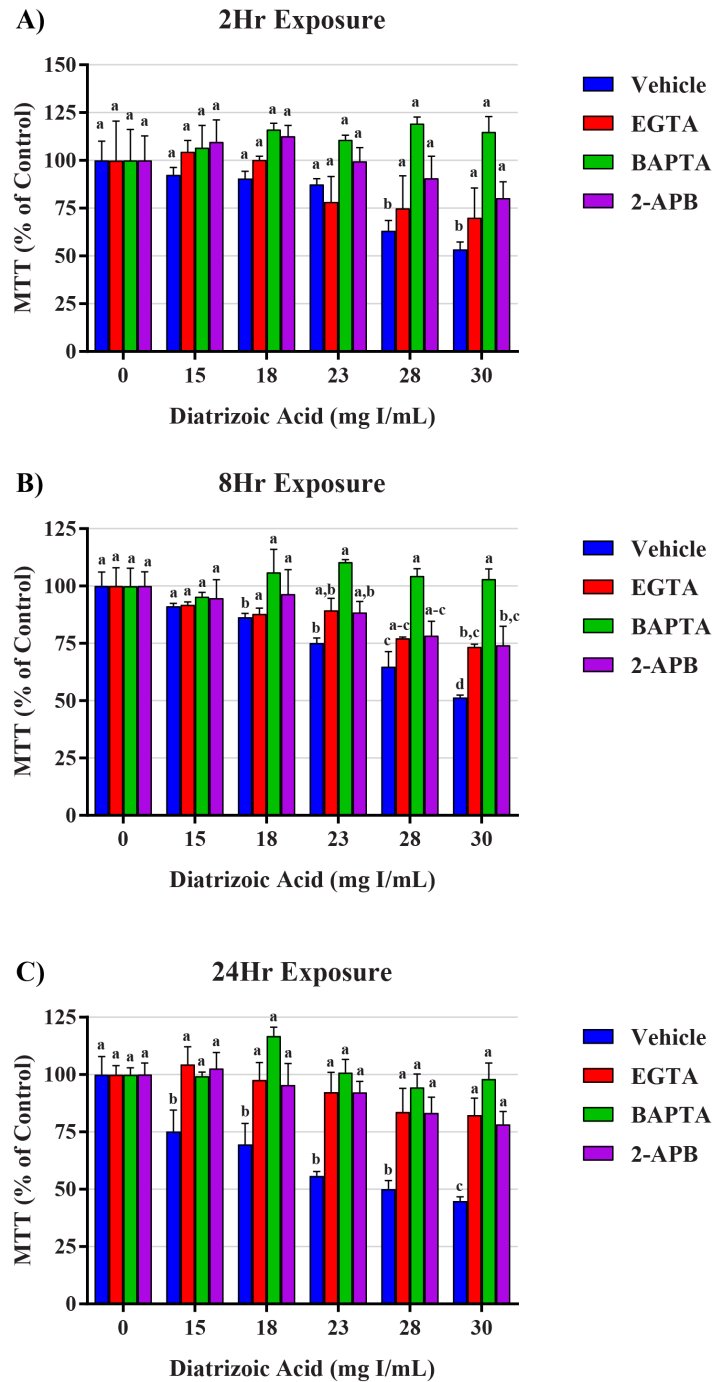


Figure 24. Effects of EGTA, BAPTA-AM, or 2-APB pretreatment on mitochondrial viability in HK-2 cells. DA induced cytotoxicity is attenuated in response to calcium concentration modulators. BAPTA-AM offered protection from DA-induced cytotoxicity within 2 hr (A), 8 hr (B), and 24 hr (C). EGTA and 2-APB provided partial protection from DA-induced cytotoxicity within 8 hr (B) and 24 hr (C). Different superscripts (a-d) indicate a statistical difference between groups. Values represent mean \pm SEM for three independent experiments with at least 4 biological replicants.

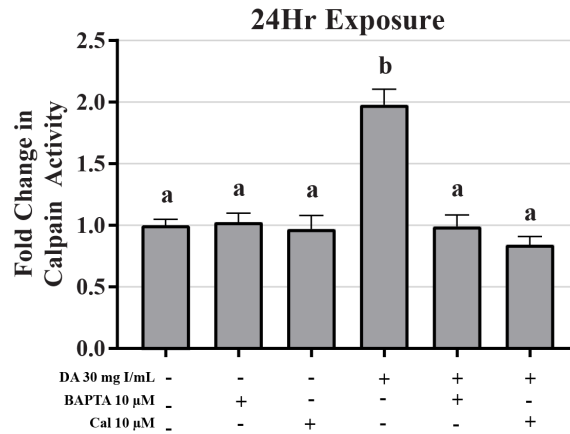


Figure 25. Diatrizoic acid effects on calpain activity in HK-2 cells. DA induced activation of calpain. HK-2 cells exposed to 30 mg I/mL DA for 24 hr demonstrated a two-fold increase in calpain activity. Pretreatment with either 10 μ M BAPTA-AM (calcium chelator) or 10 μ M calpeptin (Cal; calpain pathway inhibitor) completely abrogated DA-induced calpain activity. Different superscripts (a, b) indicate a statistical difference between groups. Values represent mean \pm SEM for three independent experiments of two biological replicants.

To investigate the role of DA-induced calcium dysregulation in mitophagy, oxidative stress, and apoptosis, protein expression of LC3BI and II, protein carbonylation, 4-HNE, and caspase 12 were measured via Western blots and Oxyblot. HK-2 cells pretreated with BAPTA-AM completely abrogated the conversion of LC3BI to LC3BII ($p < 0.05$) induced by exposure to DA (Figure 26). Pretreatment with the calpain inhibitor partially inhibited the initiation of mitophagy ($p < 0.05$) indicating that calpain activation may play a role in mitochondrial turnover (Figure 26). Chelation of intracellular calcium or inhibition of calpain activation decreased protein carbonylation, however, not to a significant degree (Figure 27). However, DA-induced 4-HNE adduct formation was completely abrogated ($P < 0.05$) in response to BAPTA-AM and calpeptin (Figure 27). Caspase 12 activation was also attenuated in response to BAPTA-AM and calpeptin ($p < 0.05$) (Figure 28) indicating that caspase 12 activity is not dependent on ER stress but can be activated in response to calpain activity.

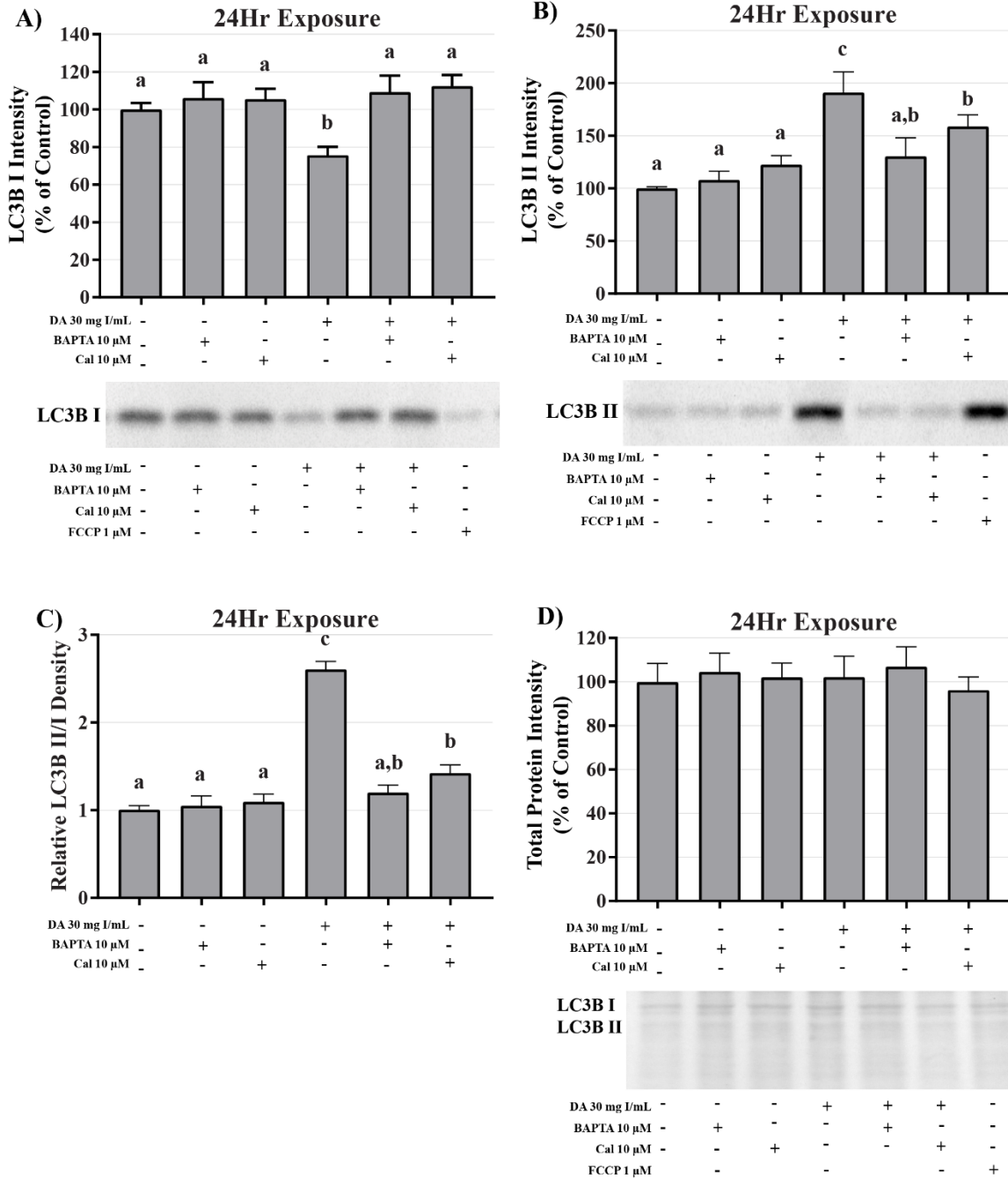


Figure 26. Effects of BAPTA-AM or calpeptin pretreatment on LC3B expression in HK-2 cells. Pretreating HK-2 cells with BAPTA-AM or calpeptin attenuated DA-induced conversion of LC3BI to LC3BII. Representative blots and cumulative densitometry included for LC3BI (A), LC3BII (B), and LC3BII/LC3B I ratio (C) following 24 hr exposure to DA. Representative blot with Memcode Reversible stain for 40 μ g loaded protein and cumulative protein densitometry depicted for 8 hr (D) exposure. Positive control for LC3B conversion was FCCP. Different superscripts (a, b, c) indicate a statistical difference between groups. Values represent mean \pm SEM for three independent experiments of two biological replicants.

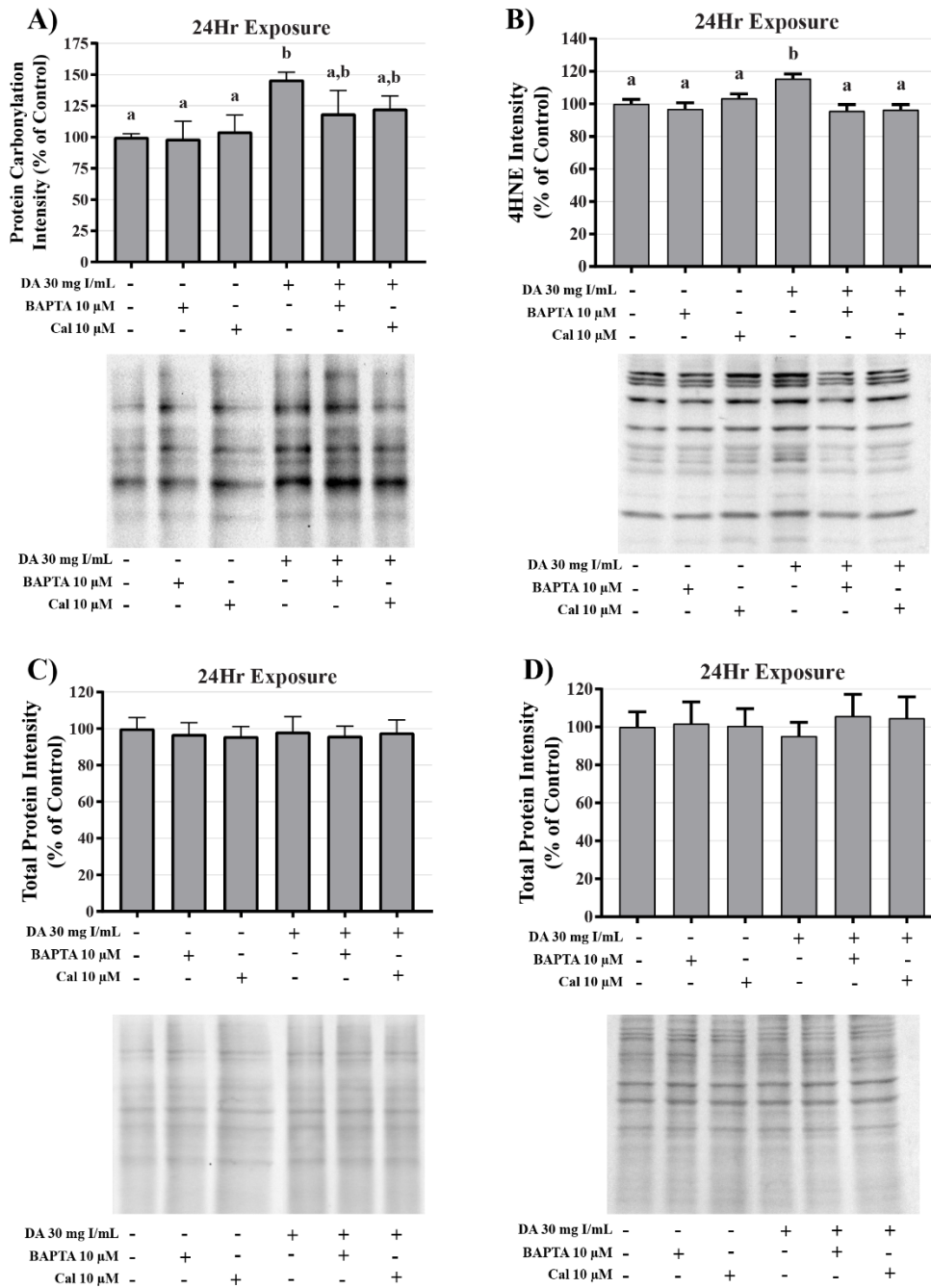


Figure 27. Effects of BAPTA-AM or calpeptin pretreatment on oxidative stress in HK-2 cells. Pretreatment with BAPTA-AM or calpeptin slightly decreased protein carbonylation and completely abrogated 4-HNE adduct formation. Representative blots and cumulative densitometry included for protein carbonylation (A) and 4-HNE adduct formation (B) following 24 hr exposure to DA. Representative blot with Memcode Reversible stain for 15 μg and 40 μg loaded protein and cumulative protein densitometry depicted for protein carbonylation (C) and 4-HNE adduct formation (D). Different superscripts (a, b) indicate a statistical difference between groups. Values represent mean ± SEM for three independent experiments of two biological replicants.

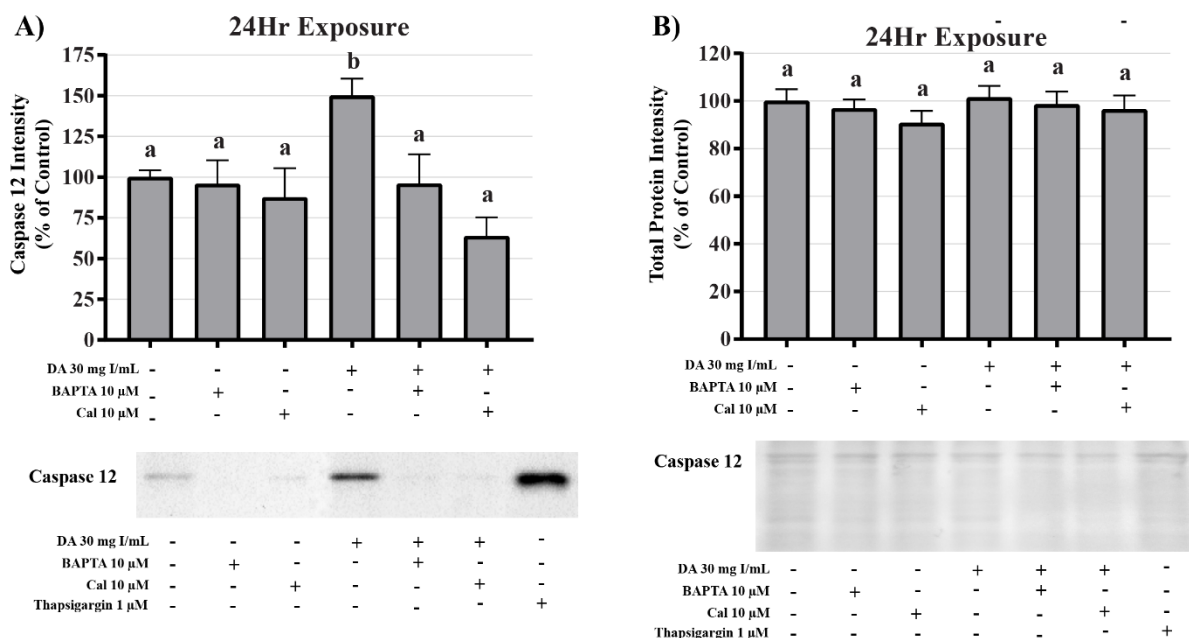


Figure 28. Effects of BAPTA-AM or calpeptin pretreatment on caspase 12 activity in HK-2 cells. Pretreatment with BAPTA-AM or calpeptin abrogated caspase 12 activation. Representative blots and cumulative densitometry included for caspase 12 (A) following 24 hr exposure to DA. Representative blot with Memcode Reversible stain for 40 μ g loaded protein and cumulative protein densitometry (B). Positive control for caspase 12 activation was thapsigargin. Different superscripts (a, b) indicate a statistical difference between groups. Values represent mean \pm SEM for three independent experiments of two biological replicants.

DISCUSSION

The use of RCM in radiographic imaging procedures does not show any sign of slowing down. Over 75 million contrast-requiring procedures are performed every year worldwide, and since 2006, the number of CT scans has increased by over 800% (Bottinor, Polkampally, & Jovin, 2013; Brown et al., 2016). As patient life expectancy increases, the need for diagnostic procedures such as percutaneous coronary intervention (PCI) and cardiac catheterizations linearly increase as well (Sawhney & Fraser, 2017). Unfortunately, the combination of comorbidities that decrease renal function and exposure to RCM leads to CI-AKI resulting in increased length of hospital stay, cardiovascular events, end-stage renal disease, and all-cause

mortality (Brown et al., 2010; Chertow et al., 2005; James et al., 2013). RCM toxicity is associated with severe renal vasoconstriction, activation of multiple inflammatory pathways, and direct tubule damage. The combination of these humoral responses can induce renal injury ranging from non-symptomatic increases in SCr to extensive damage resulting in permanent kidney failure and the need for dialysis. Although the effects of RCM exposure have been well documented, the exact mechanisms of toxicity have not been fully elucidated. A vast number of clinical reports, observational studies, and *in vivo* studies have explored the incidence of CI-AKI following exposure to RCM, most finding significant risk; however, little is known about the initial sources of renal injury and direct cellular toxicity pertaining to RCM exposure. Discovering and understanding the mechanisms of toxicity is imperative for the development of an appropriate preventative measure or treatment option to mitigate CI-AKI.

To determine the source of RCM induced cytotoxicity, *in vitro* models must be implemented to eliminate renal hemodynamic and inflammatory responses to RCM exposure. Various cell models have been utilized throughout the years including MDCK, LLC-PK1, HEK-293, and NRK-E52, however, mechanistic studies require a model that can be translated directly to human physiology. Therefore, the human kidney cell model, HK-2, was chosen. In order to determine the initial mechanisms of cellular toxicity, the model in question must be exposed to concentrations of RCM that the kidney would experience in a clinical setting. On average, the adult human male, aged 19-95 years, has blood plasma volumes of 45.2 to 53 ml/kg body weight (Yiengst & Shock, 1962). An effective dose of an RCM for CT imaging such as coronary arteriography can range from 45 to 150mL. Therefore, for a 75kg adult male, blood plasma levels of RCM will range from 4 to 15 mg I/mL (Lusic & Grinstaff, 2013). These concentrations can effectively be doubled for larger patients and dosages can continue to increase until the

effective termination limit of 300mL of a 76% DA preparation or equivalent has been injected (Skucas, 1989). It is not uncommon for mechanistic studies to expose *in vitro* models to concentrations of RCM over 150 mg I/mL, which is up to twenty-five-fold greater than blood plasma levels. In this study, a wide range of DA concentrations (0, 2, 5, 10, 15, 18, 23, 28, and 30 mg I/mL) were chosen to encompass what the kidney would experience following a modern imaging procedure. Although an extensive number of peer-reviewed studies indicate the roles of various pathways and propose multiple mechanisms of toxicity, the initial source of damage has yet to be identified at clinically relevant concentrations.

Our study is the first to show that clinically relevant concentrations of DA induces cytotoxicity. MTT conversion was used as a measure of mitochondrial viability because the reduction of the yellow tetrazolium dye to its purple formazan counterpart is performed primarily by mitochondrial dehydrogenases (Rai et al., 2018). Mitochondrial viability was decreased in HK-2 cells within 2 hr at 15 mg I/mL and continued to decrease at 8 and 24 hr at 2 mg I/mL as shown by MTT to formazan conversion. It is important to mention that a decrease in MTT conversion does not necessarily demonstrate a decrease in the total number of viable cells and vice versa (Chung, Kim, & Kim, 2015). Hence, trypan blue exclusion assays were performed to verify that a decrease in MTT conversion was due to a decrease in mitochondrial viability and not a decrease in total number of viable cells. Healthy cells with an intact cellular membrane will exclude the trypan blue dye, whereas dead cells will allow the dye to leak into the cytosol (Strober, 2015). Unlike the results obtained from the MTT assays, a decrease in cell viability was not apparent until HK-2 cells were exposed to at least 23 mg I/mL for 24 hr indicating that HK-2 cells experience a statistically significant decrease in mitochondrial viability at a much lower

concentration and at an earlier time point when compared to the noticeable decrease in cell viability.

The mitochondrial density of the kidney is relatively high compared to the rest of the body, second only in mitochondrial content and oxygen consumption to the heart (Bhargava & Schnellmann, 2017). The high mitochondrial content is due to the PT being responsible for the majority of transport within the kidney accounting for approximately 80% of all transport in the kidney (Zhuo & Li, 2013). Consequently, PT cells are fairly resistant to induction of pro-apoptotic mechanisms via multiple mitochondrial protection pathways. PT cells experiencing intracellular stressors such as ischemia, reaction to xenobiotics, or inflammatory responses will undergo mitochondrial swelling, fission, and mitophagy in an attempt to withstand the insult (Tran & Parikh, 2014). HK-2 cells have similar activity to *in situ* PT cells, and this property could explain the discrepancy between the values obtained from the MTT and Trypan blue exclusion assays.

The effects of RCM on mitochondrial function have been briefly studied in various models. Basal and uncoupled respiration measured using a Clark oxygen electrode were decreased in isolated PTs of New Zealand white rabbits after exposure to DA, ioxaglate, and iopamidol (Humes et al., 1987; Messana et al., 1990; Messana et al., 1988). It has also been shown that exposing HK-2 or LLC-PK1 cells to ioversol, iodixanol, or iohexol induces an increase in mitochondrial ROS production, as well as depolarization of mitochondrial membranes and stimulated the release of cytochrome c (Itoh et al., 2006; Lei et al., 2018). ATP production, and complex I and complex III activity were decreased in male Wistar albino rats in response to exposure to DA (Roza et al., 2011). The combination of these previous studies

indicates that there is an interaction between the mitochondria of PT cells and RCM; however, the source of this dysfunction is unclear.

This is the first study to conduct real-time screening to determine the effects of DA on the mitochondria of live, intact PT cells. Using the Seahorse XFe96 Analyzer, the effects of clinically relevant concentrations of DA on mitochondrial respiration, glycolysis, ATP production, and mitochondrial fuel utilization were determined in HK-2 cells. The cell mito stress test utilizes various compounds that have been validated to be useful in mitochondrial mechanistic studies (Eakins et al., 2016), such as the complex I and complex III inhibitors, rotenone and antimycin-A, which decrease oxygen consumption rate (OCR) and increase extracellular acidification rate (ECAR). The ATP synthase inhibitor oligomycin inhibit the electron transport chain downstream of the complexes I and III but do not affect spare respiratory capacity. Finally, the uncoupling agent, 2,4-dinitrophenol, increases both OCR and ECAR (Eakins et al., 2016). Exposure to DA induced statistically significant decreases in basal and maximal respiration, spare respiratory capacity, and ATP production within 8hr and continued to decrease these parameters through 24hr. Unfortunately, a global decrease in mitochondrial respiration does not necessarily predict the source of mitochondrial damage; for instance, the environmental agents 2,2'-methylenebis(4-chlorophenol) and pentachlorophenol were determined to be uncoupling agents because the compounds reversed oligomycin-induced inhibition of OCR (Datta et al., 2016). Previous work in our lab demonstrated that the HIV medication tenofovir may be an ATP synthase inhibitor due to its reduction of OCR and no effect on spare respiratory capacity in HK-2 cells. A study performed by Namba et al., determined that renal PTs experiencing metabolic acidosis in response to ammonium chloride showed similar results to HK-2 cells exposed to DA (Namba et al., 2014). The Namba group

concluded that the global decrease in respiration was due to an increase in mitophagy. The role of mitophagy in CI-AKI will be discussed in more depth later.

The glycolytic stress test determines the ability of a cell to utilize glycolysis as a source of ATP. The assay utilizes oligomycin to induce maximal glycolysis from which spare glycolytic capacity can be determined. Similar to mitochondrial respiration, comparing the compounds that are known to effect glycolysis can help predict the source of glycolytic damage. The pesticide maneb has been shown to decrease glycolysis and glycolytic reserve and increase OCR indicating that it differentially affects glycolysis and stimulates mitochondrial respiration (Anderson et al., 2018). Comparable to neuroblasts treated with maneb, HK-2 cells that are exposed to DA demonstrate decreases in both glycolysis and glycolytic reserve; however, this interpretation must be approached with caution. HK-2 cells depend on oxidative phosphorylation to a much greater extent than glycolysis as a source of energy production indicated by the very slight increase in ECAR following the addition of oligomycin, demonstrating that the spare glycolytic capacity of HK-2 is insignificant relative to oxidative phosphorylation. It is possible that the decrease in glycolysis is not due to damage to glycolytic machinery but, more likely, the disappearance of glycolytic substrates in response to the cells attempting to maintain ATP levels in the absence of functioning mitochondria.

In order to verify that exposure to DA results in mitochondrial dysfunction and the reduction in glycolysis and glycolytic capacity is due to downstream effects, the real-time ATP rate assay was utilized. This assay uses oligomycin and rotenone/antimycin-A to determine total ATP, mitochondria-linked ATP, and glycolysis-linked ATP production. In response to exposure to DA, HK-2 cells experienced a statistically significant decrease in total ATP and mitochondrial ATP production. Conversely, a decrease in glycolytic ATP production was apparent, however,

not to a significant degree. These results indicate that exposure to DA preferentially affects the mitochondria compared to the glycolytic pathway and the decreases that are being observed are in response to energy demand or downstream effects of mitochondrial dysfunction.

The ability of the mitochondria to utilize available fuel sources is vital for maintaining energy homeostasis. The mito fuel flex test determines the rate of oxidation of the three major mitochondrial fuels: pyruvate, glutamine, and long-chain fatty acids (LCFA). The assay determines the reliance on a particular pathway to maintain basal respiration, labeled fuel dependency, followed by the overall fuel capacity of each fuel source. The difference of these two values is the mitochondrial fuel flexibility, or the mitochondria's ability to compensate for an inhibited pathway by using the other two pathways. UK5099 is an inhibitor of the mitochondrial pyruvate carrier (MPC) thereby blocking the glucose oxidation pathway and determining the dependency and flexibility of the mitochondria to utilize pyruvate produced via glycolysis. BPTES is an allosteric inhibitor of glutaminase (GLS1) resulting in inhibition of the glutamine oxidation pathway. GLS1 converts glutamine to glutamate which is then converted to α -ketoglutarate by glutamate dehydrogenase to be used in the citric acid cycle. Finally, etomoxir inhibits the LCFA transporter carnitine-palmitoyl transferase (CPT1A) which is critical for translocating LCFA from the cytosol into the mitochondrial matrix to be used for β -oxidation.

In response to exposure to clinically relevant concentrations of DA, HK-2 cell's ability to oxidize glucose, glutamine, and fatty acid is not affected to a significant degree. The flexibility of glucose and glutamine oxidation slightly increases in response to low and intermediate concentrations of DA; however, the increase also does not reach levels of significance. Aerobic respiration is the primary mechanism of ATP production in PT cells, with the central source of ATP coming from β -oxidation of LCFA, such as palmitate, which produce 3 fold the ATP per

molecule when compared to glucose oxidation (Bhargava & Schnellmann, 2017). According to the results of the mito fuel flex test (Figure 12), the oxygen consumption linked to each oxidative pathway within the mitochondria are approximately equivalent, indicating that HK-2 cells depend on each of the three pathways to a similar degree. It is also important to note that although we are seeing a decrease in every parameter of mitochondrial function as shown by the cell mito stress tests, the ability of the mitochondria to utilize the different fuel sources is not diminished. One would expect there to be a decrease in at least one oxidative pathway as a potential source of damage within the mitochondria; for example, if there was a decrease in glutamine oxidation in response to exposure to DA, it could be concluded that the diminishment of basal and maximal respiration seen in the cell mito stress tests could be attributed to dysfunction of electron transport chain machinery, glutamine conversion to α -ketoglutarate, or transport of glutamine into the mitochondria. The ability of the HK-2 cells to utilize LCFA is very slightly decreased in response to DA, and this could be explained by accumulation of LCFA as triglycerides within the cytosol. Triglycerides have been shown to accumulate within the cytosol of injured HK-2 cells, thereby decreasing the available LCFA to be utilized as a fuel source (Johnson, Stahl, & Zager, 2005). It is possible that the damage induced by DA at 8 hr is not severe enough to induce a decrease in the ability of the mitochondria to utilize each of the fuel sources, but we can conclude that the observed decrease in mitochondrial function is not due to diminishment of the ability of the mitochondria to utilize the three major fuel sources.

A decrease in observable mitochondrial function in the absence of noticeable impairment of the oxidative machinery or transport of fuel may not indicate direct mitochondrial damage but could be caused by a decrease in the overall number of active mitochondria. Mitochondrial turnover, or mitophagy, is the main source of mitochondrial degeneration and has been

implicated in a number of diseases and conditions including CI-AKI (C. He & Klionsky, 2009; Lei et al., 2018; C. Zhao et al., 2017). The conversion of LC3BI, soluble form, to LC3BII, lipid form, is considered the major determining factor of mitophagy via the direct interaction of LC3 adapters and mitochondrial substrates (Yoo & Jung, 2018). PTEN-induced putative kinase 1 (PINK1) is continuously degraded by matrix processing peptidases within the mitochondria and subsequently cleaved by presenilin-associated rhomboid like (PARL) where it translocates to the cytosol and is entirely degraded (Matsuda et al., 2010). In the presence of mitochondrial membrane damage, the degradation of PINK1 is attenuated and it accumulates on the outer mitochondrial membrane (Park et al., 2015). The ubiquitin ligase Parkin is activated by phosphorylation on the mitochondrial membrane via interactions with PINK1, where it polyubiquinates substrates such as mitofusin I and II (MFS 1/II) (Nguyen, Padman, & Lazarou, 2016; Tanaka et al., 2010). An LC3BI adapter molecule, such as sequestrome-1 (p62), is recruited to the polyubiquinated substrates where it is recognized by LC3BI and tagged for degradation via the autophagosome (Lazarou et al., 2015). Polyubiquinated substrates contain a LC3-interacting region (LIR) in which LC3BI recognizes, binds, and is converted into LC3BII. Therefore, a decrease in the ratio of LC3BI to LC3BII is an indicator of mitophagy.

A study on the role of mitophagy in CI-AKI has already been reported using very high concentrations of RCM in an *in vitro* model. HK-2 cells exposed to 200 mg I/mL of iohexol and iodixanol expressed a statistically different increase in the ratio of LC3BII/LC3BI and an increase in p62 expression demonstrating an increase in mitophagy (Lei et al., 2018). In our study, clinically relevant concentrations of DA induced a significant increase in the ratio of LC3BII/LC3BI within 8 hr of exposure indicating that the diminishment of cellular respiration may not be due to mitochondrial damage but mitophagy. Our studies also suggest that mitophagy

may occur at levels that exist in the PT of a patient during development of CI-AKI. It has been shown that mitophagy may play a role in protecting PT cells from CI-AKI (Lei et al., 2018). Pretreatment of HK-2 cells with the inhibitor of autophagy, 3-methyladenine, resulted in more severe cellular toxicity induced by RCM (Lei et al., 2018). The increase of mitophagy seen in this study potentially explains why conversion of MTT is diminished within 2 hr of DA exposure but cell viability is not decreased until 24 hr.

Disturbances in cellular homeostasis such as alterations in available ATP, redox status, and calcium regulation will result in misfolding or unfolding of proteins within the ER. Accumulation of misfolded or unfolded proteins within the ER activates the UPR and, if the instability is prolonged, will result in ER stress and apoptosis (Faitova, Kreckac, Hrstka, & Vojtesek, 2006). The major purpose of the UPR is to reestablish the delicate balance between protein load and folding capacity of the ER. The ER is sensitive to homeostatic changes due to its dependency on a variety of fuel sources including saccharides for protein modifications, reducing equivalents for disulfide bond formation, and adequate ATP for calcium transport into and out of the ER (Bravo et al., 2013). Glucose-regulated protein 78 (GRP78) is an ER resident molecular chaperone that is considered the master regulator of UPR. Under normal physiological conditions, three ER transmembrane proteins, RNA-dependent protein kinase-like ER kinase (PERK), inositol-requiring ER-to-nucleus signal kinase 1 (IRE1), and activating transcription factor 6 (ATF6), are all kept inactive by interactions with GRP78 (Kim, Emi, Tanabe, & Murakami, 2006). Upon homeostatic disturbance, GRP78 dissociates from PERK, IRE1, and ATF6 where it binds to unfolded or misfolded protein leading to activation of the three proteins. PERK phosphorylates eukaryotic translation initiation factor 2 α (eIF2 α) resulting in attenuation of protein synthesis in an attempt to decrease ER protein load (Kim et al., 2006). Both IRE1 and

ATF6 activation leads to increased expression of ER chaperone genes and ER-associated degradation (ERAD) factors in order to fold or degrade unfolded and misfolded proteins (Kim et al., 2006; Yamamoto et al., 2007). However, if activation of the UPR regulators cannot restore homeostasis and activation of these regulators is extensively prolonged, PERK, IRE1, and ATF6 signals converge to induce transcription of the central proapoptotic transcription factor in ER stress, C/EBP homologous protein (CHOP) (Oyadomari & Mori, 2004). The final step in ER stress is activation of the pro-apoptotic protease located on the outer surface of the ER, caspase 12 (Rawlings & Salvesen, 2013).

ER stress has been shown to play a role in a large number of pathophysiological disorders including the pathogenesis of ischemia/reperfusion injury and CI-AKI (X. Gao et al., 2012). The role of ER stress has been established in HK-2 and NRK-E52 cells exposed to HOCM and LOCM has previously been established. NRK-E52 cells exposed to 60 mg I/mL DA or 100 mg I/mL iopromide resulted in significant increases in GRP78, phosphorylated PERK, phosphorylated eIF2 α , and CHOP expression (Wu et al., 2010; Y. Yang et al., 2014). HK-2 cells treated with 40 mg I/mL of DA induced statistically significant increases in GRP78, ATF4, CHOP, and caspase 12 mRNA levels (P. A. Peng et al., 2015). However, studies in our laboratory concluded that exposing HK-2 cells with clinically relevant concentrations of DA could not induce significant increases in GRP78 expression or the downstream pro-apoptotic protein CHOP. These findings indicate that activation of UPR or ER stress does not play a role in the decrease in cell viability in response to DA exposure. Interestingly, we found that exposure to 28 and 30 mg I/mL induced a significant increase in caspase 12 expression indicating activation of the ER transmembrane bound protease via another mechanism. Although the mechanism of activation of caspase 12 is not entirely understood, the role of cytokines and the

calcium dependent class of proteases called calpains may play a role (Berchtold, Prause, Storling, & Mandrup-Poulsen, 2016).

The levels of calcium within physiological systems is tightly regulated. This regulation is due to the fact that calcium acts as an essential intracellular and extracellular messenger in numerous cellular events such as hormone secretion, muscle contraction, immune responses, activation of neuronal networks, and cell survival and death. Maintenance of extracellular calcium is held in a narrow range of 8.5-10.5 mg/dL and maintaining this range is important for intracellular calcium homeostasis. Approximately 70% of filtered calcium is reabsorbed in the PT via paracellular passive diffusion, intracellular leakage via claudin-2 located within the tight junctions of basolateral membranes (Jeon, 2008), and a small, but significant, amount of calcium is actively transported into the PT (Blaine, Chonchol, & Levi, 2015). Unfortunately, little is known about the mechanism of active transport within the PT, however, preliminary studies indicate that the membrane calcium channel transient receptor potential channel vanilloid 6 (TRPV6) is distributed on the proximal tubule (J. B. Peng, 2019) potentially explaining the source of PT calcium transport.

The central mechanism in maintaining intracellular calcium balance in basically all metazoan cells is store-operated calcium entry (SOCE). SOCE is based on the theory that: 1) cells possess multiple stores of intracellular calcium; 2) endogenous and exogenous agonists can induce release of calcium from these stores; 3) intracellular calcium mobilization will cause calcium efflux from the cell; 4) as time goes on, these stores need to be replenished (Hogan & Rao, 2015). Store-operated calcium channels (SOCCs) are activated in response to calcium release from the ER. G-protein coupled receptor or tyrosine kinase activation in response to binding of an endogenous or exogenous ligand result in activation of phospholipase C (PLC) and

formation of inositol-1,4,5-triphosphate (IP₃). Binding of IP₃ to IP₃ receptors (IP₃R) on the ER membrane induces calcium release into the cytosol (Prakriya & Lewis, 2015). Excess intracellular calcium is then effluxed from the cell via plasma membrane calcium ATPases (PMCAs) and Na⁺/Ca²⁺ exchangers (NCXs) (Guerini, 1998). As the ER luminal space becomes devoid of calcium, the primary ER luminal calcium sensor, stromal interaction molecule 1 (STIM1), is activated and accumulates at ER-plasma membrane junctions (Roos et al., 2005). Accumulation of STIM1 subsequently activates the pore-forming subunit of SOCs, Orai1, and allows influx of calcium (Feske et al., 2006; Vig et al., 2006). As intracellular levels begin to rise, the sarcoplasmic/endoplasmic reticulum calcium ATPases (SERCAs) actively pump calcium back into the ER restoring intracellular calcium to appropriate and defined concentrations (Mekahli et al., 2011).

Aberrant function in intracellular calcium management has been indicated in a range of pathological conditions such as cardiovascular disease, diabetes mellitus, tumorigenesis, steatosis hepatitis, as well as ischemia reperfusion injury and CI-AKI. The relationship between calcium regulation, the ER, and the mitochondria is very complex and may play an important role in RCM-induced cytotoxicity. Soon after the characterization of carbohydrate metabolism and oxidative phosphorylation, it became clear that calcium had a special role in the mitochondrial physiology. Calcium can act as an uncoupler of oxidative phosphorylation because of the mitochondria's ability to efficiently influx and accumulate calcium within the matrix at the expense of energy consumption (Deluca & Engstrom, 1961; Vasington & Murphy, 1962). Quickly thereafter, it was verified that: 1) calcium uptake into the mitochondria is dependent on an energy source such as ATP or other oxidizable substrates; 2) uptake is saturable indicating the existence of a carrier; 3) mitochondrial calcium influx is accompanied by stoichiometric

extrusion of H^+ (Drago, Pizzo, & Pozzan, 2011). It was later discovered that two carriers were involved in mitochondrial calcium influx, the mitochondrial calcium uniporter (MCU) and the H^+/Ca^{2+} antiporter (Brand, Chen, & Lehninger, 1976; Moyle & Mitchell, 1977). In healthy cells, the levels of calcium within the mitochondrial matrix are fairly low and range from 100 nM to 1 μ M (Brinley, Tiffert, Scarpa, & Mullins, 1977; Ivannikov & Macleod, 2013; Somlyo, Bond, & Somlyo, 1985) and influx of calcium only becomes substantial when extramitochondrial calcium concentrations reach approximately 10 μ M (Rizzuto & Pozzan, 2006). Conversely, it was discovered that even though the affinity of the MCU for calcium is very low ($K_d = 20\text{-}30 \mu\text{M}$), the mitochondria are capable of quick and substantial increases in matrix calcium levels, even at physiological increases in intracellular calcium (Rizzuto, Brini, Murgia, & Pozzan, 1993). Rizzuto et al. hypothesized that the discrepancy between low MCU calcium affinity and high efficiency of mitochondrial calcium influx was due to microheterogeneity of cytoplasmic calcium following stimulation. Rizzuto et al. suggested, and later confirmed by Giorgi et al., that the area between the calcium efflux proteins of the ER and MCU of the mitochondria can form a microdomain, later named the mitochondrial-associated membranes (MAMs) (Giorgi et al., 2010). These microdomains of physiologically high concentrations of calcium were established to be approximately 10-20 μ M (Csordas et al., 2010; Giacomello et al., 2010; Rizzuto et al., 1998). These studies indicate that the mitochondria play an important role in intracellular calcium buffering at physiological and pathological concentrations.

Calcium overload within the mitochondria is considered to be one of the main driving factors of cell death. Mitochondrial membrane permeability transition (mPT) is considered the initiator of the intrinsic apoptotic pathway and induction involves numerous factors. The only dogma pertaining to mPT is the accumulation of calcium within the mitochondrial matrix.

Inhibiting calcium influx into the matrix with ruthenium red completely abrogates mPT verifying the role of calcium in mPT (Haworth & Hunter, 1979). Accumulation of large amounts of calcium within the matrix leads to the opening of a large channel within the mitochondrial inner membrane referred to as the mitochondrial membrane permeability transition pore (mPTP). As the mPTP opens, proteins (< 1.5 kD) and solutes flood into the matrix resulting in uncoupling of oxidative phosphorylation, depletion of ATP, and permeabilization of the outer mitochondrial membrane (Hunter, Haworth, & Southard, 1976; Ott et al., 2002). Mitochondrial outer membrane permeability results in leakage of cytochrome c which binds to apoptotic protease activating factor (Apaf1) to form the apoptosome. The apoptosome continues to activate caspase 9 and induce apoptosis (Morgan & Liu, 2010).

The role of calcium homeostasis in the pathogenesis of CI-AKI has been established previously by various laboratories. The Yang group demonstrated that intracellular calcium overload may play a role in ROS overproduction, p38 MAPK activation, and apoptosis in CI-AKI (D. Yang, Yang, Jia, & Ding, 2013; D. Yang, Yang, Jia, & Tan, 2013). Another study determined that exposure to 150 mg I/mL ioversol for 24 hr induced cytochrome c release and activation of caspase 3 in glomerular endothelial cells isolated from adult male Sprague-Dawley rats; however, pretreatment with the intracellular calcium chelator BAPTA-AM (5 μ mol/L) completely attenuated the cytotoxicity (J. Zhao et al., 2009). Our studies confirm the Zhao group findings as pretreatment with BAPTA-AM completely alleviated DA-induced cytotoxicity in HK-2 cells as seen by MTT conversion. Whereas the Zhao study found that the extracellular calcium chelator EGTA had no effect on protecting glomerular endothelial cells from RCM-induced cytotoxicity, pretreating HK-2 cells with EGTA did afford partial protection from DA-induced cytotoxicity (Figure 24). Additionally, pretreatment of HK-2 cells with the IP₃R

antagonist 2-APB also provided partial protection from diminished mitochondrial viability in response to DA exposure (Figure 24). Pretreatment with BAPTA-AM completely abrogated the conversion of LC3BI to LC3BII in response to DA (Figure 26), further suggesting that DA does cause intracellular calcium overload and mitophagy. It is clear from these results that calcium plays a major role in mitochondrial viability; however, the source of this calcium is still in question. It is likely that the DA-induced increase in intracellular calcium is caused by a combination of the release of calcium from the ER and calcium influx through SOCs due to the fact that both EGTA and 2-APB provided partial protection.

Aside from inducing mPT, intracellular calcium overload can also induce cellular damage by other mechanisms. Prolonged surges in intracellular calcium has long been thought to activate a class of calcium-activated non-lysosomal cysteine proteases called calpains (Goll et al., 2003). It is hypothesized that during events of high intracellular calcium, inactive calpain translocates from the cytosol to the ER membrane and autocatalyzes resulting in the dissociation of the 30kD active subunit (K. Suzuki & Sorimachi, 1998). Calpain substrates do not have a specific recognizable amino acid sequence, therefore, a large variety of proteins are targets (Momeni, 2011) including other pro-apoptotic enzymes like caspase 12. In fact, it has been previously shown that activation of caspase 12 requires calpain activation *in vivo* (Nakagawa & Yuan, 2000). Pretreatment with calpain or calpain inhibitor-1 prior to exposure to RCM results in decreased antioxidant activity or reduced renal impairment, respectively, in rats (Baykara et al., 2015; Briguori, Quintavalle, De Micco, & Condorelli, 2011; Chatterjee et al., 2001). Our studies have shown that HK-2 cells exposed to DA for 24 hr induced a two-fold increase in calpain activity and inhibiting calpain activity with calpeptin or chelating intracellular calcium with BAPTA-AM completely abrogated DA-induced calpain activation (Figure 24). To verify the role

of caspase 12 activation by calpain activity, HK-2 cells were pretreated with BAPTA-AM or the calpain inhibitor calpeptin prior to DA exposure. As a result, both BAPTA-AM and calpeptin inhibited the DA-induced increase in caspase 12 expression (Figure 28) indicating that caspase 12 activation takes place in response to intracellular calcium overload and not to ER stress.

Perhaps the most studied topic pertaining to the cytotoxicity of RCM is likely to be oxidative stress. As the production of reactive oxygen species (ROS) overwhelms the ability of a cell's innate antioxidant systems to repress ROS reactivity, the ROS continuously and cumulatively damage the cell via interactions with cellular proteins, DNA, and other cellular structures (Gracy, Talent, Kong, & Conrad, 1999). Sources of ROS production vary but the most common endogenous sources are: 1) as byproducts of cellular metabolism through the electron transport chain (ETC), specifically complexes I and III; 2) one-electron reduction of O₂ through enzymatic catalysis by NADPH oxidase (NOX) or xanthine oxidase (XO); 3) uncoupling of endothelial nitric oxide synthase (eNOS) (Mittal et al., 2014). The mitochondria ETC and NOX are the major sources of ROS generation within a cell (Di Meo, Reed, Venditti, & Victor, 2016; Phaniendra, Jestadi, & Periyasamy, 2015). In response to ROS production, cells have innate antioxidant systems to reduce oxidants to water and O₂. The most common players in the endogenous antioxidant systems include: the enzymatic ROS scavengers superoxide dismutase (SOD), catalase (CAT), glutathione peroxidase (GPx), and glutathione transferase, and the non-enzymatic scavengers glutathione (GSH) (Birben et al., 2012). In the context of CI-AKI, a plethora of studies have been performed to confirm the formation of free radicals and oxidative stress as a result of exposure to RCM (Huang et al., 2016; Liss, Nygren, Erikson, & Ulfendahl, 1998; Quintavalle et al., 2011; Rosenberger, Rosen, & Heyman, 2006); however, very few studies have addressed the source of ROS production. The purpose of this study was to verify

that clinically relevant concentrations do induce an increase in ROS and oxidative stress and identify the source of the excessive generation of ROS.

Protein carbonylation is a generic term used to describe the irreversible interaction between reactive ketones and aldehydes formed in the presence of ROS and the side chains of proteins, specifically lysine, arginine, proline, and threonine (Y. J. Suzuki, Carini, & Butterfield, 2010). This reactive carbonyl moiety will further impede biomolecule function, cause inflammation, cell toxicity, and induce apoptosis. Accumulation of proteins with carbonylated side chains indicates an increase in oxidative stress. Protein carbonyls can be recognized via derivatization with 2,4-dinitrophenylhydrazine (DNPH) to form hydrazones that can be detected using antibodies against DNPH-derivatized proteins (Levine, Williams, Stadtman, & Shacter, 1994). A more specific biomarker for oxidative stress is the formation of protein-bound carbonyls induced by excessive lipid peroxidation. Most lipid peroxidation products are strong electrophiles and readily form Michael adducts with lysine, cysteine, and histidine side chains (Fedorova, Bollineni, & Hoffmann, 2014). The primary α,β -unsaturated hydroxalkenal formed during lipid peroxidation, 4-HNE, is one of the most commonly used biomarkers for oxidative stress and can easily be detected via immunoblotting.

Our studies indicate that exposure to clinically relevant concentrations of DA induced oxidative stress in HK-2 cells as shown by an increase in protein carbonylation and 4-hydroxyl-nonenal (4-HNE) protein adduct formation within 24 hr at 18 mg I/mL; however, no increase in oxidative stress was apparent within 8 hr. It is hypothesized that a major portion of direct cytotoxicity induced by RCM is caused by oxidative stress; our results indicate mitochondrial turnover at an earlier time point. Therefore, at clinically relevant concentrations, the increase in

oxidative stress is not the initial or sole cause of HK-2 cytotoxicity but is due to damage that is already taking place within the cell.

The major source of endogenous ROS production is complex I and complex III of the electron transport chain within the mitochondria. Under normal physiological conditions, ROS generated in the mitochondria are involved in cellular crosstalk, signal integration of cell proliferation, differentiation, inflammation, repair, and apoptotic pathways (Li et al., 2017). However, in circumstances of perturbances in cellular homeostasis, such as alterations in NADH/NAD⁺ ratio, metabolic disturbances, or mitochondrial membrane damage, mitochondrial ROS generation surges (Li et al., 2013). Within the mitochondria of an affected cell, electrons leak from the intermembrane space at complex I and complex III where it interacts with O₂ to yield superoxide (O₂^{•-}) radical. The mitochondria have an internal system to dispose of excess ROS that includes manganese superoxide dismutase (MnSOD) which dismutates O₂^{•-} into H₂O₂ and glutathione peroxidase (GPx) which fully reduces H₂O₂ into water (Li et al., 2013). The mitochondria are at a disadvantage, however, due to the fact that it lacks catalase, a H₂O₂ reducing enzyme, and depends on the reduction of glutathione disulfide to glutathione via glutathione reductase (GR) to reduce H₂O₂. As concentrations of the reducing equivalent NADPH decrease and glutathione disulfide increase, the antioxidant system within the mitochondria become overwhelmed (Sung et al., 2013). Once the antioxidant systems become overwhelmed, ROS interactions disrupt the mitochondrial membrane potential and permeability transition is eminent. As previously mentioned, mitochondrial outer membrane permeability results in leakage of cytochrome c which binds to apoptotic protease activating factor (Apaf1) to form the apoptosome. A study performed by Lei et al. indicated that exposure of HK-2 cells to 200 mg I/mL iodixanol or iohexol induced statistically significant increases in mitochondrial

ROS production as shown by mitoSOX and TMRE staining (Lei et al., 2018). Our studies indicate that exposure of HK-2 cells to clinically relevant concentrations of DA induced the opposite effect. In fact, we noticed no change in 4-HNE protein adduct formation or protein carbonylation within the mitochondria and the statistically significant increases in 4-HNE adduction and protein carbonylation takes place solely within the cytosol. To verify these findings, SOD activity assays were performed. We discovered that there was no change in MnSOD expression or activity, and the overall decrease in SOD activity was due, entirely, to a decrease in activity of the cytosolic SOD, Cu/ZnSOD.

The role of the cytokine tumor necrosis factor alpha (TNF α) was measured in response to DA exposure as a possible initiator of ROS generation. TNF α is an important cytokine in inflammation and is involved in many cellular responses including pro-survival and pro-apoptotic pathways that have been shown to be affected in response to RCM exposure (Saritemur et al., 2015). TNF α has been shown to induce ROS production in a number of different pathways but most noticeably is through activation of NOX, specifically NOX4, in renal parenchymal cells (Sedeek, Nasrallah, Touyz, & Hebert, 2013). TNF α induces an increase in various NADPH oxidase components such as the NOX regulatory proteins p22phox and p47phox, NADPH oxidase organizer 1 (NOXO1) and NOX4 (De Keulenaer et al., 1998; Moe et al., 2006; Yoshida & Tsunawaki, 2008). A study performed by Jeong et al. demonstrated that exposing HK-2 cells to 150 μ M iohexol induced statistically significant increases in NOX4 within 5 min; however, the group did not verify if the increase in NOX4 induced an increase in ROS at this time point (Jeong et al., 2018). In response to clinically relevant concentrations of DA, a statistically significant increase in TNF α in cell media and decrease in TNF α in cell lysate of HK-2 cells was apparent, indicating that DA does induce a mild inflammatory response *in vitro*.

However, NOX4 expression was unaffected in response to the increase in active TNF α . From these results, we can conclude that although TNF α is activated in response to DA exposure, the intracellular signaling is not strong enough to induce NOX4 transcription or activation. We can also conclude that TNF α and NOX4 are not playing a role in ROS generation or apoptosis in HK-2 cells.

Excessive ROS generation induced by intracellular calcium dysregulation may play a role in CI-AKI. Intracellular calcium levels have been linked to ROS production in response to RCM (D. Yang, Yang, Jia, & Ding, 2013; D. Yang, Yang, Jia, & Tan, 2013). Calcium induced ROS production is linked to the interactions between mitochondrial calcium and increased ATP production and ROS generation, and calcium induced activation of NOX (Gorlach, Bertram, Hudecova, & Krizanova, 2015). However, our studies indicate that there is no change in NOX4 activation and mitochondrial oxidative stress in response to DA exposure (Figure 20, Figure 21). Calcium may be inducing ROS production via calpain activation. In diabetic mouse and human umbilical vein endothelial cells, activation of calpain correlated with an increase in ROS production; whereas, transgenic mice over-expressing the endogenous calpain inhibitor calpastatin experienced significant reduction in ROS production (B. Chen et al., 2014). Our study indicates that pretreatment with BAPTA-AM or calpeptin completely abrogates 4-HNE adduct formation; however, protein carbonylation is not decreased to a significant degree. From these results, it can be concluded that the increase in lipid peroxidation that takes place in response to DA exposure is linked to calcium dysregulation and calpain activity.

Apoptosis can be induced via two main pathways: the mitochondrial, or intrinsic, pathway; the ligand-mediated, or extrinsic, pathway. Both pathways involve two types of caspases: the initiator caspases (caspase 2, 4, 8, 9, 10, 11, and 12) and the effector caspases

(caspase 3, 6, 7). Activation of specific apoptotic pathways can be determined by measuring the appropriate caspase. Cleavage of caspase 9, for example, occurs in response to activation of the apoptosome and can be used as a determinant of initiation of the intrinsic apoptotic pathway. The apoptosome will then interact with and cleave executioner caspases such as caspase 3 resulting in programmed cell death. As previously mentioned, exposure to DA induces an increase in expression of the initiator caspase, caspase 12; however, caspase 12 activation occurs in the absence of initiation of the UPR or ER stress. Caspase 4 was measured as an indicator of the extrinsic apoptotic pathway. Caspase 4 is in response to binding of TNF α to the TNF α receptor 1 (TNFR1), activation of the TNF α receptor-associated death domain (TRADD), and induction of extrinsic apoptosis. Caspase 4 has also been linked to ER stress linked apoptosis. HK-2 cells exposed to clinically relevant concentration of DA for 24 hr experience a statistically significant increase in TNF α activation but there was no noticeable change in caspase 4, indicating that ER stress and the extrinsic apoptotic pathway do not play roles in DA-induced apoptosis. Cleavage of caspase 3 was statistically increased in response to clinically relevant concentrations of DA, indicating that apoptosis is occurring within 24 hr and mitochondrial dysfunction may be the major contributing factor to the decrease in cell viability as seen by leakage of cytochrome c and the increase in mitophagy.

CONCLUSION

This study provides additional insight into the mechanisms of DA-induced renal epithelial cytotoxicity. DA induces a decrease in mitochondrial and cell viability within 2 hr and 24 hr, respectively, as shown by MTT assays and trypan blue exclusion studies. Exposure to DA resulted in a decrease in basal and maximal respiration, spare respiratory capacity and ATP production within 8 hr as seen by changes in OCR and ECAR in Seahorse XFe assays; however,

the ability of the mitochondria to utilize the three major fuel sources (glucose, glutamine, and fatty acid oxidation) was unchanged, indicating that the decrease in mitochondrial respiration could be due to an increase in mitophagy. The ratio of LC3BII/I was increased after 8 hr exposure demonstrating that DA does, in fact, increase mitochondrial turnover. An increase in oxidative stress was apparent within the cytosol but not in the mitochondria as shown by protein carbonylation and 4-HNE protein adduct formation. Exposure to DA induced no change in MnSOD expression or activity confirming that the source of ROS overproduction is not within the mitochondria. Alternatively, the activity of Cu/ZnSOD was decreased in response to DA exposure. The role of TNF α in DA-induced cytotoxicity was evaluated by measuring NOX4 and caspase 4 expression but no change was detected. Therefore, the source of ROS overproduction remains elusive at this time. Caspase 3 and 12 activation was evident following a 24 hr exposure of HK-2 cells to clinically relevant concentrations of DA indicating that DA is inducing apoptosis. Caspase 12 expression is increased despite the fact that these concentrations of DA do not induce the UPR or ER stress as shown by GRP78 and CHOP expression. Pretreatment of HK-2 cells with calcium concentration modulators such as BAPTA-AM, EGTA, and 2-APB resulted in partial or complete protection from DA-induced mitochondrial toxicity demonstrating that calcium dysregulation plays a crucial role in CI-AKI. To determine if calpains play a role in caspase 12 activation, calpain activity assays were performed and determined that HK-2 cells exposed to 30 μ M DA induces an increase in calpain activity. Pretreatment with BAPTA-AM completely abrogated the activation of calpain, caspase 12 activation, and the increase in 4-HNE adduct formation in response to DA exposure. Additional studies need to be conducted to determine the sources of ROS overproduction and calcium dysregulation, as well as the role of calcium in cellular homeostasis in response to RCM.

ACKNOWLEDGMENTS

This work was supported by NIH Grant P20GM103434 to the West Virginia IDeA Network for Biomedical Research Excellence. Dakota B. Ward was supported by a graduate fellowship from the West Virginia NASA Space Grant Consortium.

CHAPTER 4: SUMMARY, CONCLUSIONS, AND FUTURE DIRECTIONS

As the research for my dissertation comes to an end, my interest in CI-AKI and renal pathology has only been reinforced in the last five years. RCM are one of the most commonly administered drugs in a clinical setting and administration is only going to increase further in the future. As advances in human longevity are continuously made, the need for radiopaque diagnostic procedures will rise alongside, and cases of CI-AKI will increase as a result. Discovering the exact mechanisms of RCM-induced renal cytotoxicity are particularly relevant, as the overall number of patients with conditions causing advanced renal impairment such as diabetes mellitus, congestive heart failure, and advanced age are rising. The general goal of this project was to determine the mechanism of DA-induced proximal tubule cytotoxicity and to explore potential methods to alleviate this toxicity. My work provides insight into these mechanisms as well as evidence that pretreatment with calcium modulators mitigate this toxicity; this evidence warrants further study and may have potential clinical implications.

CLINICALLY RELEVANT CONCENTRATIONS OF DA IS CYTOTOXIC TO HK-2 CELLS

The vast majority of studies pertaining to the discovery of the mechanisms of direct toxicity of RCM use concentrations that greatly exceed the concentrations within the kidney following RCM administration. It is not uncommon for studies to use concentrations that exceed twenty-fold the normal plasma levels of RCM following clinical administration in *in vitro* experiments. During a routine radiopaque imaging procedure, 45-150 mg I/mL RCM are administered intravenous for a 75 kg man and these concentrations can double as patients' weight increase. It is at the clinician's discretion to select the appropriate amount of RCM to use during these procedures, and the effective termination limit of a 76% DA preparation is 300mL (Skucas, 1989). For a 75kg adult male, blood plasma levels will range from ~4 to 15 mg I/mL

but can reach as high as 30 mg I/mL as administered volumes increase (Lusic & Grinstaff, 2013). Mechanistic studies attempting to determine the mechanisms of cytotoxicity frequently expose *in vitro* models to concentrations of RCM well over 100 mg I/mL. In a study to determine the role of NOX4 and oxidative stress in response to RCM, HK-2 cells were exposed to 150 mg I/mL of iohexol (Jeong et al., 2018). The Yang group exposed NRK-52E cells to 150 mg I/mL of iopromide to determine the effects of RCM on the induction of ER stress (Y. Yang et al., 2014). Multiple studies attempting to verify the origin of cytotoxicity expose various models to 200 mg I/mL RCM (X. He et al., 2016; Netti et al., 2014; Quintavalle et al., 2011). It is possible that exposing cells to concentrations of RCM of this magnitude is inducing changes in cellular homeostasis that would not occur at clinically relevant concentrations of RCM. Therefore, the conclusions obtained from the results of these previous studies may be misleading.

In this study, a wide range of clinically relevant DA concentrations (0, 2, 5, 10, 15, 18, 23, 28, and 30 mg I/mL) were chosen to encompass what the kidney would experience following one of the plethora of imaging procedures used today. In response to clinically relevant concentrations of DA, mitochondrial and cell viability was diminished in HK-2 cells in a time-dependent and concentration-dependent manner. Therefore, concentrations of DA that the normal, healthy kidney would experience in a clinical setting induce cytotoxicity, and this model can be used to examine the mechanisms of toxicity without the compounding *in situ* factors that are involved in CI-AKI.

DA ALTERS MITOCHONDRIAL FUNCTION AND INDUCES MITOPHAGY IN HK-2 CELLS

Renal PT cells have high energy demands in order to maintain normal cellular function. To sustain appropriate levels of ATP, PT cells have the second highest mitochondrial density within the body (Bhargava & Schnellmann, 2017). A decline in basal respiration and maximal

respiration, and subsequent decrease in ATP production, in response to DA exposure would impair cellular homeostasis. Our studies determined that DA induces a global decrease in mitochondria-linked oxygen consumption resulting in diminished ATP production within 8 hr and 24 hr exposure at 23 and 15 mg I/mL, respectively (Figure 10, Chapter 3) as shown by Seahorse XFe cell mito stress tests. The Seahorse ATP-rate assay was utilized to determine if the decrease in ATP production was due partially to an interaction between DA and glycolysis. Exposure of HK-2 cells to DA does not induce a statistically significant change in ATP linked to glycolysis (Figure 11, Chapter 3) and the decrease in total ATP production was due to the decrease in mitochondria-linked ATP production (Figure 11, Chapter 3). In an effort to determine the source of mitochondrial dysfunction, the Seahorse mito fuel flex test was used. This assay measures mitochondrial fuel utilization and represents changes in cellular machinery. Exposure to DA did not affect the ability of HK-2 cells to utilize any of the three major fuel sources (Figure 12, Chapter 3) indicating that DA does not alter the function of glycolytic or mitochondrial energy utilization machinery.

A global decrease in mitochondria-linked oxygen consumption in response to DA could indicate that DA is not directly damaging the mitochondria but inducing mitophagy via alternative mechanisms. One study utilizing Seahorse technology determined that an increase in mitophagy induced by metabolic acidosis in ammonium chloride treated transgenic mice containing green fluorescence protein tagged LC3 resulted in a global decrease in OCR in renal PTs (Namba et al., 2014). To determine if an increase in mitochondrial turnover is taking place, the expression of the biomarker for mitophagy, LC3B, was measured. HK-2 cells exposed to DA experienced a statistically significant increase in the ratio of LC3BII/I at 8 and 24 hr (Figure 13 and 12, Chapter 3) indicating that DA induces an increase in mitophagy. The increase in

mitophagy, i.e. a decrease in the total number of viable mitochondria, could explain the decrease in the mitochondria-linked OCR and ATP production.

DA CAUSES OXIDATIVE STRESS IN HK-2 CELLS

In this study, we probed HK-2 cell whole cell lysate for the biomarkers of oxidative stress, protein carbonylation, and 4-HNE protein adduct formation. An imbalance between the production and removal of ROS in the favor of the former results in oxidative damage and stress (Birben et al., 2012). Various studies have indicated that exposure to RCM induces oxidative stress *in vitro*; however, this is the first study to show that clinically relevant blood plasma levels of DA cause oxidative stress in HK-2 cells. The concentrations in the higher range of what is considered clinically relevant induced a 50% increase in protein carbonylation and a subtle but significant increase in 4-HNE protein adduction formation within 24 hr (Figure 17 and 16, Chapter 3).

We further investigated the oxidative damage following DA exposure in mitochondrial fractions. Previous studies have indicated that the mitochondria might be a potential target for DA-induced toxicity. Studies performed on PT isolated from New Zealand white rabbits exposed to approximately 160 mg I/mL DA or iopamidol demonstrated mitochondrial damage in the form of decreased basal respiration, uncoupled respiration, and ATP production (Humes et al., 1987; Messana et al., 1988). It is important to mention that although these studies expose PT cells to 25mM DA or iopamidol, which is within the clinically relevant range, the cells were incubated with or without hypoxic conditions. Only the PT cells that encountered concomitant hypoxia experienced significantly greater metabolic alterations compared to control conditions, indicating that the HK-2 cell model is more susceptible to DA induced cytotoxicity than PT collected from New Zealand white rabbits. Our studies show that exposure to clinically relevant concentrations

of DA does not induce oxidative stress within the mitochondria. No change in protein carbonylation or 4-HNE protein adduct formation was evident within 24 hr (Figure 20, Chapter 3).

To verify these findings, total SOD, MnSOD, and Cu/ZnSOD activity assays were performed to determine the effect of DA exposure on HK-2 cell antioxidant systems. MnSOD is a nuclearly encoded antioxidant enzyme found specifically in the mitochondria responsible for the detoxification of $O_2^{\cdot-}$. Multiple studies indicate that exposure to RCM decrease MnSOD activity *in vivo* and *in vitro* (Gong et al., 2016; Jeong et al., 2018; Tasanarong et al., 2014); however, the concentrations of RCM used in these studies were at least 150 mg I/mL, well above clinical relevance. Our studies indicate that exposure to DA results in a significant decrease in total SOD activity caused solely by diminished activity of the cytosolic SOD, Cu/ZnSOD. No change in activity was noticed in MnSOD (Figure 19, Chapter 3). To further verify that DA exposure had no effect on mitochondrial antioxidant capability, MnSOD expression was measured as well. As before, there was no noticeable change in MnSOD expression (Figure 19, Chapter 3). These results are contradictory to previously published data indicating that the initial source of oxidative stress is not within the mitochondria but via an alternative mechanism within the cytosol.

TNF α is a pro-inflammatory cytokine that is expressed in PT epithelial cells and secreted in the inflammatory response to exogenous compounds (Gu et al., 2016). Binding of TNF α to TNFR1 can induce oxidative stress by downstream activation of NOXs and mitochondrial involvement (Morgan & Liu, 2010). TNF α levels have been seen to rise in response to various toxicants and ischemia alongside oxidative stress, activation of the inflammatory response, and apoptosis (Gong, Ivanov, Davidson, & Hei, 2015; Zager, Johnson, & Geballe, 2007). We

examined TNF α as a potential initiator of oxidative stress. Our studies showed that TNF α was released into the media and cell lysates showed diminished expression at 24 hr (Figure 21, Chapter 3). To verify the role of TNF α in the induction of oxidative stress and apoptosis, NOX4 and caspase 4 expression were measured. Although there was a statistically significant increase in TNF α release into the media, no change in NOX4 or caspase 4 expression was apparent (Figure 21, Chapter 3) indicating that it is unlikely that TNF α plays a role in the observed oxidative stress or loss of cell viability noticed in response to DA exposure.

DA INDUCES APOPTOSIS IN HK-2 CELLS

Our study shows that a loss of cell viability occurs in HK-2 cells following a 24 hr exposure period to 23-30 mg I/mL DA. Cytochrome c leakage from the mitochondrial inner membrane space into the cytosol induces apoptosis by binding to the apoptotic protease activating factor 1 (Apaf-1) to form a complex that binds to and activates caspase 9 leading to caspase 3 activation (Jiang & Wang, 2000; X. Liu et al., 1996). Following a 24 hr exposure to clinically relevant concentrations of DA, there is an observable release of cytochrome c into the cytosol and a statistically significant increase in caspase 3 cleavage (Figure 22 and 21, Chapter 3). Alternatively, DA exposure also induces an increase in expression of caspase 12 (Figure 23, Chapter 3). Although the mechanism of caspase 12 activation is not fully understood, interaction with calpains on the ER membrane surface (Tan et al., 2006) or via the IRE-xBP1 pathway (Faitova et al., 2006) have been hypothesized. Our results indicate that caspase 12 activation induced by exposure to DA occurs via calpain activity and in the absence of components of ER stress (Figure 15, 14, and 26, Chapter 3). These results indicate that clinically relevant concentrations of DA causes calcium dysregulation and mitochondrial dysfunction that initiates apoptosis.

DA CAUSES DYSREGULATION OF CALCIUM HOMEOSTASIS IN HK-2 CELLS

Intracellular calcium concentrations are tightly regulated as calcium acts as an essential intracellular and extracellular messenger in numerous cellular events such as hormone secretion, muscle contraction, immune responses, activation of neuronal networks, and cell survival and death. A rise in intracellular calcium levels can induce a variety of cellular responses including induction of mitophagy, activation of a class of calcium-dependent cysteine proteases called calpains, or activation of mitochondrial membrane permeability transition, induction of the mitochondrial membrane transition pore, and induce cytochrome c release from the inner membrane space (Hunter et al., 1976; Ott et al., 2002).

Our study demonstrates that exposure of HK-2 cells to DA causes dysregulation of intracellular calcium concentrations as shown by the results of the MTT assays with calcium chelators (Figure 24, Chapter 3). Pretreatment of cells with BAPTA-AM, EGTA, or 2-APB provides partial or total protection from DA-induced decreases in mitochondrial viability. The intracellular calcium chelator, BAPTA-AM, completely abrogated DA-induced mitochondrial damage indicating that DA causes dysregulation of intracellular calcium concentrations. To determine the source of excess intracellular calcium, the extracellular calcium chelator, EGTA, and the IP₃R antagonist, 2-APB, were used. Both compounds provide partial protection indicating that calcium influx from outside the cell and calcium released from the ER both play a role in DA-induced calcium dysregulation. Prolonged increases in intracellular calcium activates calpains which are pro-apoptotic proteases. Calpain activity is increased two-fold in response to exposure to DA for 24 hr (Figure 25, Chapter 3) in HK-2 cells. To determine if calpain activity is linked to oxidative stress and caspase 12 activation, HK-2 cells were pretreated with BAPTA-

AM or the calpain inhibitor, calpeptin. BAPTA-AM completely inhibited calpain activity, as well as abrogated the activation of caspase 12 in response to DA exposure.

CONCLUSIONS

Bridging the gap in knowledge pertaining to the mechanistic understanding of DA-induced PT cytotoxicity is critical in determining clinical applications of preventing CI-AKI. We have determined that DA diminishes mitochondrial and cell viability with 2 and 24 hr, respectively. DA exposure induces aberrant regulation of intracellular calcium by intracellular and extracellular means. Calcium dysregulation within the PT induces an increase in mitophagy, cellular energy depletion, a loss in mitochondrial membrane integrity, and activation of calpains. The combination of calcium dysregulation and mitochondrial dysfunction results in a secondary response of lipid peroxidation and protein carbonylation. Loss of mitochondrial membrane integrity leads to cytochrome c leakage into the cytosol and activation of the executioner caspase, caspase 3. Calpain activation near the ER activates caspase 12 furthering the apoptotic cell signals in response to DA exposure (Chapter 3, Figure 29). Pretreatment of HK-2 cells with an intracellular or extracellular calcium chelator, or IP₃R antagonist protects against DA-induced cytotoxicity within 24 hr. There are currently several intracellular calcium modulators available on the market and further studies are warranted to determine the role of these drugs in preventing CI-AKI.

FUTURE DIRECTIONS

My study was the first to intensively investigate the mechanisms of cytotoxicity induced by clinically relevant concentrations of DA. Certain conclusions can be made from the results obtained from this study; however, many questions are still left unanswered. Several things still remain unknown such as the initial mechanisms of calcium dysregulation and ROS production.

The role of the IP₃R-induced calcium efflux from the ER has been partially established in this study; however, there are various other calcium transport mechanisms. The sodium calcium exchanger (NCX), voltage-dependent anion channels (VDAC), and SERCA all transport calcium into and out of numerous compartments of the cell and could play a role in DA-induced cytotoxicity. More work needs to be done to determine if these transporters play a role in CI-AKI. Although this study eliminates the mitochondria and NOX4 as potential sources of ROS overproduction, the initial source still eludes us. Additional research needs to be conducted to determine the role of calcium dysregulation and oxidative stress in regard to RCM exposure. Finally, calcium dysregulation, mitophagy, and ER stress are mechanisms that are co-dependent under normal circumstances. However, during DA-induced cytotoxicity, calcium dysregulation and mitochondrial turnover take place in the absence of ER stress. Further studies need to be performed to determine intracellular calcium concentrations within the different cellular compartments to verify the findings of this study. As previously mentioned, there are currently several intracellular calcium modulators such as calcium channel blockers. Several studies have shown various results pertaining to the use of calcium modulators and CI-AKI and more research is needed to determine the efficacy of calcium channel blockers (Beyazal, Caliskan, & Utac, 2014; Oguzhan et al., 2013; Quintavalle et al., 2013).

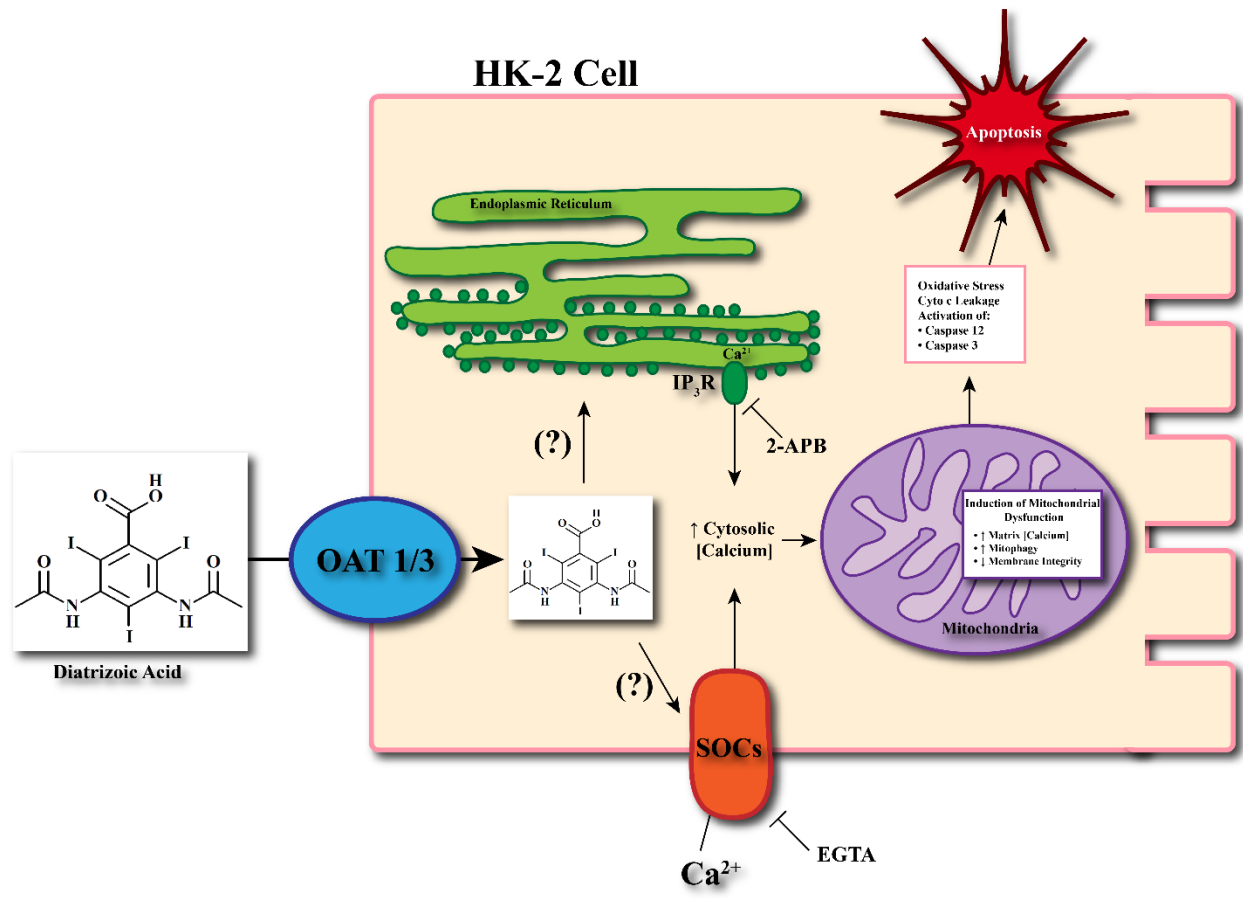


Figure 29. Summary of DA-induced cytotoxicity. DA enters the proximal tubule cell via the OAT 1/3 transporters. Through an unknown mechanism, DA induces the release of calcium from the ER and influx via the store-operated calcium entry. As a result, calcium accumulates within the mitochondrial matrix where it induces the conversion of LC3BI to LC3BII triggering mitophagy. Prolonged periods of calcium accumulation within the mitochondria induces mitochondrial membrane transition and permeability, leakage of cytochrome c, activation of the intrinsic apoptotic pathway. Intracellular calcium overload in response to DA also induces calpain activity and activation of caspase 12, furthering the apoptotic cascade. Extracellular and intracellular modulation can attenuate DA-induced cytotoxicity.

REFERENCES

- Alobaidi, R., Basu, R. K., Goldstein, S. L., & Bagshaw, S. M. (2015). Sepsis-associated acute kidney injury. *Semin Nephrol*, 35(1), 2-11. doi:10.1016/j.semnephrol.2015.01.002
- Amersham-Health. (2007). Hypaque (diatrizoate meglumine) [Package Insert]. Princeton, NJ.
- Andersen, K. J., Christensen, E. I., & Vik, H. (1994). Effects of iodinated x-ray contrast media on renal epithelial cells in culture. *Invest Radiol*, 29(11), 955-962.
- Andersen, K. J., Vik, H., Eikesdal, H. P., & Christensen, E. I. (1995). Effects of contrast media on renal epithelial cells in culture. *Acta Radiol Suppl*, 399, 213-218.
- Anderson, C. C., Aivazidis, S., Kuzyk, C. L., Jain, A., & Roede, J. R. (2018). Acute Maneb Exposure Significantly Alters Both Glycolysis and Mitochondrial Function in Neuroblastoma Cells. *Toxicol Sci*, 165(1), 61-73. doi:10.1093/toxsci/kfy116
- Andreucci, M., Faga, T., Pisani, A., Sabbatini, M., & Michael, A. (2014). Acute kidney injury by radiographic contrast media: pathogenesis and prevention. *Biomed Res Int*, 2014, 362725. doi:10.1155/2014/362725
- Andreucci, M., Solomon, R., & Tasanarong, A. (2014). Side effects of radiographic contrast media: pathogenesis, risk factors, and prevention. *Biomed Res Int*, 2014, 741018. doi:10.1155/2014/741018
- Angus, D. C., & van der Poll, T. (2013). Severe sepsis and septic shock. *N Engl J Med*, 369(9), 840-851. doi:10.1056/NEJMra1208623
- Arend, L. J., Bakris, G. L., Burnett, J. C., Jr., Megerian, C., & Spielman, W. S. (1987). Role for intrarenal adenosine in the renal hemodynamic response to contrast media. *J Lab Clin Med*, 110(4), 406-411.
- Banerjee, A. K., Grainger, S. L., & Thompson, R. P. (1990). Trial of low versus high osmolar contrast media in endoscopic retrograde cholangiopancreatography. *Br J Clin Pract*, 44(11), 445-447.
- Barrett, B. J., & Parfrey, P. S. (1994). Prevention of nephrotoxicity induced by radiocontrast agents. *N Engl J Med*, 331(21), 1449-1450. doi:10.1056/NEJM199411243312111
- Bartels, E. D., Brun, G. C., Gammeltoft, A., & Gjorup, P. A. (1954). Acute anuria following intravenous pyelography in a patient with myelomatosis. *Acta Med Scand*, 150(4), 297-302.
- Baykara, M., Silici, S., Ozcelik, M., Guler, O., Erdogan, N., & Bilgen, M. (2015). In vivo nephroprotective efficacy of propolis against contrast-induced nephropathy. *Diagn Interv Radiol*, 21(4), 317-321. doi:10.5152/dir.2015.14075

- Berchtold, L. A., Prause, M., Storling, J., & Mandrup-Poulsen, T. (2016). Cytokines and Pancreatic B-Cell Apoptosis In G. S. Makowski (Ed.), *Advances in Clinical Chemistry* (pp. 99-158). New York, NY.
- Berns, A. S. (1989). Nephrotoxicity of contrast media. *Kidney Int*, 36(4), 730-740.
- Beyazal, H., Caliskan, Z., & Utac, C. (2014). Comparison of effects of isotonic sodium chloride with diltiazem in prevention of contrast-induced nephropathy. *Ren Fail*, 36(3), 351-355. doi:10.3109/0886022X.2013.866016
- Bhargava, P., & Schnellmann, R. G. (2017). Mitochondrial energetics in the kidney. *Nat Rev Nephrol*, 13(10), 629-646. doi:10.1038/nrneph.2017.107
- Birben, E., Sahiner, U. M., Sackesen, C., Erzurum, S., & Kalayci, O. (2012). Oxidative stress and antioxidant defense. *World Allergy Organ J*, 5(1), 9-19. doi:10.1097/WOX.0b013e3182439613
- Blaine, J., Chonchol, M., & Levi, M. (2015). Renal control of calcium, phosphate, and magnesium homeostasis. *Clin J Am Soc Nephrol*, 10(7), 1257-1272. doi:10.2215/CJN.09750913
- Bottinor, W., Polkampally, P., & Jovin, I. (2013). Adverse reactions to iodinated contrast media. *Int J Angiol*, 22(3), 149-154. doi:10.1055/s-0033-1348885
- Bradford, M. M. (1976). A rapid and sensitive method for the quantitation of microgram quantities of protein utilizing the principle of protein-dye binding. *Anal Biochem*, 72, 248-254.
- Brand, M. D., Chen, C. H., & Lehninger, A. L. (1976). Stoichiometry of H⁺ ejection during respiration-dependent accumulation of Ca²⁺ by rat liver mitochondria. *J Biol Chem*, 251(4), 968-974.
- Bravo, R., Parra, V., Gatica, D., Rodriguez, A. E., Torrealba, N., Paredes, F., . . . Lavandero, S. (2013). Endoplasmic reticulum and the unfolded protein response: dynamics and metabolic integration. *Int Rev Cell Mol Biol*, 301, 215-290. doi:10.1016/B978-0-12-407704-1.00005-1
- Briguori, C., Airoldi, F., D'Andrea, D., Bonizzoni, E., Morici, N., Focaccio, A., . . . Colombo, A. (2007). Renal Insufficiency Following Contrast Media Administration Trial (REMEDIAL): a randomized comparison of 3 preventive strategies. *Circulation*, 115(10), 1211-1217. doi:10.1161/CIRCULATIONAHA.106.687152
- Briguori, C., Colombo, A., Violante, A., Balestrieri, P., Manganelli, F., Paolo Elia, P., . . . Ricciardelli, B. (2004). Standard vs double dose of N-acetylcysteine to prevent contrast agent associated nephrotoxicity. *Eur Heart J*, 25(3), 206-211. doi:10.1016/j.ehj.2003.11.016

- Briguori, C., Quintavalle, C., De Micco, F., & Condorelli, G. (2011). Nephrotoxicity of contrast media and protective effects of acetylcysteine. *Arch Toxicol*, *85*(3), 165-173. doi:10.1007/s00204-010-0626-5
- Brinley, F. J., Jr., Tiffert, T., Scarpa, A., & Mullins, L. J. (1977). Intracellular calcium buffering capacity in isolated squid axons. *J Gen Physiol*, *70*(3), 355-384.
- Brown, J. R., Rezaee, M. E., Nichols, E. L., Marshall, E. J., Siew, E. D., & Matheny, M. E. (2016). Incidence and In-Hospital Mortality of Acute Kidney Injury (AKI) and Dialysis-Requiring AKI (AKI-D) After Cardiac Catheterization in the National Inpatient Sample. *J Am Heart Assoc*, *5*(3), e002739. doi:10.1161/JAHA.115.002739
- Brown, J. R., Robb, J. F., Block, C. A., Schoolwerth, A. C., Kaplan, A. V., O'Connor, G. T., . . . Malenka, D. J. (2010). Does safe dosing of iodinated contrast prevent contrast-induced acute kidney injury? *Circ Cardiovasc Interv*, *3*(4), 346-350. doi:10.1161/CIRCINTERVENTIONS.109.910638
- Cavaillon, J. M., Adib-Conquy, M., Fitting, C., Adrie, C., & Payen, D. (2003). Cytokine cascade in sepsis. *Scand J Infect Dis*, *35*(9), 535-544. doi:10.1080/00365540310015935
- Chatterjee, P. K., Brown, P. A., Cuzzocrea, S., Zacharowski, K., Stewart, K. N., Mota-Filipe, H., . . . Thiernemann, C. (2001). Calpain inhibitor-1 reduces renal ischemia/reperfusion injury in the rat. *Kidney Int*, *59*(6), 2073-2083. doi:10.1046/j.1523-1755.2001.00722.x
- Chen, B., Zhao, Q., Ni, R., Tang, F., Shan, L., Cepinskas, I., . . . Peng, T. (2014). Inhibition of calpain reduces oxidative stress and attenuates endothelial dysfunction in diabetes. *Cardiovasc Diabetol*, *13*, 88. doi:10.1186/1475-2840-13-88
- Chen, S. Q., Liu, Y., Bei, W. J., Wang, Y., Duan, C. Y., Wu, D. X., . . . Li, L. W. (2018). Optimal hydration volume among high-risk patients with advanced congestive heart failure undergoing coronary angiography. *Oncotarget*, *9*(34), 23738-23748. doi:10.18632/oncotarget.25315
- Chertow, G. M., Burdick, E., Honour, M., Bonventre, J. V., & Bates, D. W. (2005). Acute kidney injury, mortality, length of stay, and costs in hospitalized patients. *J Am Soc Nephrol*, *16*(11), 3365-3370. doi:10.1681/ASN.2004090740
- Cho, D. H., Nakamura, T., & Lipton, S. A. (2010). Mitochondrial dynamics in cell death and neurodegeneration. *Cell Mol Life Sci*, *67*(20), 3435-3447. doi:10.1007/s00018-010-0435-2
- Cho, J. Y., Jeong, M. H., Hwan Park, S., Kim, I. S., Park, K. H., Sim, D. S., . . . Kang, J. C. (2010). Effect of contrast-induced nephropathy on cardiac outcomes after use of nonionic isosmolar contrast media during coronary procedure. *J Cardiol*, *56*(3), 300-306. doi:10.1016/j.jjcc.2010.07.002

- Chung, D. M., Kim, J. H., & Kim, J. K. (2015). Evaluation of MTT and Trypan Blue assays for radiation-induced cell viability test in HepG2 cells. *International Journal of Radiation Research*, 13(4), 331-335. doi:10.7508/ijrr.2015.04.006
- Clark, B. A., Kim, D., & Epstein, F. H. (1997). Endothelin and atrial natriuretic peptide levels following radiocontrast exposure in humans. *Am J Kidney Dis*, 30(1), 82-86.
- Cronin, R. E. (2010). Contrast-induced nephropathy: pathogenesis and prevention. *Pediatr Nephrol*, 25(2), 191-204. doi:10.1007/s00467-009-1204-z
- Csordas, G., Varnai, P., Golenar, T., Roy, S., Purkins, G., Schneider, T. G., . . . Hajnoczky, G. (2010). Imaging interorganelle contacts and local calcium dynamics at the ER-mitochondrial interface. *Mol Cell*, 39(1), 121-132. doi:10.1016/j.molcel.2010.06.029
- Datta, S., Sahdeo, S., Gray, J. A., Morriseau, C., Hammock, B. D., & Cortopassi, G. (2016). A high-throughput screen for mitochondrial function reveals known and novel mitochondrial toxicants in a library of environmental agents. *Mitochondrion*, 31, 79-83. doi:10.1016/j.mito.2016.10.001
- Dawney, A. B., Thornley, C., Nockler, I., Webb, J. A., & Cattell, W. R. (1985). Tamm-Horsfall glycoprotein excretion and aggregation during intravenous urography. Relevance to acute renal failure. *Invest Radiol*, 20(1), 53-57.
- De Keulenaer, G. W., Alexander, R. W., Ushio-Fukai, M., Ishizaka, N., & Griendling, K. K. (1998). Tumour necrosis factor alpha activates a p22phox-based NADH oxidase in vascular smooth muscle. *Biochem J*, 329 (Pt 3), 653-657.
- Deluca, H. F., & Engstrom, G. W. (1961). Calcium uptake by rat kidney mitochondria. *Proc Natl Acad Sci U S A*, 47, 1744-1750.
- Denic, A., Glasscock, R. J., & Rule, A. D. (2016). Structural and Functional Changes With the Aging Kidney. *Adv Chronic Kidney Dis*, 23(1), 19-28. doi:10.1053/j.ackd.2015.08.004
- Detrenis, S., Meschi, M., Musini, S., & Savazzi, G. (2005). Lights and shadows on the pathogenesis of contrast-induced nephropathy: state of the art. *Nephrol Dial Transplant*, 20(8), 1542-1550. doi:10.1093/ndt/gfh868
- Di Meo, S., Reed, T. T., Venditti, P., & Victor, V. M. (2016). Role of ROS and RNS Sources in Physiological and Pathological Conditions. *Oxid Med Cell Longev*, 2016, 1245049. doi:10.1155/2016/1245049
- Dickenmann, M., Oetl, T., & Mihatsch, M. J. (2008). Osmotic nephrosis: acute kidney injury with accumulation of proximal tubular lysosomes due to administration of exogenous solutes. *Am J Kidney Dis*, 51(3), 491-503. doi:10.1053/j.ajkd.2007.10.044
- Drago, I., Pizzo, P., & Pozzan, T. (2011). After half a century mitochondrial calcium in- and efflux machineries reveal themselves. *EMBO J*, 30(20), 4119-4125. doi:10.1038/emboj.2011.337

- Duan, S. B., Liu, F. Y., Luo, J. A., Wu, H. W., Liu, R. H., Peng, Y. M., & Yang, X. L. (2000). Nephrotoxicity of high- and low-osmolar contrast media. The protective role of amlodipine in a rat model. *Acta Radiol*, *41*(5), 503-507.
- Eakins, J., Bauch, C., Woodhouse, H., Park, B., Bevan, S., Dilworth, C., & Walker, P. (2016). A combined in vitro approach to improve the prediction of mitochondrial toxicants. *Toxicol In Vitro*, *34*, 161-170. doi:10.1016/j.tiv.2016.03.016
- El-Refai, M., Krivospitskaya, O., Peterson, E. L., Wells, K., Williams, L. K., & Lanfear, D. E. (2011). Relationship of Loop Diuretic Dosing and Acute Changes in Renal Function during Hospitalization for Heart Failure. *J Clin Exp Cardiol*, *2*(10). doi:10.4172/2155-9880.1000164
- Faggioni, L., & Gabelloni, M. (2016). Iodine Concentration and Optimization in Computed Tomography Angiography: Current Issues. *Invest Radiol*, *51*(12), 816-822. doi:10.1097/RLI.0000000000000283
- Fahling, M., Seeliger, E., Patzak, A., & Persson, P. B. (2017). Understanding and preventing contrast-induced acute kidney injury. *Nat Rev Nephrol*, *13*(3), 169-180. doi:10.1038/nrneph.2016.196
- Faitova, J., Krekac, D., Hrstka, R., & Vojtesek, B. (2006). Endoplasmic reticulum stress and apoptosis. *Cell Mol Biol Lett*, *11*(4), 488-505. doi:10.2478/s11658-006-0040-4
- Fanos, V., & Cataldi, L. (2000). Amphotericin B-induced nephrotoxicity: a review. *J Chemother*, *12*(6), 463-470. doi:10.1179/joc.2000.12.6.463
- Fedorova, M., Bollineni, R. C., & Hoffmann, R. (2014). Protein carbonylation as a major hallmark of oxidative damage: update of analytical strategies. *Mass Spectrom Rev*, *33*(2), 79-97. doi:10.1002/mas.21381
- Feske, S., Gwack, Y., Prakriya, M., Srikanth, S., Puppel, S. H., Tanasa, B., . . . Rao, A. (2006). A mutation in Orai1 causes immune deficiency by abrogating CRAC channel function. *Nature*, *441*(7090), 179-185. doi:10.1038/nature04702
- Gafter, U., Creter, D., Zevin, D., Catz, R., & Djaldetti, M. (1979). Inhibition of platelet aggregation by contrast media. *Radiology*, *132*(2), 341-342. doi:10.1148/132.2.341
- Gao, X., Fu, L., Xiao, M., Xu, C., Sun, L., Zhang, T., . . . Mei, C. (2012). The nephroprotective effect of tauroursodeoxycholic acid on ischaemia/reperfusion-induced acute kidney injury by inhibiting endoplasmic reticulum stress. *Basic Clin Pharmacol Toxicol*, *111*(1), 14-23. doi:10.1111/j.1742-7843.2011.00854.x
- Gao, Z., Han, Y., Hu, Y., Wu, X., Wang, Y., Zhang, X., . . . Zeng, C. (2016). Targeting HO-1 by Epigallocatechin-3-Gallate Reduces Contrast-Induced Renal Injury via Anti-Oxidative Stress and Anti-Inflammation Pathways. *PLoS One*, *11*(2), e0149032. doi:10.1371/journal.pone.0149032

- Gaut, J. R., & Hendershot, L. M. (1993). The modification and assembly of proteins in the endoplasmic reticulum. *Curr Opin Cell Biol*, 5(4), 589-595.
- GE-Healthcare. (2006). Visipaque (iodixanol) [Package Insert], Mississauga, ON, Canada.
- Giacomello, M., Drago, I., Bortolozzi, M., Scorzeto, M., Gianelle, A., Pizzo, P., & Pozzan, T. (2010). Ca²⁺ hot spots on the mitochondrial surface are generated by Ca²⁺ mobilization from stores, but not by activation of store-operated Ca²⁺ channels. *Mol Cell*, 38(2), 280-290. doi:10.1016/j.molcel.2010.04.003
- Giorgi, C., Ito, K., Lin, H. K., Santangelo, C., Wieckowski, M. R., Lebedzinska, M., . . . Pandolfi, P. P. (2010). PML regulates apoptosis at endoplasmic reticulum by modulating calcium release. *Science*, 330(6008), 1247-1251. doi:10.1126/science.1189157
- Gleeson, T. G., & Bulugahapitiya, S. (2004). Contrast-induced nephropathy. *AJR Am J Roentgenol*, 183(6), 1673-1689. doi:10.2214/ajr.183.6.01831673
- Goll, D. E., Thompson, V. F., Li, H., Wei, W., & Cong, J. (2003). The calpain system. *Physiol Rev*, 83(3), 731-801. doi:10.1152/physrev.00029.2002
- Gong, X., Duan, Y., Zheng, J., Wang, Y., Wang, G., Norgren, S., & Hei, T. K. (2016). Nephroprotective Effects of N-Acetylcysteine Amide against Contrast-Induced Nephropathy through Upregulating Thioredoxin-1, Inhibiting ASK1/p38MAPK Pathway, and Suppressing Oxidative Stress and Apoptosis in Rats. *Oxid Med Cell Longev*, 2016, 8715185. doi:10.1155/2016/8715185
- Gong, X., Ivanov, V. N., Davidson, M. M., & Hei, T. K. (2015). Tetramethylpyrazine (TMP) protects against sodium arsenite-induced nephrotoxicity by suppressing ROS production, mitochondrial dysfunction, pro-inflammatory signaling pathways and programmed cell death. *Arch Toxicol*, 89(7), 1057-1070. doi:10.1007/s00204-014-1302-y
- Gorlach, A., Bertram, K., Hudecova, S., & Krizanova, O. (2015). Calcium and ROS: A mutual interplay. *Redox Biol*, 6, 260-271. doi:10.1016/j.redox.2015.08.010
- Gracy, R. W., Talent, J. M., Kong, Y., & Conrad, C. C. (1999). Reactive oxygen species: the unavoidable environmental insult? *Mutat Res*, 428(1-2), 17-22.
- Grosser, N., Erdmann, K., Hemmerle, A., Berndt, G., Hinkelmann, U., Smith, G., & Schroder, H. (2004). Rosuvastatin upregulates the antioxidant defense protein heme oxygenase-1. *Biochem Biophys Res Commun*, 325(3), 871-876. doi:10.1016/j.bbrc.2004.10.123
- Gruberg, L., Pinnow, E., Flood, R., Bonnet, Y., Tebeica, M., Waksman, R., . . . Lindsay, J., Jr. (2000). Incidence, management, and outcome of coronary artery perforation during percutaneous coronary intervention. *Am J Cardiol*, 86(6), 680-682, A688.
- Gu, L. L., Zhang, X. Y., Xing, W. M., Xu, J. D., & Lu, H. (2016). Andrographolide-induced apoptosis in human renal tubular epithelial cells: Roles of endoplasmic reticulum stress

- and inflammatory response. *Environ Toxicol Pharmacol*, 45, 257-264.
doi:10.1016/j.etap.2016.02.004
- Guerini, D. (1998). The Ca²⁺ pumps and the Na⁺/Ca²⁺ exchangers. *Biometals*, 11(4), 319-330.
- Gunness, P., Aleksa, K., Kosuge, K., Ito, S., & Koren, G. (2010). Comparison of the novel HK-2 human renal proximal tubular cell line with the standard LLC-PK1 cell line in studying drug-induced nephrotoxicity. *Can J Physiol Pharmacol*, 88(4), 448-455.
doi:10.1139/y10-023
- Gussenhoven, M. J., Ravensbergen, J., van Bockel, J. H., Feuth, J. D., & Aarts, J. C. (1991). Renal dysfunction after angiography; a risk factor analysis in patients with peripheral vascular disease. *J Cardiovasc Surg (Torino)*, 32(1), 81-86.
- Haeussler, U., Riedel, M., & Keller, F. (2004). Free reactive oxygen species and nephrotoxicity of contrast agents. *Kidney Blood Press Res*, 27(3), 167-171. doi:10.1159/000079805
- Hall, K. A., Wong, R. W., Hunter, G. C., Camazine, B. M., Rappaport, W. A., Smyth, S. H., . . . Misorowski, R. L. (1992). Contrast-induced nephrotoxicity: the effects of vasodilator therapy. *J Surg Res*, 53(4), 317-320.
- Haller, C., & Hizoh, I. (2004). The cytotoxicity of iodinated radiocontrast agents on renal cells in vitro. *Invest Radiol*, 39(3), 149-154.
- Hanigan, M. H., & Devarajan, P. (2003). Cisplatin nephrotoxicity: molecular mechanisms. *Cancer Ther*, 1, 47-61.
- Haworth, R. A., & Hunter, D. R. (1979). The Ca²⁺-induced membrane transition in mitochondria. II. Nature of the Ca²⁺ trigger site. *Arch Biochem Biophys*, 195(2), 460-467.
- He, C., & Klionsky, D. J. (2009). Regulation mechanisms and signaling pathways of autophagy. *Annu Rev Genet*, 43, 67-93. doi:10.1146/annurev-genet-102808-114910
- He, X., Li, L., Tan, H., Chen, J., & Zhou, Y. (2016). Atorvastatin attenuates contrast-induced nephropathy by modulating inflammatory responses through the regulation of JNK/p38/Hsp27 expression. *J Pharmacol Sci*, 131(1), 18-27.
doi:10.1016/j.jphs.2016.03.006
- Heyman, S. N., Brezis, M., Epstein, F. H., Spokes, K., Silva, P., & Rosen, S. (1991). Early renal medullary hypoxic injury from radiocontrast and indomethacin. *Kidney Int*, 40(4), 632-642.
- Heyman, S. N., Brezis, M., Reubinoff, C. A., Greenfeld, Z., Lechene, C., Epstein, F. H., & Rosen, S. (1988). Acute renal failure with selective medullary injury in the rat. *J Clin Invest*, 82(2), 401-412. doi:10.1172/JCI113612

- Heyman, S. N., Rosen, S., & Brezis, M. (1997). The renal medulla: life at the edge of anoxia. *Blood Purif*, *15*(4-6), 232-242. doi:10.1159/000170341
- Heyman, S. N., Rosen, S., Khamaisi, M., Idee, J. M., & Rosenberger, C. (2010). Reactive oxygen species and the pathogenesis of radiocontrast-induced nephropathy. *Invest Radiol*, *45*(4), 188-195. doi:10.1097/RLI.0b013e3181d2eed8
- Ho, L. M., Nelson, R. C., & DeLong, D. M. (2007). Determining contrast medium dose and rate on basis of lean body weight: does this strategy improve patient-to-patient uniformity of hepatic enhancement during multi-detector row CT? *Radiology*, *243*(2), 431-437. doi:10.1148/radiol.2432060390
- Hogan, P. G., & Rao, A. (2015). Store-operated calcium entry: Mechanisms and modulation. *Biochem Biophys Res Commun*, *460*(1), 40-49. doi:10.1016/j.bbrc.2015.02.110
- Holscher, B., Heitmeyer, C., Fobker, M., Breithardt, G., Schaefer, R. M., & Reinecke, H. (2008). Predictors for contrast media-induced nephropathy and long-term survival: prospectively assessed data from the randomized controlled Dialysis-Versus-Diuresis (DVD) trial. *Can J Cardiol*, *24*(11), 845-850.
- Horl, W. H. (2010). Nonsteroidal Anti-Inflammatory Drugs and the Kidney. *Pharmaceuticals (Basel)*, *3*(7), 2291-2321. doi:10.3390/ph3072291
- Huang, Y. T., Chen, Y. Y., Lai, Y. H., Cheng, C. C., Lin, T. C., Su, Y. S., . . . Lai, P. C. (2016). Resveratrol alleviates the cytotoxicity induced by the radiocontrast agent, ioxitalamate, by reducing the production of reactive oxygen species in HK-2 human renal proximal tubule epithelial cells in vitro. *Int J Mol Med*, *37*(1), 83-91. doi:10.3892/ijmm.2015.2404
- Humes, H. D., Hunt, D. A., & White, M. D. (1987). Direct toxic effect of the radiocontrast agent diatrizoate on renal proximal tubule cells. *Am J Physiol*, *252*(2 Pt 2), F246-255. doi:10.1152/ajprenal.1987.252.2.F246
- Humphrey, M. L., Cole, M. P., Pendergrass, J. C., & Kinningham, K. K. (2005). Mitochondrial mediated thimerosal-induced apoptosis in a human neuroblastoma cell line (SK-N-SH). *Neurotoxicology*, *26*(3), 407-416. doi:10.1016/j.neuro.2005.03.008
- Hunter, D. R., Haworth, R. A., & Southard, J. H. (1976). Relationship between configuration, function, and permeability in calcium-treated mitochondria. *J Biol Chem*, *251*(16), 5069-5077.
- Ichijo, H. (1999). From receptors to stress-activated MAP kinases. *Oncogene*, *18*(45), 6087-6093. doi:10.1038/sj.onc.1203129
- Ikeda, N., Nishimura, S., Kyo, S., Komiyama, N., Matsumoto, K., Inoue, T., & Suzuki, H. (2006). Valsartan cardio-renal protection in patients undergoing coronary angiography complicated with chronic renal insufficiency (VAL-CARP) trial: rationale and design. *Circ J*, *70*(5), 548-552.

- Ip, Y. T., & Davis, R. J. (1998). Signal transduction by the c-Jun N-terminal kinase (JNK)--from inflammation to development. *Curr Opin Cell Biol*, *10*(2), 205-219.
- Itoh, Y., Yano, T., Sendo, T., Sueyasu, M., Hirano, K., Kanaide, H., & Oishi, R. (2006). Involvement of de novo ceramide synthesis in radiocontrast-induced renal tubular cell injury. *Kidney Int*, *69*(2), 288-297. doi:10.1038/sj.ki.5000057
- Ivannikov, M. V., & Macleod, G. T. (2013). Mitochondrial free Ca²⁺(+) levels and their effects on energy metabolism in Drosophila motor nerve terminals. *Biophys J*, *104*(11), 2353-2361. doi:10.1016/j.bpj.2013.03.064
- James, M. T., Samuel, S. M., Manning, M. A., Tonelli, M., Ghali, W. A., Faris, P., . . . Hemmelgarn, B. R. (2013). Contrast-induced acute kidney injury and risk of adverse clinical outcomes after coronary angiography: a systematic review and meta-analysis. *Circ Cardiovasc Interv*, *6*(1), 37-43. doi:10.1161/CIRCINTERVENTIONS.112.974493
- Jeon, U. S. (2008). Kidney and calcium homeostasis. *Electrolyte Blood Press*, *6*(2), 68-76. doi:10.5049/EBP.2008.6.2.68
- Jeong, B. Y., Lee, H. Y., Park, C. G., Kang, J., Yu, S. L., Choi, D. R., . . . Yoon, S. H. (2018). Oxidative stress caused by activation of NADPH oxidase 4 promotes contrast-induced acute kidney injury. *PLoS One*, *13*(1), e0191034. doi:10.1371/journal.pone.0191034
- Jiang, X., & Wang, X. (2000). Cytochrome c promotes caspase-9 activation by inducing nucleotide binding to Apaf-1. *J Biol Chem*, *275*(40), 31199-31203. doi:10.1074/jbc.C000405200
- Jin, S., Orabi, A. I., Le, T., Javed, T. A., Sah, S., Eisses, J. F., . . . Husain, S. Z. (2015). Exposure to Radiocontrast Agents Induces Pancreatic Inflammation by Activation of Nuclear Factor-kappaB, Calcium Signaling, and Calcineurin. *Gastroenterology*, *149*(3), 753-764 e711. doi:10.1053/j.gastro.2015.05.004
- Jo, S. H., Koo, B. K., Park, J. S., Kang, H. J., Cho, Y. S., Kim, Y. J., . . . Kim, H. S. (2008). Prevention of radiocontrast medium-induced nephropathy using short-term high-dose simvastatin in patients with renal insufficiency undergoing coronary angiography (PROMISS) trial--a randomized controlled study. *Am Heart J*, *155*(3), 499 e491-498. doi:10.1016/j.ahj.2007.11.042
- Johnson, A. C., Stahl, A., & Zager, R. A. (2005). Triglyceride accumulation in injured renal tubular cells: alterations in both synthetic and catabolic pathways. *Kidney Int*, *67*(6), 2196-2209. doi:10.1111/j.1523-1755.2005.00325.x
- Jones, L. J., Gray, M., Yue, S. T., Haugland, R. P., & Singer, V. L. (2001). Sensitive determination of cell number using the CyQUANT cell proliferation assay. *J Immunol Methods*, *254*(1-2), 85-98.
- Kellum, J. A. (2012). *Kidney Disease: Improving Global Outcomes (KDIGO) Acute Kidney Injury Work Group*. Retrieved from

- Killmann, S. A., Gjorup, S., & Thaysen, J. H. (1957). Fatal acute renal failure following intravenous pyelography in a patient with multiple myeloma. *Acta Med Scand*, *158*(1), 43-46.
- Kim, R., Emi, M., Tanabe, K., & Murakami, S. (2006). Role of the unfolded protein response in cell death. *Apoptosis*, *11*(1), 5-13. doi:10.1007/s10495-005-3088-0
- Koc, E., Reis, K. A., Ebinc, F. A., Pasaoglu, H., Demirtas, C., Omeroglu, S., . . . Sindel, S. (2011). Protective effect of beta-glucan on contrast induced-nephropathy and a comparison of beta-glucan with nebivolol and N-acetylcysteine in rats. *Clin Exp Nephrol*, *15*(5), 658-665. doi:10.1007/s10157-011-0451-z
- Kolonko, A., Kokot, F., & Wiecek, A. (1998). Contrast-associated nephropathy--old clinical problem and new therapeutic perspectives. *Nephrol Dial Transplant*, *13*(3), 803-806.
- Kongkham, S., Sriwong, S., & Tasanarong, A. (2013). Protective effect of alpha tocopherol on contrast-induced nephropathy in rats. *Nefrologia*, *33*(1), 116-123. doi:10.3265/Nefrologia.pre2012.Nov.11736
- Krebs, J., Agellon, L. B., & Michalak, M. (2015). Ca(2+) homeostasis and endoplasmic reticulum (ER) stress: An integrated view of calcium signaling. *Biochem Biophys Res Commun*, *460*(1), 114-121. doi:10.1016/j.bbrc.2015.02.004
- Langenberg, C., Bellomo, R., May, C., Wan, L., Egi, M., & Morgera, S. (2005). Renal blood flow in sepsis. *Crit Care*, *9*(4), R363-374. doi:10.1186/cc3540
- Langenberg, C., Wan, L., Egi, M., May, C. N., & Bellomo, R. (2006). Renal blood flow in experimental septic acute renal failure. *Kidney Int*, *69*(11), 1996-2002. doi:10.1038/sj.ki.5000440
- Lazarou, M., Sliter, D. A., Kane, L. A., Sarraf, S. A., Wang, C., Burman, J. L., . . . Youle, R. J. (2015). The ubiquitin kinase PINK1 recruits autophagy receptors to induce mitophagy. *Nature*, *524*(7565), 309-314. doi:10.1038/nature14893
- Lee, D., Choi, Y. O., Kim, K. H., Chin, Y. W., Namgung, H., Yamabe, N., & Jung, K. (2016). Protective effect of alpha-mangostin against iodixanol-induced apoptotic damage in LLC-PK1 cells. *Bioorg Med Chem Lett*, *26*(15), 3806-3809. doi:10.1016/j.bmcl.2016.05.031
- Lee, D., Kim, C. E., Park, S. Y., Kim, K. O., Hiep, N. T., Lee, D., . . . Kang, K. S. (2018). Protective Effect of *Artemisia argyi* and Its Flavonoid Constituents against Contrast-Induced Cytotoxicity by Iodixanol in LLC-PK1 Cells. *Int J Mol Sci*, *19*(5). doi:10.3390/ijms19051387
- Lei, R., Zhao, F., Tang, C. Y., Luo, M., Yang, S. K., Cheng, W., . . . Duan, S. B. (2018). Mitophagy Plays a Protective Role in Iodinated Contrast-Induced Acute Renal Tubular Epithelial Cells Injury. *Cell Physiol Biochem*, *46*(3), 975-985. doi:10.1159/000488827

- Leong, C. L., Anderson, W. P., O'Connor, P. M., & Evans, R. G. (2007). Evidence that renal arterial-venous oxygen shunting contributes to dynamic regulation of renal oxygenation. *Am J Physiol Renal Physiol*, *292*(6), F1726-1733. doi:10.1152/ajprenal.00436.2006
- Levine, R. L., Williams, J. A., Stadtman, E. R., & Shacter, E. (1994). Carbonyl assays for determination of oxidatively modified proteins. *Methods Enzymol*, *233*, 346-357.
- Li, X., Fang, P., Mai, J., Choi, E. T., Wang, H., & Yang, X. F. (2013). Targeting mitochondrial reactive oxygen species as novel therapy for inflammatory diseases and cancers. *J Hematol Oncol*, *6*, 19. doi:10.1186/1756-8722-6-19
- Li, X., Fang, P., Yang, W. Y., Chan, K., Lavalley, M., Xu, K., . . . Yang, X. (2017). Mitochondrial ROS, uncoupled from ATP synthesis, determine endothelial activation for both physiological recruitment of patrolling cells and pathological recruitment of inflammatory cells. *Can J Physiol Pharmacol*, *95*(3), 247-252. doi:10.1139/cjpp-2016-0515
- Liss, P., Nygren, A., Erikson, U., & Ulfendahl, H. R. (1998). Injection of low and iso-osmolar contrast medium decreases oxygen tension in the renal medulla. *Kidney Int*, *53*(3), 698-702. doi:10.1046/j.1523-1755.1998.00811.x
- Liu, N., Chen, J., Gao, D., Li, W., & Zheng, D. (2018). Astaxanthin attenuates contrast agent-induced acute kidney injury in vitro and in vivo via the regulation of SIRT1/FOXO3a expression. *Int Urol Nephrol*, *50*(6), 1171-1180. doi:10.1007/s11255-018-1788-y
- Liu, X., Kim, C. N., Yang, J., Jemmerson, R., & Wang, X. (1996). Induction of apoptotic program in cell-free extracts: requirement for dATP and cytochrome c. *Cell*, *86*(1), 147-157.
- Liu, Z. Z., Viegas, V. U., Perlewitz, A., Lai, E. Y., Persson, P. B., Patzak, A., & Sendeski, M. M. (2012). Iodinated contrast media differentially affect afferent and efferent arteriolar tone and reactivity in mice: a possible explanation for reduced glomerular filtration rate. *Radiology*, *265*(3), 762-771. doi:10.1148/radiol.12120044
- Lusic, H., & Grinstaff, M. W. (2013). X-ray-computed tomography contrast agents. *Chem Rev*, *113*(3), 1641-1666. doi:10.1021/cr200358s
- Majumdar, S. R., Kjellstrand, C. M., Tymchak, W. J., Hervas-Malo, M., Taylor, D. A., & Teo, K. K. (2009). Forced euvolemic diuresis with mannitol and furosemide for prevention of contrast-induced nephropathy in patients with CKD undergoing coronary angiography: a randomized controlled trial. *Am J Kidney Dis*, *54*(4), 602-609. doi:10.1053/j.ajkd.2009.03.024
- Martin-Paredero, V., Dixon, S. M., Baker, J. D., Takiff, H., Gomes, A. S., Busuttil, R. W., & Moore, W. S. (1983). Risk of renal failure after major angiography. *Arch Surg*, *118*(12), 1417-1420.

- Matejovic, M., Chvojka, J., Radej, J., Ledvinova, L., Karvunidis, T., Krouzecky, A., & Novak, I. (2011). Sepsis and acute kidney injury are bidirectional. *Contrib Nephrol*, *174*, 78-88. doi:10.1159/000329239
- Matsuda, N., Sato, S., Shiba, K., Okatsu, K., Saisho, K., Gautier, C. A., . . . Tanaka, K. (2010). PINK1 stabilized by mitochondrial depolarization recruits Parkin to damaged mitochondria and activates latent Parkin for mitophagy. *J Cell Biol*, *189*(2), 211-221. doi:10.1083/jcb.200910140
- Matsuzawa, A., & Ichijo, H. (2008). Redox control of cell fate by MAP kinase: physiological roles of ASK1-MAP kinase pathway in stress signaling. *Biochim Biophys Acta*, *1780*(11), 1325-1336. doi:10.1016/j.bbagen.2007.12.011
- McNair, J. D. (1972). Selective coronary angiography. Report of a fatality in a patient with sickle cell hemoglobin. *Calif Med*, *117*(5), 71-75.
- Mehran, R., & Nikolsky, E. (2006). Contrast-induced nephropathy: definition, epidemiology, and patients at risk. *Kidney Int Suppl*(100), S11-15. doi:10.1038/sj.ki.5000368
- Mekahli, D., Bultynck, G., Parys, J. B., De Smedt, H., & Missiaen, L. (2011). Endoplasmic-reticulum calcium depletion and disease. *Cold Spring Harb Perspect Biol*, *3*(6). doi:10.1101/cshperspect.a004317
- Melartin, E., Tuohimaa, P. J., & Dabb, R. (1970). Neurotoxicity of iothalamates and diatrizoates. I. Significance of concentration and cation. *Invest Radiol*, *5*(1), 13-21.
- Messana, J. M., Cieslinski, D. A., & Humes, H. D. (1990). Comparison of toxicity of radiocontrast agents to renal tubule cells in vitro. *Ren Fail*, *12*(2), 75-82.
- Messana, J. M., Cieslinski, D. A., Nguyen, V. D., & Humes, H. D. (1988). Comparison of the toxicity of the radiocontrast agents, iopamidol and diatrizoate, to rabbit renal proximal tubule cells in vitro. *J Pharmacol Exp Ther*, *244*(3), 1139-1144.
- Michael, A., Faga, T., Pisani, A., Riccio, E., Bramanti, P., Sabbatini, M., . . . Andreucci, M. (2014). Molecular mechanisms of renal cellular nephrotoxicity due to radiocontrast media. *Biomed Res Int*, *2014*, 249810. doi:10.1155/2014/249810
- Mittal, M., Siddiqui, M. R., Tran, K., Reddy, S. P., & Malik, A. B. (2014). Reactive oxygen species in inflammation and tissue injury. *Antioxid Redox Signal*, *20*(7), 1126-1167. doi:10.1089/ars.2012.5149
- Moe, K. T., Aulia, S., Jiang, F., Chua, Y. L., Koh, T. H., Wong, M. C., & Dusting, G. J. (2006). Differential upregulation of Nox homologues of NADPH oxidase by tumor necrosis factor-alpha in human aortic smooth muscle and embryonic kidney cells. *J Cell Mol Med*, *10*(1), 231-239.
- Momeni, H. R. (2011). Role of calpain in apoptosis. *Cell J*, *13*(2), 65-72.

- Morcos, S. K. (1998). Contrast media-induced nephrotoxicity--questions and answers. *Br J Radiol*, 71(844), 357-365. doi:10.1259/bjr.71.844.9659127
- Morgan, M. J., & Liu, Z. G. (2010). Reactive oxygen species in TNF α -induced signaling and cell death. *Mol Cells*, 30(1), 1-12. doi:10.1007/s10059-010-0105-0
- Moyle, J., & Mitchell, P. (1977). Electric charge stoichiometry of calcium translocation in rat liver mitochondria. *FEBS Lett*, 73(2), 131-136.
- Mudge, G. H., Berndt, W. O., Saunders, A., & Beattie, B. (1971). Renal transport of diatrizoate in the rabbit, dog, and rat. *Nephron*, 8(2), 156-172. doi:10.1159/000179916
- Murakami, R., Kumita, S., Hayashi, H., Sugizaki, K., Okazaki, E., Kiriyama, T., . . . Takeda, M. (2013). Anemia and the risk of contrast-induced nephropathy in patients with renal insufficiency undergoing contrast-enhanced MDCT. *Eur J Radiol*, 82(10), e521-524. doi:10.1016/j.ejrad.2013.06.004
- Murphy, R. A., Stafford, R. M., Petrasovits, B. A., Boone, M. A., & Valentovic, M. A. (2017). Establishment of HK-2 Cells as a Relevant Model to Study Tenofovir-Induced Cytotoxicity. *Int J Mol Sci*, 18(3). doi:10.3390/ijms18030531
- Nakagawa, T., & Yuan, J. (2000). Cross-talk between two cysteine protease families. Activation of caspase-12 by calpain in apoptosis. *J Cell Biol*, 150(4), 887-894.
- Namba, T., Takabatake, Y., Kimura, T., Takahashi, A., Yamamoto, T., Matsuda, J., . . . Rakugi, H. (2014). Autophagic clearance of mitochondria in the kidney copes with metabolic acidosis. *J Am Soc Nephrol*, 25(10), 2254-2266. doi:10.1681/ASN.2013090986
- Nash, K., Hafeez, A., & Hou, S. (2002). Hospital-acquired renal insufficiency. *Am J Kidney Dis*, 39(5), 930-936. doi:10.1053/ajkd.2002.32766
- Nasri, H., Hajian, S., Ahmadi, A., Baradaran, A., Kohi, G., Nasri, P., & Rafieian-Kopaei, M. (2015). Ameliorative effect of green tea against contrast-induced renal tubular cell injury. *Iran J Kidney Dis*, 9(6), 421-426.
- Navas, J. P., & Martinez-Maldonado, M. (1993). Pathophysiology of edema in congestive heart failure. *Heart Dis Stroke*, 2(4), 325-329.
- Netti, G. S., Prattichizzo, C., Montemurno, E., Simone, S., Cafiero, C., Rascio, F., . . . Gesualdo, L. (2014). Exposure to low- vs iso-osmolar contrast agents reduces NADPH-dependent reactive oxygen species generation in a cellular model of renal injury. *Free Radic Biol Med*, 68, 35-42. doi:10.1016/j.freeradbiomed.2013.11.016
- Nguyen, T. N., Padman, B. S., & Lazarou, M. (2016). Deciphering the Molecular Signals of PINK1/Parkin Mitophagy. *Trends Cell Biol*, 26(10), 733-744. doi:10.1016/j.tcb.2016.05.008

- Nikolsky, E., Mehran, R., Lasic, Z., Mintz, G. S., Lansky, A. J., Na, Y., . . . Dangas, G. (2005). Low hematocrit predicts contrast-induced nephropathy after percutaneous coronary interventions. *Kidney Int*, 67(2), 706-713. doi:10.1111/j.1523-1755.2005.67131.x
- Oguzhan, N., Cilan, H., Sipahioglu, M., Unal, A., Kocyigit, I., Kavuncuoglu, F., . . . Oymak, O. (2013). The lack of benefit of a combination of an angiotensin receptor blocker and calcium channel blocker on contrast-induced nephropathy in patients with chronic kidney disease. *Ren Fail*, 35(4), 434-439. doi:10.3109/0886022X.2013.766566
- Ott, M., Robertson, J. D., Gogvadze, V., Zhivotovsky, B., & Orrenius, S. (2002). Cytochrome c release from mitochondria proceeds by a two-step process. *Proc Natl Acad Sci U S A*, 99(3), 1259-1263. doi:10.1073/pnas.24165498
- Oyadomari, S., & Mori, M. (2004). Roles of CHOP/GADD153 in endoplasmic reticulum stress. *Cell Death Differ*, 11(4), 381-389. doi:10.1038/sj.cdd.4401373
- Pacher, P., Beckman, J. S., & Liaudet, L. (2007). Nitric oxide and peroxynitrite in health and disease. *Physiol Rev*, 87(1), 315-424. doi:10.1152/physrev.00029.2006
- Pahade, J. K., LeBedis, C. A., Raptopoulos, V. D., Avigan, D. E., Yam, C. S., Kruskal, J. B., & Pedrosa, I. (2011). Incidence of contrast-induced nephropathy in patients with multiple myeloma undergoing contrast-enhanced CT. *AJR Am J Roentgenol*, 196(5), 1094-1101. doi:10.2214/AJR.10.5152
- Palli, E., Makris, D., Papanikolaou, J., Garoufalis, G., Tsilioni, I., Zygoulis, P., & Zakyntinos, E. (2017). The impact of N-acetylcysteine and ascorbic acid in contrast-induced nephropathy in critical care patients: an open-label randomized controlled study. *Crit Care*, 21(1), 269. doi:10.1186/s13054-017-1862-3
- Paolicchi, A., Sotiropoulou, M., Perego, P., Daubeuf, S., Visvikis, A., Lorenzini, E., . . . Pompella, A. (2003). gamma-Glutamyl transpeptidase catalyses the extracellular detoxification of cisplatin in a human cell line derived from the proximal convoluted tubule of the kidney. *Eur J Cancer*, 39(7), 996-1003.
- Park, S., Choi, S. G., Yoo, S. M., Nah, J., Jeong, E., Kim, H., & Jung, Y. K. (2015). Pyruvate stimulates mitophagy via PINK1 stabilization. *Cell Signal*, 27(9), 1824-1830. doi:10.1016/j.cellsig.2015.05.020
- Patel, K., King, C. A., & Jovin, I. S. (2011). Angiotensin-converting enzyme inhibitors and their effects on contrast-induced nephropathy after cardiac catheterization or percutaneous coronary intervention. *Cardiovasc Revasc Med*, 12(2), 90-93. doi:10.1016/j.carrev.2010.01.002
- Peng, J. B. (2019). Hypercalciuria and TRPV6-mediated Active Calcium Reabsorption in the Proximal Tubule *Unpublished Manuscript, University of Alabama Birmingham, Birmingham, AL.*

- Peng, P. A., Wang, L., Ma, Q., Xin, Y., Zhang, O., Han, H. Y., . . . Zhao, Y. X. (2015). Valsartan protects HK-2 cells from contrast media-induced apoptosis by inhibiting endoplasmic reticulum stress. *Cell Biol Int*, 39(12), 1408-1417. doi:10.1002/cbin.10521
- Persson, P. B., Hansell, P., & Liss, P. (2005). Pathophysiology of contrast medium-induced nephropathy. *Kidney Int*, 68(1), 14-22. doi:10.1111/j.1523-1755.2005.00377.x
- Phaniendra, A., Jestadi, D. B., & Periyasamy, L. (2015). Free radicals: properties, sources, targets, and their implication in various diseases. *Indian J Clin Biochem*, 30(1), 11-26. doi:10.1007/s12291-014-0446-0
- Prakriya, M., & Lewis, R. S. (2015). Store-Operated Calcium Channels. *Physiol Rev*, 95(4), 1383-1436. doi:10.1152/physrev.00020.2014
- Quintavalle, C., Brenca, M., De Micco, F., Fiore, D., Romano, S., Romano, M. F., . . . Condorelli, G. (2011). In vivo and in vitro assessment of pathways involved in contrast media-induced renal cells apoptosis. *Cell Death Dis*, 2, e155. doi:10.1038/cddis.2011.38
- Quintavalle, C., Donnarumma, E., Fiore, D., Briguori, C., & Condorelli, G. (2013). Therapeutic strategies to prevent contrast-induced acute kidney injury. *Curr Opin Cardiol*, 28(6), 676-682. doi:10.1097/HCO.0b013e3283653f41
- Quintavalle, C., Fiore, D., De Micco, F., Visconti, G., Focaccio, A., Golia, B., . . . Condorelli, G. (2012). Impact of a high loading dose of atorvastatin on contrast-induced acute kidney injury. *Circulation*, 126(25), 3008-3016. doi:10.1161/CIRCULATIONAHA.112.103317
- Radiology, A. C. o. (2018). American College of Radiology Committee on Drugs and Contrast Media. 11. Retrieved from https://www.acr.org/-/media/ACR/Files/Clinical-Resources/Contrast_Media.pdf
- Rai, Y., Pathak, R., Kumari, N., Sah, D. K., Pandey, S., Kalra, N., . . . Bhatt, A. N. (2018). Mitochondrial biogenesis and metabolic hyperactivation limits the application of MTT assay in the estimation of radiation induced growth inhibition. *Sci Rep*, 8(1), 1531. doi:10.1038/s41598-018-19930-w
- Rawlings, N. D., & Salvesen, G. (2013). *Handbook of proteolytic enzymes* (Third edition. / ed.). Amsterdam: Elsevier/AP.
- Rees, J. A., Old, S. L., & Rowlands, P. C. (1997). An ultrastructural histochemistry and light microscopy study of the early development of renal proximal tubular vacuolation after a single administration of the contrast enhancement medium "Iotrolan". *Toxicol Pathol*, 25(2), 158-164. doi:10.1177/019262339702500205
- Rizzuto, R., Brini, M., Murgia, M., & Pozzan, T. (1993). Microdomains with high Ca²⁺ close to IP₃-sensitive channels that are sensed by neighboring mitochondria. *Science*, 262(5134), 744-747.

- Rizzuto, R., Pinton, P., Carrington, W., Fay, F. S., Fogarty, K. E., Lifshitz, L. M., . . . Pozzan, T. (1998). Close contacts with the endoplasmic reticulum as determinants of mitochondrial Ca²⁺ responses. *Science*, *280*(5370), 1763-1766.
- Rizzuto, R., & Pozzan, T. (2006). Microdomains of intracellular Ca²⁺: molecular determinants and functional consequences. *Physiol Rev*, *86*(1), 369-408.
doi:10.1152/physrev.00004.2005
- Robinson, M. J., & Cobb, M. H. (1997). Mitogen-activated protein kinase pathways. *Curr Opin Cell Biol*, *9*(2), 180-186.
- Romano, G., Briguori, C., Quintavalle, C., Zanca, C., Rivera, N. V., Colombo, A., & Condorelli, G. (2008). Contrast agents and renal cell apoptosis. *Eur Heart J*, *29*(20), 2569-2576.
doi:10.1093/eurheartj/ehn197
- Roos, J., DiGregorio, P. J., Yeromin, A. V., Ohlsen, K., Liudyno, M., Zhang, S., . . . Stauderman, K. A. (2005). STIM1, an essential and conserved component of store-operated Ca²⁺ channel function. *J Cell Biol*, *169*(3), 435-445.
doi:10.1083/jcb.200502019
- Rosenberger, C., Rosen, S., & Heyman, S. N. (2006). Renal parenchymal oxygenation and hypoxia adaptation in acute kidney injury. *Clin Exp Pharmacol Physiol*, *33*(10), 980-988.
doi:10.1111/j.1440-1681.2006.04472.x
- Rosenstock, J. L., Bruno, R., Kim, J. K., Lubarsky, L., Schaller, R., Panagopoulos, G., . . . Michelis, M. F. (2008). The effect of withdrawal of ACE inhibitors or angiotensin receptor blockers prior to coronary angiography on the incidence of contrast-induced nephropathy. *Int Urol Nephrol*, *40*(3), 749-755. doi:10.1007/s11255-008-9368-1
- Roza, C. A., Scaini, G., Jeremias, I. C., Ferreira, G. K., Rochi, N., Benedet, J., . . . Streck, E. L. (2011). Evaluation of brain and kidney energy metabolism in an animal model of contrast-induced nephropathy. *Metab Brain Dis*, *26*(2), 115-122. doi:10.1007/s11011-011-9240-3
- Ryan, M. J., Johnson, G., Kirk, J., Fuerstenberg, S. M., Zager, R. A., & Torok-Storb, B. (1994). HK-2: an immortalized proximal tubule epithelial cell line from normal adult human kidney. *Kidney Int*, *45*(1), 48-57.
- Sands, J. M. (2012). Urine concentrating and diluting ability during aging. *J Gerontol A Biol Sci Med Sci*, *67*(12), 1352-1357. doi:10.1093/gerona/gls128
- Saritemur, M., Un, H., Cadirci, E., Karakus, E., Akpinar, E., Halici, Z., . . . Atmaca, H. T. (2015). Tnf-alpha inhibition by infliximab as a new target for the prevention of glycerol-contrast-induced nephropathy. *Environ Toxicol Pharmacol*, *39*(2), 577-588.
doi:10.1016/j.etap.2015.01.002

- Sawhney, S., & Fraser, S. D. (2017). Epidemiology of AKI: Utilizing Large Databases to Determine the Burden of AKI. *Adv Chronic Kidney Dis*, 24(4), 194-204. doi:10.1053/j.ackd.2017.05.001
- Scheitlin, W., Martz, G., & Brunner, U. (1960). [Acute renal failure following intravenous pyelography in multiple myeloma]. *Schweiz Med Wochenschr*, 90, 84-87.
- Schick, C. S., Bangert, R., Kubler, W., & Haller, C. (2002). Ionic radiocontrast media disrupt intercellular contacts via an extracellular calcium-independent mechanism. *Exp Nephrol*, 10(3), 209-215. doi:10.1159/000058347
- Schoolwerth, A. C., Sica, D. A., Ballermann, B. J., Wilcox, C. S., Council on the Kidney in Cardiovascular, D., & the Council for High Blood Pressure Research of the American Heart, A. (2001). Renal considerations in angiotensin converting enzyme inhibitor therapy: a statement for healthcare professionals from the Council on the Kidney in Cardiovascular Disease and the Council for High Blood Pressure Research of the American Heart Association. *Circulation*, 104(16), 1985-1991.
- Schreiner, G. E. (1966). Nephrotoxicity and diagnostic agents. *JAMA*, 196(5), 413-415.
- Schroder, M., & Kaufman, R. J. (2005). The mammalian unfolded protein response. *Annu Rev Biochem*, 74, 739-789. doi:10.1146/annurev.biochem.73.011303.074134
- Sedeek, M., Nasrallah, R., Touyz, R. M., & Hebert, R. L. (2013). NADPH oxidases, reactive oxygen species, and the kidney: friend and foe. *J Am Soc Nephrol*, 24(10), 1512-1518. doi:10.1681/ASN.2012111112
- Sekiguchi, H., Ajiro, Y., Uchida, Y., Jujo, K., Iwade, K., Tanaka, N., . . . Hagiwara, N. (2018). Contrast-Induced Nephropathy and Oxygen Pretreatment in Patients With Impaired Renal Function. *Kidney Int Rep*, 3(1), 65-72. doi:10.1016/j.ekir.2017.08.002
- Skucas, J. (1989). *Radiographic contrast agents* (2nd ed.). Rockville, Md.: Aspen Publishers.
- Solomon, R., & Dauerman, H. L. (2010). Contrast-induced acute kidney injury. *Circulation*, 122(23), 2451-2455. doi:10.1161/CIRCULATIONAHA.110.953851
- Somlyo, A. P., Bond, M., & Somlyo, A. V. (1985). Calcium content of mitochondria and endoplasmic reticulum in liver frozen rapidly in vivo. *Nature*, 314(6012), 622-625.
- Spargias, K., Alexopoulos, E., Kyrzopoulos, S., Iokovis, P., Greenwood, D. C., Manginas, A., . . . Cokkinos, D. V. (2004). Ascorbic acid prevents contrast-mediated nephropathy in patients with renal dysfunction undergoing coronary angiography or intervention. *Circulation*, 110(18), 2837-2842. doi:10.1161/01.CIR.0000146396.19081.73
- Stacul, F., Bertolotto, M., Thomsen, H. S., Pozzato, G., Ugolini, D., Bellin, M. F., . . . Committee, E. C. M. S. (2018). Iodine-based contrast media, multiple myeloma and monoclonal gammopathies: literature review and ESUR Contrast Media Safety Committee guidelines. *Eur Radiol*, 28(2), 683-691. doi:10.1007/s00330-017-5023-5

- Stokes, J. M., & Bernard, H. R. (1961). Nephrotoxicity of Iodinated Contrast Media: Quantitative Effects of High Concentration Upon Glomerular and Tubular Functions. *Ann Surg*, *153*(2), 299-309.
- Stoll, L. L., McCormick, M. L., Denning, G. M., & Weintraub, N. L. (2004). Antioxidant effects of statins. *Drugs Today (Barc)*, *40*(12), 975-990.
- Stratta, P., Quaglia, M., Airoidi, A., & Aime, S. (2012). Structure-function relationships of iodinated contrast media and risk of nephrotoxicity. *Curr Med Chem*, *19*(5), 736-743.
- Strober, W. (2015). Trypan Blue Exclusion Test of Cell Viability. *Curr Protoc Immunol*, *111*, A3 B 1-3. doi:10.1002/0471142735.ima03bs111
- Su, J., Zou, W., Cai, W., Chen, X., Wang, F., Li, S., . . . Cao, Y. (2014). Atorvastatin ameliorates contrast medium-induced renal tubular cell apoptosis in diabetic rats via suppression of Rho-kinase pathway. *Eur J Pharmacol*, *723*, 15-22. doi:10.1016/j.ejphar.2013.10.025
- Sung, C. C., Hsu, Y. C., Chen, C. C., Lin, Y. F., & Wu, C. C. (2013). Oxidative stress and nucleic acid oxidation in patients with chronic kidney disease. *Oxid Med Cell Longev*, *2013*, 301982. doi:10.1155/2013/301982
- Suzuki, K., & Sorimachi, H. (1998). A novel aspect of calpain activation. *FEBS Lett*, *433*(1-2), 1-4.
- Suzuki, Y. J., Carini, M., & Butterfield, D. A. (2010). Protein carbonylation. *Antioxid Redox Signal*, *12*(3), 323-325. doi:10.1089/ars.2009.2887
- Swan, S. K. (1997). Aminoglycoside nephrotoxicity. *Semin Nephrol*, *17*(1), 27-33.
- Swick, M. (1930). Intravenous Urography By Means Of The Sodium Salt Of 5-Iodo2-Pyridon-N-Acetic Acid. *J Am Med Assoc*, *95*(19), 1403-1409.
- Szegezdi, E., Logue, S. E., Gorman, A. M., & Samali, A. (2006). Mediators of endoplasmic reticulum stress-induced apoptosis. *EMBO Rep*, *7*(9), 880-885. doi:10.1038/sj.embor.7400779
- Takasu, O., Gaut, J. P., Watanabe, E., To, K., Fagley, R. E., Sato, B., . . . Hotchkiss, R. S. (2013). Mechanisms of cardiac and renal dysfunction in patients dying of sepsis. *Am J Respir Crit Care Med*, *187*(5), 509-517. doi:10.1164/rccm.201211-1983OC
- Tan, Y., Dourdin, N., Wu, C., De Veyra, T., Elce, J. S., & Greer, P. A. (2006). Ubiquitous calpains promote caspase-12 and JNK activation during endoplasmic reticulum stress-induced apoptosis. *J Biol Chem*, *281*(23), 16016-16024. doi:10.1074/jbc.M601299200
- Tanaka, A., Cleland, M. M., Xu, S., Narendra, D. P., Suen, D. F., Karbowski, M., & Youle, R. J. (2010). Proteasome and p97 mediate mitophagy and degradation of mitofusins induced by Parkin. *J Cell Biol*, *191*(7), 1367-1380. doi:10.1083/jcb.201007013

- Tang, C., Han, H., Yan, M., Zhu, S., Liu, J., Liu, Z., . . . Dong, Z. (2018). PINK1-PRKN/PARK2 pathway of mitophagy is activated to protect against renal ischemia-reperfusion injury. *Autophagy*, *14*(5), 880-897. doi:10.1080/15548627.2017.1405880
- Tasanarong, A., Kongkham, S., & Itharat, A. (2014). Antioxidant effect of *Phyllanthus emblica* extract prevents contrast-induced acute kidney injury. *BMC Complement Altern Med*, *14*, 138. doi:10.1186/1472-6882-14-138
- Tasanarong, A., Vohakiat, A., Hutayanon, P., & Piyayotai, D. (2013). New strategy of alpha- and gamma-tocopherol to prevent contrast-induced acute kidney injury in chronic kidney disease patients undergoing elective coronary procedures. *Nephrol Dial Transplant*, *28*(2), 337-344. doi:10.1093/ndt/gfs525
- Tepel, M., van der Giet, M., Schwarzfeld, C., Laufer, U., Liermann, D., & Zidek, W. (2000). Prevention of radiographic-contrast-agent-induced reductions in renal function by acetylcysteine. *N Engl J Med*, *343*(3), 180-184. doi:10.1056/NEJM200007203430304
- Terneus, M. V., Kiningham, K. K., Carpenter, A. B., Sullivan, S. B., & Valentovic, M. A. (2007). Comparison of S-Adenosyl-L-methionine and N-acetylcysteine protective effects on acetaminophen hepatic toxicity. *J Pharmacol Exp Ther*, *320*(1), 99-107. doi:10.1124/jpet.106.111872
- Tervahartiala, P., Kivisaari, L., Kivisaari, R., Vehmas, T., & Virtanen, I. (1997). Structural changes in the renal proximal tubular cells induced by iodinated contrast media. *Nephron*, *76*(1), 96-102. doi:10.1159/000190147
- Tervahartiala, P., Kivisaari, L., Kivisaari, R., Virtanen, I., & Standertskjold-Nordenstam, C. G. (1991). Contrast media-induced renal tubular vacuolization. A light and electron microscopic study on rat kidneys. *Invest Radiol*, *26*(10), 882-887.
- Thomsen, H. S., & Morcos, S. K. (2000). Radiographic contrast media. *BJU Int*, *86 Suppl 1*, 1-10.
- Thomsen, H. S., & Morcos, S. K. (2003). Contrast media and the kidney: European Society of Urogenital Radiology (ESUR) guidelines. *Br J Radiol*, *76*(908), 513-518. doi:10.1259/bjr/26964464
- Tongqiang, L., Shaopeng, L., Xiaofang, Y., Nana, S., Xialian, X., Jiachang, H., . . . Xiaoqiang, D. (2016). Salvianolic Acid B Prevents Iodinated Contrast Media-Induced Acute Renal Injury in Rats via the PI3K/Akt/Nrf2 Pathway. *Oxid Med Cell Longev*, *2016*, 7079487. doi:10.1155/2016/7079487
- Toprak, O. (2007). Conflicting and new risk factors for contrast induced nephropathy. *J Urol*, *178*(6), 2277-2283. doi:10.1016/j.juro.2007.08.054
- Toprak, O., Cirit, M., Tanrisev, M., Yazici, C., Canoz, O., Sipahioglu, M., . . . Sozmen, E. Y. (2008). Preventive effect of nebivolol on contrast-induced nephropathy in rats. *Nephrol Dial Transplant*, *23*(3), 853-859. doi:10.1093/ndt/gfm691

- Toso, A., Maioli, M., Leoncini, M., Gallopin, M., Tedeschi, D., Micheletti, C., . . . Bellandi, F. (2010). Usefulness of atorvastatin (80 mg) in prevention of contrast-induced nephropathy in patients with chronic renal disease. *Am J Cardiol*, *105*(3), 288-292. doi:10.1016/j.amjcard.2009.09.026
- Touati, C., Idee, J. M., Deray, G., Santus, R., Balut, C., Beaufile, H., . . . Bonnemain, B. (1993). Modulation of the renal effects of contrast media by endothelium-derived nitric oxide in the rat. *Invest Radiol*, *28*(9), 814-820.
- Tran, M., & Parikh, S. M. (2014). Mitochondrial biogenesis in the acutely injured kidney. *Nephron Clin Pract*, *127*(1-4), 42-45. doi:10.1159/000363715
- Tran, M., Tam, D., Bardia, A., Bhasin, M., Rowe, G. C., Kher, A., . . . Parikh, S. M. (2011). PGC-1 α promotes recovery after acute kidney injury during systemic inflammation in mice. *J Clin Invest*, *121*(10), 4003-4014. doi:10.1172/JCI58662
- Tropeano, F., Leoncini, M., Toso, A., Maioli, M., Dabizzi, L., Biagini, D., . . . Bellandi, F. (2016). Impact of Rosuvastatin in Contrast-Induced Acute Kidney Injury in the Elderly: Post Hoc Analysis of the PRATO-ACS Trial. *J Cardiovasc Pharmacol Ther*, *21*(2), 159-166. doi:10.1177/1074248415599062
- Tsai, T. T., Patel, U. D., Chang, T. I., Kennedy, K. F., Masoudi, F. A., Matheny, M. E., . . . Spertus, J. A. (2014). Contemporary incidence, predictors, and outcomes of acute kidney injury in patients undergoing percutaneous coronary interventions: insights from the NCDR Cath-PCI registry. *JACC Cardiovasc Interv*, *7*(1), 1-9. doi:10.1016/j.jcin.2013.06.016
- Ueda, J., Nygren, A., Hansell, P., & Ulfendahl, H. R. (1993). Effect of intravenous contrast media on proximal and distal tubular hydrostatic pressure in the rat kidney. *Acta Radiol*, *34*(1), 83-87.
- Vasington, F. D., & Murphy, J. V. (1962). Ca ion uptake by rat kidney mitochondria and its dependence on respiration and phosphorylation. *J Biol Chem*, *237*, 2670-2677.
- Vig, M., Beck, A., Billingsley, J. M., Lis, A., Parvez, S., Peinelt, C., . . . Penner, R. (2006). CRACM1 multimers form the ion-selective pore of the CRAC channel. *Curr Biol*, *16*(20), 2073-2079. doi:10.1016/j.cub.2006.08.085
- Wallingford, V. H. (1953). The development of organic iodine compounds as x-ray contrast media. *J Am Pharm Assoc Am Pharm Assoc*, *42*(12), 721-728.
- Wang, Y., Zhang, H., Yang, Z., Miao, D., & Zhang, D. (2018). Rho Kinase Inhibitor, Fasudil, Attenuates Contrast-induced Acute Kidney Injury. *Basic Clin Pharmacol Toxicol*, *122*(2), 278-287. doi:10.1111/bcpt.12895
- Weisbord, S. D., Gallagher, M., Jneid, H., Garcia, S., Cass, A., Thwin, S. S., . . . Group, P. T. (2018). Outcomes after Angiography with Sodium Bicarbonate and Acetylcysteine. *N Engl J Med*, *378*(7), 603-614. doi:10.1056/NEJMoa1710933

- Weisbord, S. D., & Palevsky, P. M. (2008). Prevention of contrast-induced nephropathy with volume expansion. *Clin J Am Soc Nephrol*, 3(1), 273-280. doi:10.2215/CJN.02580607
- Widmark, J. M. (2007). Imaging-related medications: a class overview. *Proc (Bayl Univ Med Cent)*, 20(4), 408-417.
- Wiersinga, W. J., Leopold, S. J., Cranendonk, D. R., & van der Poll, T. (2014). Host innate immune responses to sepsis. *Virulence*, 5(1), 36-44. doi:10.4161/viru.25436
- Wu, C. T., Sheu, M. L., Tsai, K. S., Weng, T. I., Chiang, C. K., & Liu, S. H. (2010). The role of endoplasmic reticulum stress-related unfolded protein response in the radiocontrast medium-induced renal tubular cell injury. *Toxicol Sci*, 114(2), 295-301. doi:10.1093/toxsci/kfq006
- Wu, C. T., Weng, T. I., Chen, L. P., Chiang, C. K., & Liu, S. H. (2013). Involvement of caspase-12-dependent apoptotic pathway in ionic radiocontrast urografin-induced renal tubular cell injury. *Toxicol Appl Pharmacol*, 266(1), 167-175. doi:10.1016/j.taap.2012.10.012
- Xiao, X., Hu, Y., Quiros, P. M., Wei, Q., Lopez-Otin, C., & Dong, Z. (2014). OMA1 mediates OPA1 proteolysis and mitochondrial fragmentation in experimental models of ischemic kidney injury. *Am J Physiol Renal Physiol*, 306(11), F1318-1326. doi:10.1152/ajprenal.00036.2014
- Xie, X. C., Cao, Y., Yang, X., Xu, Q. H., Wei, W., & Wang, M. (2017). Relaxin Attenuates Contrast-Induced Human Proximal Tubular Epithelial Cell Apoptosis by Activation of the PI3K/Akt Signaling Pathway In Vitro. *Biomed Res Int*, 2017, 2869405. doi:10.1155/2017/2869405
- Yamamoto, K., Sato, T., Matsui, T., Sato, M., Okada, T., Yoshida, H., . . . Mori, K. (2007). Transcriptional induction of mammalian ER quality control proteins is mediated by single or combined action of ATF6alpha and XBP1. *Dev Cell*, 13(3), 365-376. doi:10.1016/j.devcel.2007.07.018
- Yang, D., & Yang, D. (2013). Role of intracellular Ca²⁺ and Na⁺/Ca²⁺ exchanger in the pathogenesis of contrast-induced acute kidney injury. *Biomed Res Int*, 2013, 678456. doi:10.1155/2013/678456
- Yang, D., Yang, D., Jia, R., & Ding, G. (2013). Selective inhibition of the reverse mode of Na⁽⁺⁾/Ca⁽²⁺⁾ exchanger attenuates contrast-induced cell injury. *Am J Nephrol*, 37(3), 264-273. doi:10.1159/000348526
- Yang, D., Yang, D., Jia, R., & Tan, J. (2013). Na⁺/Ca²⁺ exchange inhibitor, KB-R7943, attenuates contrast-induced acute kidney injury. *J Nephrol*, 26(5), 877-885. doi:10.5301/jn.5000259
- Yang, J. S., Peng, Y. R., Tsai, S. C., Tyan, Y. S., Lu, C. C., Chiu, H. Y., . . . Tsai, F. J. (2018). The molecular mechanism of contrast-induced nephropathy (CIN) and its link to in vitro

- studies on iodinated contrast media (CM). *Biomedicine (Taipei)*, 8(1), 1. doi:10.1051/bmdcn/2018080101
- Yang, X., Yan, X., Yang, D., Zhou, J., Song, J., & Yang, D. (2018). Rapamycin attenuates mitochondrial injury and renal tubular cell apoptosis in experimental contrast-induced acute kidney injury in rats. *Biosci Rep*, 38(6). doi:10.1042/BSR20180876
- Yang, Y., Yang, D., Yang, D., Jia, R., & Ding, G. (2014). Role of reactive oxygen species-mediated endoplasmic reticulum stress in contrast-induced renal tubular cell apoptosis. *Nephron Exp Nephrol*, 128(1-2), 30-36. doi:10.1159/000366063
- Yeganehkhah, M. R., Iranirad, L., Dorri, F., Pazoki, S., Akbari, H., Miryounesi, M., . . . Vafaeimanesh, J. (2014). Comparison between three supportive treatments for prevention of contrast-induced nephropathy in high-risk patients undergoing coronary angiography. *Saudi J Kidney Dis Transpl*, 25(6), 1217-1223.
- Yiengst, M. J., & Shock, N. W. (1962). Blood and plasma volume in adult males. *J Appl Physiol*, 17, 195-198. doi:10.1152/jappl.1962.17.2.195
- Yokomaku, Y., Sugimoto, T., Kume, S., Araki, S., Isshiki, K., Chin-Kanasaki, M., . . . Kashiwagi, A. (2008). Asialoerythropoietin prevents contrast-induced nephropathy. *J Am Soc Nephrol*, 19(2), 321-328. doi:10.1681/ASN.2007040481
- Yoo, S. M., & Jung, Y. K. (2018). A Molecular Approach to Mitophagy and Mitochondrial Dynamics. *Mol Cells*, 41(1), 18-26. doi:10.14348/molcells.2018.2277
- Yoshida, L. S., & Tsunawaki, S. (2008). Expression of NADPH oxidases and enhanced H₂O₂-generating activity in human coronary artery endothelial cells upon induction with tumor necrosis factor- α . *Int Immunopharmacol*, 8(10), 1377-1385. doi:10.1016/j.intimp.2008.05.004
- Zager, R. A., Johnson, A. C., & Geballe, A. (2007). Gentamicin suppresses endotoxin-driven TNF- α production in human and mouse proximal tubule cells. *Am J Physiol Renal Physiol*, 293(4), F1373-1380. doi:10.1152/ajprenal.00333.2007
- Zager, R. A., Johnson, A. C., & Hanson, S. Y. (2003). Radiographic contrast media-induced tubular injury: evaluation of oxidant stress and plasma membrane integrity. *Kidney Int*, 64(1), 128-139. doi:10.1046/j.1523-1755.2003.00059.x
- Zhang, B., Wu, X., Liu, J., Song, L., Song, Q., Wang, L., . . . Wu, Z. (2019). beta-Actin: Not a Suitable Internal Control of Hepatic Fibrosis Caused by *Schistosoma japonicum*. *Front Microbiol*, 10, 66. doi:10.3389/fmicb.2019.00066
- Zhao, C., Chen, Z., Xu, X., An, X., Duan, S., Huang, Z., . . . Yuan, Y. (2017). Pink1/Parkin-mediated mitophagy play a protective role in cisplatin induced renal tubular epithelial cells injury. *Exp Cell Res*, 350(2), 390-397. doi:10.1016/j.yexcr.2016.12.015

Zhao, J., Huang, Y., Song, Y., Zhao, X., Jin, J., Wang, J., & Huang, L. (2009). Low osmolar contrast medium induces cellular injury and disruption of calcium homeostasis in rat glomerular endothelial cells in vitro. *Toxicol Lett*, 185(2), 124-131.
doi:10.1016/j.toxlet.2008.12.009

Zhuo, J. L., & Li, X. C. (2013). Proximal nephron. *Compr Physiol*, 3(3), 1079-1123.
doi:10.1002/cphy.c110061

APPENDIX A: OFFICE OF RESEARCH INTEGRITY APPROVAL LETTER



Office of Research Integrity

May 10, 2019

Dakota Ward
Department of Biomedical Sciences
Joan C. Edwards School of Medicine
Marshall University

Dear Mr. Ward:

This letter is in response to the submitted dissertation abstract entitled "*A Mechanistic Study of Diatrizoic Acid Induced Proximal Tubule Cytotoxicity.*" After assessing the abstract it has been deemed not to be human subject research and therefore exempt from oversight of the Marshall University Institutional Review Board (IRB). The Code of Federal Regulations (45CFR46) has set forth the criteria utilized in making this determination. Since the study does not involve human subjects as defined in DHHS regulation 45 CFR §46.102(e) it is not considered human subject research. If there are any changes to the abstract you provided then you would need to resubmit that information to the Office of Research Integrity for review and determination.

I appreciate your willingness to submit the abstract for determination. Please feel free to contact the Office of Research Integrity if you have any questions regarding future protocols that may require IRB review.

Sincerely,

Bruce F. Day, ThD, CIP
Director

WE ARE... MARSHALL.

One John Marshall Drive • Huntington, West Virginia 25755 • Tel 304/696-4303
A State University of West Virginia • An Affirmative Action/Equal Opportunity Employer

APPENDIX B: LIST OF ABBREVIATIONS

2-APB...2-aminoethoxydiphenyl borate

4-HNE...4-hydroxynonenal

8-OHdG...8-hydroxy-2'-deoxyguanosine

ACEI...angiotensin-converting enzyme inhibitors

Akt... protein kinase B

Apaf1...apoptotic protease activating factor 1

ARB...angiotensin-II receptor blockers

ATCC...American Type Culture Collection

ATF4...activating transcription factor 6

ATF6...activating transcription factor 6

BAPTA-AM...1, 2-bis (*o*-aminophenoxy) ethane-*N,N,N',N'*-tetra-acetic acid

BSA...bovine serum albumin

CAT...catalase

CHF...congestive heart failure

CHOP...C/EBP homologous protein

CI-AKI...contrast-induced acute kidney injury

CPT1A...carnitine-palmitoyl transferase

DA...diatrizoic acid

DDTC... diethyldithiocarbamate

DNPH...dinitrophenylhydrazine

ECAR...extracellular acidification rate

EGCG...epigallocatechin gallate

eGFR...estimated glomerular filtration rate

EGTA...ethyleneglycol-bis(β -aminoethyl)-*N,N,N',N'*-tetra-acetic acid

eIF2 α ...eukaryotic translation initiation factor 2 α

eNOS...endothelial nitric oxide synthase

ER...endoplasmic reticulum

ERAD...endoplasmic reticulum-associated degradation

ERK...extracellular signal-regulated kinase

ETC...electron transport chain

FCCP... carbonyl cyanide-4-(trifluoromethoxy)phenylhydrazone

GFR...glomerular filtration rate

GLS1... glutaminase

GPx...glutathione peroxidase

GR...glutathione reductase

GRP78...glucose-regulated protein 78

GSH...glutathione

H₂O₂...hydrogen peroxide

HEK-293...human embryonic kidney cells

HK-2...human kidney 2 cells

HOCM...high-osmolar contrast media

IOCM...iso-osmolar contrast media

IP₃...inositol-1,4,5-triphosphate

IP₃R... inositol triphosphate receptor

IRE1...inositol-requiring ER-to-nucleus signal kinase 1

JAK...Janus kinase

JNK...c-Jun N-terminal kinase

LC3B...Microtubule-associated proteins 1A/1B light chain 3B

LCFA...long-chain fatty acids

LIR...LC3-interacting region

LLC-PK1...porcine kidney proximal tubule cells

LOCM...low-osmolar contrast media

MAM...mitochondrial-associated membranes

MAPK...mitogen-activated protein kinase

MCU...mitochondrial calcium uniporter

MFS I/II...Mitofusin I and II

MnSOD...manganese superoxide dismutase

MPC...mitochondrial pyruvate carrier

mPT...mitochondrial membrane permeability transition

mPTP...mitochondrial membrane permeability transition pore

MTT... 3-(4,5-dimethylthiazol-2-yl)-2,5-diphenyltetrazolium bromide

NAC...N-acetylcysteine

NCX...Sodium calcium exchanger

NO...nitric oxide

NOX...NADPH oxidase

NOX4...NADPH oxidase 4

NOXO1...NADPH oxidase organizer 1

NRK52E...rat renal proximal tubule cells

NSAID...nonsteroidal anti-inflammatory drug

$O_2^{\cdot -}$...superoxide anion

OAT...organic ion transporter

OH^{\cdot} ...hydroxyl radical

OCR...oxygen consumption rate

P62...sequestrome-1

PARK2...Parkin

PARL...presenilin-associated Rhomboid like

PBS...phosphate buffered saline

PBST...phosphate buffered saline plus Tween 20

PCI...percutaneous coronary intervention

PER...proton efflux rate

PERK...RNA-dependent protein kinase-like ER kinase

PI...propidium iodide

PI3...phosphoinositide 3

PLC...phospholipase C

PMCA...plasma membrane calcium ATPase

PINK1...PTEN-induced putative kinase

PT...proximal tubule

RAAS...renin-angiotensin-aldosterone system

RCM...radiocontrast media

ROCK...Rho-associated protein kinase

ROS...reactive oxygen species

RSB...reducing sample buffer

SERCA...sarco/endoplasmic reticulum calcium ATPase

SOCE...store-operated calcium entry

SOCC...store-operated calcium channel

SOD...superoxide dismutase

STAT...signal transducer and activator of transcription proteins

STIM1...stromal interaction molecule 1

SCr...serum creatinine

TAL...thick ascending limb

TBST...tris buffered saline plus Tween 20

TMB...3,3t,5,5t-tetramethylbenzidine

TNF α ...tumor necrosis factor alpha

TNFR1...TNF α receptor 1

TRADD...TNF α receptor-associated death domain

TRPV6...transient receptor potential cation channel subfamily V member 6

UPR...unfolded protein response

VDAC...voltage-dependent anion channel

XO...xanthine oxidase

APPENDIX C: VITA

DAKOTA B. WARD

3349 McCoy Road, Huntington, WV 25701 | 304-951-3742 | warddb13@outlook.com

EDUCATION

- **Marshall University, Huntington, WV**

Ph.D. in Biomedical Research

July 2014 – July 2019

Dissertation: A Mechanistic Study of Diatrizoic Acid induced Proximal Tubule Cytotoxicity

- **Bachelor of Science in Biochemistry**

August 2009 – December 2013

Minor: Biology

Graduating Study: Synthesis of the NDPS Fungicide Analog 1-(3,5-dichloro-4-pyridyl)-2,5-pyrrolidinedione

PROFESSIONAL AND RESEARCH EXPERIENCE

- **Scientist I**

June 2019 - Present

BioAgilytix Labs, LLC, Research Triangle Park, NC

- **Research Assistant**

November 2011 – January 2014

Marshall University, Department of Biomedical Sciences, Huntington, WV

Principle Investigator: Dr. Gary Rankin

Laboratory duties including experimental design, conducting biochemical toxicity assays, compiling data and completing statistical analyses.

- **Teaching Assistant**

August 2011 – May 2013

Marshall University, College of Science, Principles of Chemistry I/II

Professor: Dr. John L. Hubbard

Teaching duties included collaborating on curriculum and exam development, meeting with students upon request, and grading all written work including final examinations.

MANUSCRIPTS SUBMITTED

Ward D. B.; Brown K; Valentovic M; Contrast Induced Acute Kidney Injury and Direct Cytotoxicity of Iodinated Radiocontrast Media on Renal Proximal Tubule Cells. Journal of Pharmacology and Experimental Therapeutics, May 2019. Minireview, revised manuscript submitted

Ward D. B.; Brown K; Valentovic M; Radiocontrast Agent Diatrizoic Acid Induces Mitophagy and Oxidative Stress Via Calcium Dysregulation. Submitted to International Journal of Molecular Sciences, Special Nephrotoxicity Issue, May 2019.

PUBLICATIONS

Racine CR, Ferguson T, Preston D, **Ward D**, Ball J, Anestis DK, Valentovic M, Rankin GO. The Role of Biotransformation and Oxidative Stress in 3,5-Dichloroaniline (3,5-DCA) Induced Nephrotoxicity in Isolated Renal Cortical Cells from Male Fischer 344 Rats. *Toxicology*. 2016; 3;341-343:47-55

Racine CR, **Ward D**, Anestis, DK, Ferguson T, Preston D, Rankin, GO. 3,4,5-trichloroaniline nephrotoxicity in vitro: potential role of free radicals and renal biotransformation. *International Journal of Molecular Sciences* 2014; 11:20900-20912

PRESENTATIONS

Oral Presentations

Ward D, Brown K, Valentovic M. Cytotoxicity, Mitochondrial Function, and Endoplasmic Reticulum (ER) Stress Associated with the Radiocontrast Agent Diatrizoate (DA) in a Human Proximal Tubule Cell Line. Marshall University School of Medicine 31th Annual Research Day. March 22, 2019. Huntington, WV

Ward D, Brown K, Valentovic M. Characterization of Renal Cytotoxicity and Oxidative Stress Induced by the Radiocontrast Agent Diatrizoate (DA) in Human Proximal Tubular Cell Line. Marshall University School of Medicine 30th Annual Research Day. March 28, 2018. Huntington, WV

Poster Presentations

Ward D, Brown K, Valentovic M. Cytotoxicity, Mitochondrial Function, and Endoplasmic Reticulum (ER) Stress Associated with the Radiocontrast Agent Diatrizoate (DA) in a Human Proximal Tubule Cell Line. Society of Toxicology Annual Meeting. March 10-14, 2019. Baltimore, MD

Ward D; Brown K; Valentovic M. Characterization of Renal Cytotoxicity and Oxidative Stress by the Radiographic Agent Diatrizoic Acid (DA) in a Human Kidney Cell Line. Appalachian Regional Cell Conference. December 2, 2017. Athens, OH.

Racine CR; Ferguson T; Preston D; **Ward D**; Ball J; Anestis DK; Valentovic M; Rankin GO. The Role of Gender, Biotransformation and Oxidative Stress in 3,5-Dichloroaniline Induced Nephrotoxicity in Isolated Renal Cortical Cells from Fischer 344 Rats. Society of Toxicology Annual Meeting. March 13-17, 2016. New Orleans, LA.

Racine CR; **Ward D**; Tyree C; Pope D; Sharp J; Anestis DK; Rankin GO. In Vitro Cytotoxicity Induced by Putative Metabolites of 3,5-Dichloroaniline. Society of Toxicology Annual Meeting. March 13–17, 2016. New Orleans, LA.

Tate J; Racine CR; Vermudez S; Tyree C; **Ward D**; Anestis DK; Rankin GO. Role of renal bioactivation enzyme systems on 3,5-dichloronitrobenzene (3,5-DCNB) induced nephrotoxicity in vitro. Society of Toxicology Annual Meeting. March 22-26, 2015. San Diego, CA. *Toxicologist* 144 (1), 489, 2015. Program #2278

LEADERSHIP EXPERIENCE

Graduate Student Organization

Marshall University, Joan C. Edwards School of Medicine, Huntington, WV

President May 2017 – May 2018

Vice-President May 2016 – May 2017

COMMUNITY SERVICE EXPERIENCE

The Jared Box Project

Cabell Huntington Hospital, Huntington, WV

Event Organizer December 2018

Volunteer December 2016-2017, 2019

GRANTS

WV NASA Space Consortium Graduate Fellowship 2017, 2019

AWARDS

Graduate Student Organization Leadership Scholarship 2018

Marshall University School of Medicine 30th Annual Research Day

Oral Presentation Runner-Up 2018

Dr. Frederick J. Lotspeich Award for Academic Excellence 2016